

PRODUCTION OF VIRUS LIKE PARTICLES EXPRESSING ALPHA (B.1.1.7)
OR DELTA PLUS (B.1.617.2.1) SPIKE VARIANTS AND DEVELOPMENT OF
A PSEUDOTYPED VIRUS NEUTRALIZATION ASSAY

A THESIS SUBMITTED TO
THE GRADUATE SCHOOL OF NATURAL AND APPLIED SCIENCES
OF
MIDDLE EAST TECHNICAL UNIVERSITY

BY
NEŞE GÜVENÇLİ

IN PARTIAL FULFILLMENT OF THE REQUIREMENTS
FOR
THE DEGREE OF MASTER OF SCIENCE
IN
MOLECULAR BIOLOGY AND GENETICS

FEBRUARY 2022

Approval of the thesis:

**PRODUCTION OF VIRUS LIKE PARTICLES EXPRESSING ALPHA
(B.1.1.7) OR DELTA PLUS (B.1.617.2.1) SPIKE VARIANTS AND
DEVELOPMENT OF A PSEUDOTYPED VIRUS NEUTRALIZATION
ASSAY**

submitted by **NEŞE GÜVENÇLİ** in partial fulfillment of the requirements for the degree of **Master of Science in Molecular Biology and Genetics, Middle East Technical University** by,

Prof. Dr. Halil Kalıpçılar
Dean, Graduate School of **Natural and Applied Sciences**

Prof. Dr. Ayşegül Gözen
Head of the Department, **Biology**

Prof. Dr. Mayda Gürsel
Supervisor, **Biology, METU**

Examining Committee Members:

Prof. Dr. Kamil Can Akçalı
Biophysics Dept., Ankara University

Prof. Dr. Mayda Gürsel
Biological Sciences, METU

Assoc. Prof. Banu Bayyurt Kocabaş
Biological Sciences, METU

Date:10.02.2022

I hereby declare that all information in this document has been obtained and presented in accordance with academic rules and ethical conduct. I also declare that, as required by these rules and conduct, I have fully cited and referenced all material and results that are not original to this work.

Name Last name: Neşe Güvençli

Signature:

ABSTRACT

PRODUCTION OF VIRUS LIKE PARTICLES EXPRESSING ALPHA (B.1.1.7) OR DELTA PLUS (B.1.617.2.1) SPIKE VARIANTS AND DEVELOPMENT OF A PSEUDOTYPED VIRUS NEUTRALIZATION ASSAY

Güvençli, Neşe
Master of Science, Molecular Biology and Genetics
Supervisor : Prof. Dr. Mayda Gürsel

February 2022, 146 pages

Vaccines are one of the most important public health interventions to combat the spread of infectious diseases. All currently approved COVID-19 vaccines target Spike antigen derived from the authentic Wuhan strain. However, with the emergence of new variants effectiveness of the current vaccines declined, commensurate to their ability to generate neutralizing antibodies against some variants of concern (VOC). Since new VOCs are predicted to emerge the next 2-4 years, variant specific vaccines are urgently needed. In this study, we aimed to design vaccine antigens against Delta plus (B 1.617.2.1) and Alpha (B.1.1.7) variants of concern by exploiting the Virus Like Particle (VLP) vaccine platform. Consequently, these variant specific VLPs were formed by assembling the Membrane (M), Nucleocapsid (N), Envelope (E) proteins of the authentic virus and Spike (S) proteins bearing mutations of Delta plus (B 1.617.2.1) and Alpha (B.1.1.7) variants of concern. For this, the M and N genes were cloned into the pVITro1 expression vector, whereas variant specific Spike genes were cloned together with the Envelope gene into the pVITro2 expression vector. Transfection of these vectors to Hek293

suspension cells resulted in VLP accumulation in the supernatant. Herein, we demonstrate the feasibility of producing variant spike expressing VLPs derived from Alpha (B.1.1.7) and Delta plus (B.1.617.2.1) VOCs. Furthermore, we established a pseudotyped virus neutralization assay and tested its utility using sera taken from volunteers and mice immunized with Delta plusS-6p-VLP or AlphaS-6p-VLP vaccines.

Keywords: SARS-CoV-2, Variants of Concern, Vaccine, Virus Like Particle, Neutralization Assay

ÖZ

ALPHA (B.1.1.7) VEYA DELTA PLUS (B.1.617.2.1) SPIKE VARYANTLARINI İFADE EDEN VİRÜS BENZERİ PARÇACIKLARIN (VBP) ÜRETİMİ VE YALANCI TİP VİRÜSLE NÖTRALİZASYON ANALİZİ GELİŞTİRME

Güvençli, Neşe
Yüksek Lisans, Moleküler Biyoloji ve Genetik
Tez Yöneticisi: Prof. Dr. Mayda Gürsel

Şubat 2022, 146 sayfa

Aşılar, bulaşıcı hastalıkların yayılmasıyla mücadelede en önemli halk sağlığı müdahalelerinden biridir. Hali hazırda onaylanmış olan tüm COVID-19 aşıları, orijinal Wuhan soyundan türetilen Spike antijenini hedefler. Fakat, yeni varyantların ortaya çıkmasıyla birlikte, mevcut aşuların etkinliği, bazı endişe uyandıran varyantlara (VOC) karşı nötralizan antikor üretme yetenekleriyle orantılı olarak azaldı. Önümüzdeki 2 ila 4 yıl içinde yeni VOC'ların ortaya çıkacağı tahmin edildiğinden, varyant spesifik aşılar acilen ihtiyaç duyulmaktadır. Bu çalışmada, Virüs Benzeri Parçacık (VBP) aşı platformundan yararlanarak, Delta plus (B 1.617.2.1) ve Alpha (B.1.1.7) varyantlarına karşı aşı antijenleri tasarlamayı amaçladık. Bu nedenle, bu varyantlara özgü VBP'ler, orijinal virüsün M, N, E proteinleri ve endişe uyandıran Delta plus (B 1.617.2.1) ve Alpha (B.1.1.7) varyantlarının mutasyonlarını taşıyan Spike (S) proteinlerinin birleştirilmesiyle oluşturulmuştur. Bunun için M ve N genleri, pVitro1 ekspresyon vektörüne klonlanırken, varyantlara özgü Spike genleri, Envelope geni ile birlikte pVitro2 ekspresyon vektörüne klonlandı. Bu vektörlerin Hek293 süspansiyon hücrelerine transfeksiyonu, süpernatantta VLP birikmesiyle sonuçlandı. Burada, Alpha (B.1.1.7) ve Delta plus (B.1.617.2.1) VOC'larından türetilen Spike versiyonlarının ifade

edildiđi VBPlerin üretiminin uygulanabilirliđini gösteriyoruz. Ayrıca, yalancı tip virüs nötralizasyon analizi oluşturduk ve analizin kullanılabilirliđini Delta plusS-6p-VLP veya AlphaS-6p-VLP aşıları ile aşılanmış gönüllülerden ve farelerden alınan serumları kullanarak test ettik.

Anahtar Kelimeler: SARS-CoV-2, Endişe Uyandıran Varyantlar, Aşı, Virüs Benzeri Parçacık, Nötralizasyon Analizi

ACKNOWLEDGEMENTS

First of all, I am heartily grateful to my supervisor, Prof. Dr. Mayda Gürsel, for accepting me in her lab and giving me the chance of working in this kind of scientific environment with lots of valuable people. She has filled my heart with wonder and desire and became my role model with her tender heart in academia.

I want to thank members in my thesis examining committee: Asst. Prof. Banu Bayyurt Kocabaş and Prof. Dr. Kamil Can Akçalı for evaluating my thesis, sparing their valuable times and their appreciated comments.

I also want to thank my precious lab mates: Başak Kayaoğlu, Yağmur Aydın, Emre Dünüroğlu, Emre Mert İpekoğlu who kindly shared their experiences. I am also thankful to İsmail Cem Yılmaz who is more than a postdoc for me with his tremendous supports and understanding. Moreover, I am very glad to have such friendships with Öykü Yağmur Başar, İlayda Baydemir and Hatice Asena Şanlı who stand near me and improve my motivation all the time with their cheer and mature supports. I want to thank Naz Sürücü for being my sister, who is free from evil and shines all the time with her kindness, wisdom and warm heart. She has become my lifeline every time when I feel devastated.

I would like to thank to Prof. Dr. İhsan Gürsel for always look after me and make me smile after every discussion. I will never forget his delicious wraps. I also thank İG lab members, especially Nilsu Turay and Artun Bülbül for their kind friendships during the Nobel times.

I am indebted to all my beloved ones, Fatma Türk, Beste Baba, Özlem Neyişçi, Arif Gür, Hasan Eray İğneler, Burak Kemal Kara who are always near me, for giving me morale in every step of my life.

I would like to express my gratitude to my dearest little engineer Fethi Umur Ersoy for sharing a life with me with an eternal love and support.

Finally, I would like to express my deepest love to my little woman Nezihe Güvençli. She tried every path to provide me a qualified education. I wouldn't be such an energetic person without her.

I also want to thank The Scientific and Technological Research Council of Turkey (TÜBİTAK) for the financial support.

TABLE OF CONTENTS

ABSTRACT	v
ÖZ	vii
ACKNOWLEDGEMENTS	ix
TABLE OF CONTENTS	xi
LIST OF TABLES	xvi
LIST OF FIGURES	xvii
LIST OF ABBREVIATIONS	xix
1 INTRODUCTION	1
1.1 SARS-CoV-2	1
1.1.1 The Emergence of SARS-CoV-2	1
1.1.2 General Characteristics of SARS-CoV-2	2
1.1.2.1 Phylogenetic Analyses of SARS-CoV-2	2
1.1.2.2 Genome Organization of SARS-CoV-2	3
1.1.3 Nonstructural and accessory proteins of SARS-CoV-2	5
1.1.4 Structural proteins of SARS-CoV-2	6
1.1.4.1 Spike Glycoprotein	7
1.1.4.2 Nucleocapsid protein (N) of SARS-CoV-2	9
1.1.4.3 Membrane (M) and Envelope (E) Proteins of SARS-CoV-2	9
1.2 COVID-19 Disease	10
1.2.1 SARS-CoV-2 Entry and Replication of the Virus	11
1.2.2 Immune Response to COVID-19 disease	12
1.2.2.1 Innate Immunity to SARS-CoV-2	13

1.2.2.2	Adaptive Immunity to SARS-CoV-2	14
1.3	Vaccine platforms against SARS-CoV-2	16
1.3.1	mRNA based vaccines	18
1.3.2	DNA vaccines	18
1.3.3	Inactivated vaccines	19
1.3.4	Vector Based vaccines	19
1.3.5	Protein Based Vaccines	20
1.4	Emergence of SARS-CoV-2 Variants of Concern	21
1.5	Aim of the Study	24
2	MATERIALS & METHODS	25
2.1	Materials	25
2.1.1	HEK293 Suspension Cell line and HEK293-FT-hACE 2 Adherent Cell line	25
2.1.2	Cell Culture Media, Buffers and Solutions	25
2.1.3	Bacteria Strain and Bacterial Culture Media	26
2.1.4	Plasmids, Enzymes and Related Reagents	26
2.1.5	Solutions and tools of VLP purification	27
2.1.6	Protein analyses tools for purified and concentrated VLP samples	28
2.1.6.1	Device and tools for Nanoparticle analyses	28
2.1.6.2	Solutions, instruments and antibodies for SDS-PAGE & Western-blotting, Dot Blotting& micro BCA	28
2.1.7	DNA amount determination with Picogreen Assay	30
2.1.8	Serums and reagents used in neutralization assay	30
2.2	Methods	31

2.2.1	Cloning of SARS-CoV-2 Spike, Membrane, Nucleocapsid and Envelope expressing plasmids	31
2.2.1.1	Sequences of the proteins & expressing vectors and cloning strategy	31
2.2.1.2	Transformation of the genes and ligated plasmids	32
2.2.1.3	Plasmid DNA isolation	32
2.2.1.4	Restriction enzyme digestion, Gel elution and Ligation	33
2.2.1.5	Agarose Gel Electrophoresis and Next Generation Sequencing	34
2.2.2	Transient Transfection of HEK293 Suspension Cells	34
2.2.3	Virus Like Particle Purification	35
2.2.3.1	First clarification of harvest and removal of host cell-derived nucleic acids	35
2.2.3.2	Fast Protein Liquid Chromatography System for VLP purification	35
2.2.3.3	Tangential Flow Filtration of VLPs	36
2.2.4	Characterization and Quantification of VLPs	38
2.2.4.1	Nanoparticle Analysis with Tunable Resistive Pulse Sensing	38
2.2.4.2	SDS-PAGE, Western and Dot Blotting for the Characterization of VLPs	39
2.2.4.3	VLP protein content determination with micro BCA	41
2.2.5	Determination of residual DNA amount in purified VLPs with the PicoGreen Assay	42
2.2.6	Pseudovirus Neutralization Assay	42
2.2.6.1	SARS-CoV-2 Spike Protein expressing Pseudotyped virus Production	43

2.2.6.2	Pseudotyped virus Neutralization Assay	45
2.2.7	Statistical Analysis	46
2.3	Ethical Statement	46
3	RESULTS & DISCUSSION	47
3.1	Cloning of Alpha (B.1.1.7) and Delta (B.1.617.2.1) Variant expressing genes and Confirmation of Structural Protein Expression Vectors	49
3.2	Optimization of PEIpro Mediated Transfection of HEK293 Suspension Cells Using Green Fluorescence Protein Expressing Plasmid	54
3.3	Transient Transfection of HEK293 Suspension Cells Generates Virus Like Particles in the Culture Supernatant	56
3.3.1	Virus Like Particle Accumulation Rates in the Culture Supernatant on 2, 4 and 5 Days After Transfection	56
3.3.2	Characterization of Purified VLPs	58
3.4	Size Distributions of the Alpha- and Delta-6p-VLPs	60
3.5	Protein and DNA contents of Alpha-S and Delta-S-6p-VLPs	62
3.6	Establishment of Pseudotyped Virus Neutralization Assay	64
3.6.1	Spike Bearing Pseudotyped Virus Production	64
3.6.2	Evaluation of Neutralizing Activity of the Sera Taken from Volunteers Vaccinated with Alpha- S-6p-VLP and Mice Vaccinated with Deltaplus-S-6p-VLP	65
4	CONCLUSION	79
	APPENDICES	103
	Sequence of Envelope protein gene of SARS-CoV-2:	103
	Sequence of Membrane glycoprotein gene of SARS-CoV-2:	103
	Sequence of Nucleocapsid gene of SARS-CoV-2:	104

Sequence of 6p-Spike gene of SARS-CoV-2:	105
Sequence of Spike gene of Alpha variant:	108
Sequence of Spike gene of Delta variant:	110
pVITRO1-hygro-mcs Vector map:	113
pVITRO2-hygro-mcs vector map:	114
Next Generation Sequencing result of pVITRO2 hexapS-E for Alpha variant:	114
Next Generation Sequencing result of pVITRO2 hexapS-E for Delta variant:	121
Next Generation Sequencing Result of pVITRO1 M+N:	130
B. Media and Buffer Recipes	137
C. Gating Strategy for tracking pcDNA 3.1 (+) eGFP transfected HEK293 Suspension Cells	139
D. Viability Tracking of pVITRO2 6p-Delta-Variant-S+E and pVITRO1 M+N transfected HEK293 Suspension Cells (Representative for Both Variants)	140
E. Negative and Positive Controls of Pseudotyped Virus Neutralization Assay	141
F. Flow Cytometric Analysis of Mean Fluorescent Intensity Levels	143

LIST OF TABLES

Table 1.1. Functions of the SARS-CoV-2 nonstructural proteins.	6
Table 2.1. Antibodies used in western and dot blots.	29
Table 2.2. Plasmid amounts used for pseudotyped virus production.	43
Table 3.1. Protein and DNA contents of Alpha-, Delta- and WT-6p-VLPs.	63

LIST OF FIGURES

Figure 1.1. Placement of SARS-CoV-2, SARS-CoV, MERS-CoV and other betacoronaviruses in the phylogenetic tree based on whole genome analysis. (Adapted from Hu, Guo, Zhou & Shi, 2021)	3
Figure 1.2. Genome organization of SARS-CoV-2 non-structural, structural and accessory proteins. (Adapted from Redondo, Zaldivar-Lopez , Garrido & Montoya, 2021)	4
Figure 1.3. Model of SARS-CoV-2 virion structure with an emphasis on four structural proteins (S, M, E, N) (Adapted from (Kumar, Nyodu, Maurya et al. 2020).	7
Figure 1.4. SARS-CoV-2- Spike protein structural domains and cleavage sites (Adapted from Takeda, 2021).	8
Figure 1.5. SARS-CoV-2 Nucleocapsid protein encoding gene (Adapted from Satarker & Nampoothiri, 2020).	9
Figure 1.6. SARS-CoV-2 entry into target cell and virion exocytosis after viral genome processing (Adapted from Lebeau, Vagner, Frumence & Gasque, 2020).	12
Figure 1.7. Immune response in alveoli against SARS-CoV-2 infection during mild and severe cases (Lebeau, Vagner, Frumence & Gasque, 2020).	14
Figure 1.8. The underlying mechanism of immunization through vaccination (Adapted from (Pollard & Bijker, 2021)).	17
Figure 1.9. Spike protein Mutations in Emerging SARS-CoV-2 Variants of Concern (Adapted from He X., Hong W., Pan X., Lu G. & Wei X., 2021).	22
Figure 2.1. Diagram of Tangential Flow System	37
Figure 2.2. Western blot transfer stack for transfer of proteins form gel to membrane.	40
Figure 2.3. Pseudotyped virus production scheme starting with transfection of the Hek293ft cells to the cryopreservation of the pseudoviruses at -80°C.	44
Figure 2.4. Summary of Pseudotyped Virus Neutralization Protocol	46

Figure 3.1. Schematic Representation of Spike Gene Design with the Inclusion of Mutations that were found in Alpha and Delta plus Variants (Adapted from Mohammadi et al., 2021)	50
Figure 3.2. Confirmation of isolated plasmid constructs digested with various restriction enzymes.	52
Figure 3.3. Flow Cytometric Analysis of GFP expression following transfection of Hek293 suspension cells.	55
Figure 3.4. Determination of VLP Secretion Rate into the Culture Supernatant on Different Days through Dot Blot Analysis.	57
Figure 3.5. Verification of expression of the four structural proteins in purified VLPs incorporating the WT, Alpha- or Delta- 6p-VLP Spikes (a,b) and comparison of their Spike expression rates in gels loaded with equal protein amounts of VLPs (c,d).	59
Figure 3.6. Size distributions of the Alpha-6p-VLP (a), WT-6p-VLP (b) and Delta-6p-VLPs (c).	62
Figure 3.7. Confirmation of Spike protein expression in isolated Pseudotyped Viruses via Dot Blot Analysis.	65
Figure 3.8. GFP expression levels of hACE2 expressing HEK293FT cells infected with/out pseudoviruses in the absence of neutralizing antibodies.	66
Figure 3.9. Fluorescent Microscopy Images and Neutralization Activity Analysis from the Sera of DeltaS-6p-VLP, BioNTech and SinoVac Vaccinated Mice/Volunteers (DF: dilution factor, BN: Balb/c number).	70
Figure 3.10. Fluorescent Microscopy Images and Neutralization Activity Analysis from the Sera of AlphaS-6p-VLP Vaccinated Volunteers (DF: dilution factor, VN: volunteer number).	76

LIST OF ABBREVIATIONS

VLP: Virus Like Particle

VOC: Variants of Concern

SARS-CoV-2: Severe Acute Respiratory Syndrome Coronavirus 2

MERS-CoV: Middle East Respiratory Syndrome Coronavirus

COVID-19: Coronavirus Disease 19

WHO: World Health Organization

ORF: Open Reading Frame

UTR: Untranslated Region

RTC: Replication/Transcription Complex

Nsp: Nonstructural Protein

S: Spike glycoprotein

E: Envelope

N: Nucleocapsid

M: Membrane glycoprotein

IL: Interleukin

MHC: Major Histocompatibility Complex

IFN: Interferon

ER: Endoplasmic Reticulum

RBD: Receptor Binding Domain

HR: Heptad Repeats

FP: Fusion Peptide

TM: Transmembrane

ACE2: Angiotensin Converting Enzyme 2

TMPRSS2: Transmembrane Protease Serine 2

NTD: N Terminal Domain

CTD: C Terminal Domain

PRR: Pattern Recognition Receptors

NET: Neutrophil Extracellular Traps

NAbs: Neutralizing Antibodies

DC: Dendritic Cell

TAE: Tris-Acetate-EDTA

BCA: Bicinchoninic acid Assay

TFM: Transfection Medium

TFF: Tangential Flow Filtration

FBS: Fetal Bovine Serum

BSL: Biosafety Level

GFP: Green Fluorescent Protein

NGS: Next Generation Sequencing

TRPS: Tunable-resistive pulse sensing

MFI: Mean Fluorescent Intensity

CHAPTER 1

INTRODUCTION

1.1 SARS-CoV-2

1.1.1 The Emergence of SARS-CoV-2

The increase in mysterious pneumonia cases in Wuhan on December 31, 2019 was followed by the discovery of a highly transmissible unknown coronavirus with similar genomic organization to SARS-CoV (J. Li et al., 2021). It was reported that a novel virus from the same *Coronaviridae* family appeared after the emergence of SARS-CoV in 2003 and MERS-CoV in 2012 (Keni et al., 2020).

The first four cases showed similar symptoms to SARS-CoV, which were fever, low lymphocyte count and pneumonia, yet none of them responded to antimicrobial treatment (Q. Li et al., 2020). After the discovery of the epidemiologic link of the first cases to the Huanan Seafood Wholesale Market, thorough analysis suggested that this infectious agent had evolved from the viruses in bats and *Rhinolophus* species (J. Li et al., 2021). The novel virus was named SARS-CoV-2 by the International Committee on Taxonomy of Viruses because of its genomic similarity to severe acute respiratory syndrome related coronaviruses (Gorbalenya et al., 2020). The disease resulting from SARS-CoV-2 infection was later named COVID-19 (World Health Organization, 2020).

At the beginning of the epidemic, cases doubled every week. When infected patients commonly displayed pneumonia, cough, fever and acute respiratory distress syndrome, elder patients who had diabetes, obesity, hypertension, asthma showed

higher mortality rates resulting from cytokine storm (Keni et al., 2020). Following the alarming level of spread of the virus across countries, World Health Organization (WHO) declared COVID-19 a pandemic on 11 March 2020 (World Health Organization, 2020). At the end of two years, more than 350 million people have been infected with a death toll of 5.5 million.

1.1.2 General Characteristics of SARS-CoV-2

1.1.2.1 Phylogenetic Analyses of SARS-CoV-2

SARS-CoV-2 is a member of the *Coronaviridae* family comprised of positive strand enveloped RNA viruses (Pereson et al., 2021). In the early twenty-first century, humanity had come across with two zoonotic coronaviruses classified as MERS-CoV and SARS-CoV, and grouped under the *Merbecovirus* and *Sarbecovirus* subgenera of the *Betacoronavirus* genus (Gorbalenya et al., 2020b; X. Li et al., 2020). With the emergence of SARS-CoV-2, the third zoonotic human coronavirus has been identified.

Through the high-level genome organization studies with *Betacoronaviruses*, it was revealed that SARS-CoV-2 shares 79% and 50% similarity with SARS-CoV and MERS-CoV, respectively. Furthermore, SARS-CoV and SARS-CoV-2 share more than 90% amino acid homology in terms of three structural proteins (Membrane -M-, Nucleocapsid -N-, Envelope -E-) (Hu et al., 2021a). Thus, whole genome analysis suggested to place the SARS-CoV-2 under the *Betacoronavirus* genus and *Sarbecovirus* subgenus on the phylogenetic tree. However, SARS-CoV-2 pairwise distance demarcation with other species in *Coronaviridae* family indicated the separation between SARS-CoV related lineage from SARS-CoV-2 (Gorbalenya et al., 2020b). Therefore, together with parallel existing SARS-CoV and SARS- related coronaviruses groups, SARS-CoV-2 was grouped with four horseshoe bat

coronaviruses and two pangolin coronaviruses -with 88% sequence identity- under *Sarbecovirus* subgenus (Lu et al., 2020). (Figure 1.1)

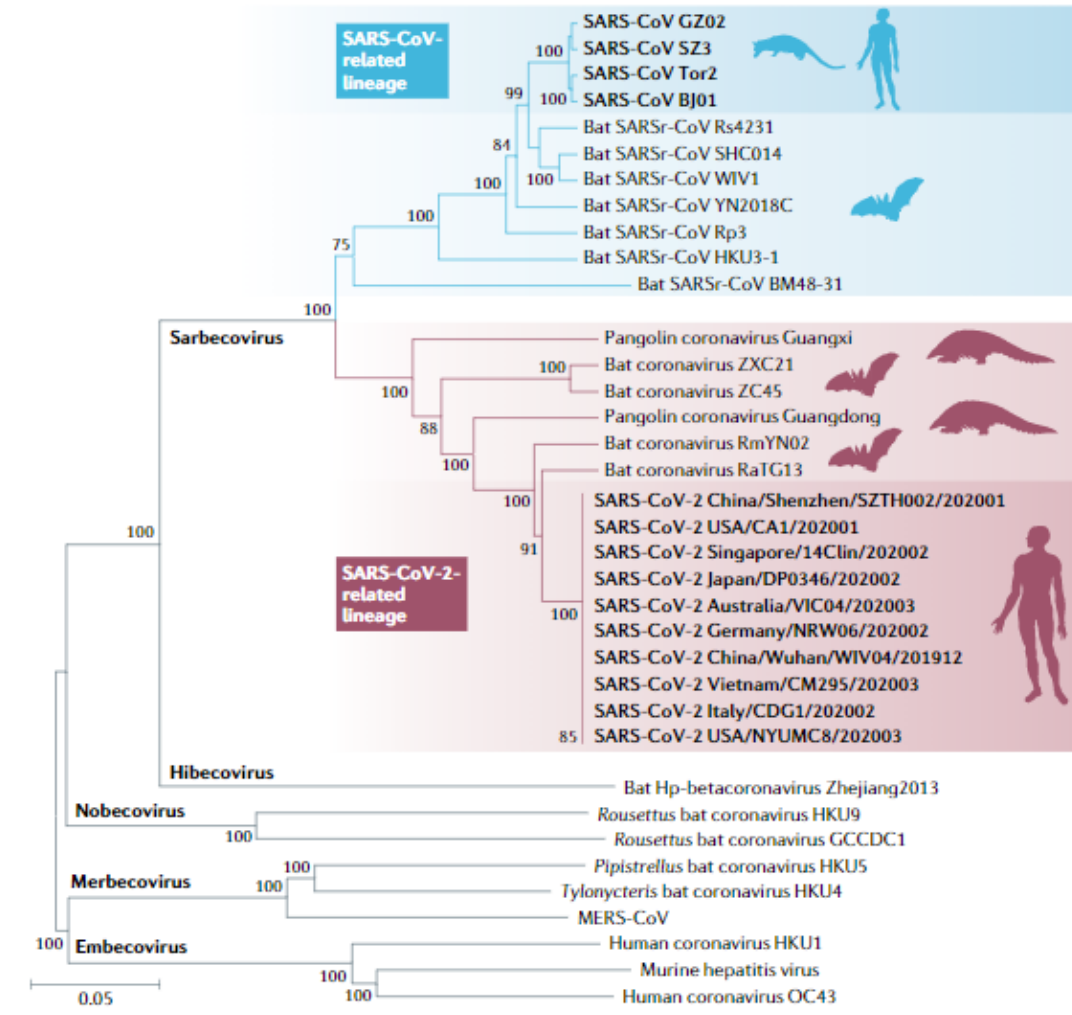


Figure 1.1. Placement of SARS-CoV-2, SARS-CoV, MERS-CoV and other betacoronaviruses in the phylogenetic tree based on whole genome analysis. (Adapted from Hu, Guo, Zhou & Shi, 2021)

1.1.2.2 Genome Organization of SARS-CoV-2

The size of SARS-CoV-2 genome is ~29.9 kb. The full-length SARS-CoV-2 genome is made of 29903 nucleotides, and 29 proteins are encoded by 14 open reading frames

(ORFs) (Gordon et al., 2020). The flanking 265 nucleotides at the 5' cap form the 5' untranslated region (UTR), which is followed by localization of ORF1a and ORF1b encoding replication/transcription complex (RTC) (F. Wu, Zhao, et al., 2020). ORF1a and ORF1ab constitute 67% of the whole SARS-CoV-2 genome. While the ORF1a gene encodes polyprotein 1a (pp1a), made up of 10 nonstructural proteins (nsp1-nsp10), the ORF1ab gene encodes polyprotein 1ab (pp1ab) consisting of 16 nonstructural proteins including nsp1-nsp10 (Rastogi et al., 2020; A. Wu et al., 2020).

At the 3' UTR site, formed by flanking 358 nucleotides, one third of the whole genome is formed from the four major structural protein genes, encoding Spike glycoprotein (S), Envelope (E), Membrane glycoprotein (M) and Nucleocapsid (N). These are accompanied by genes of eleven accessory proteins (Redondo et al., 2021). The 3' end genomic sequence order is as follows: Spike, ORF3a/b/c/d, Envelope, Membrane, ORF6, ORF7a/b, ORF8, ORF9, Nucleocapsid and ORF10 from 5' to 3' (Rahimi et al., 2021) (Figure 1.2).

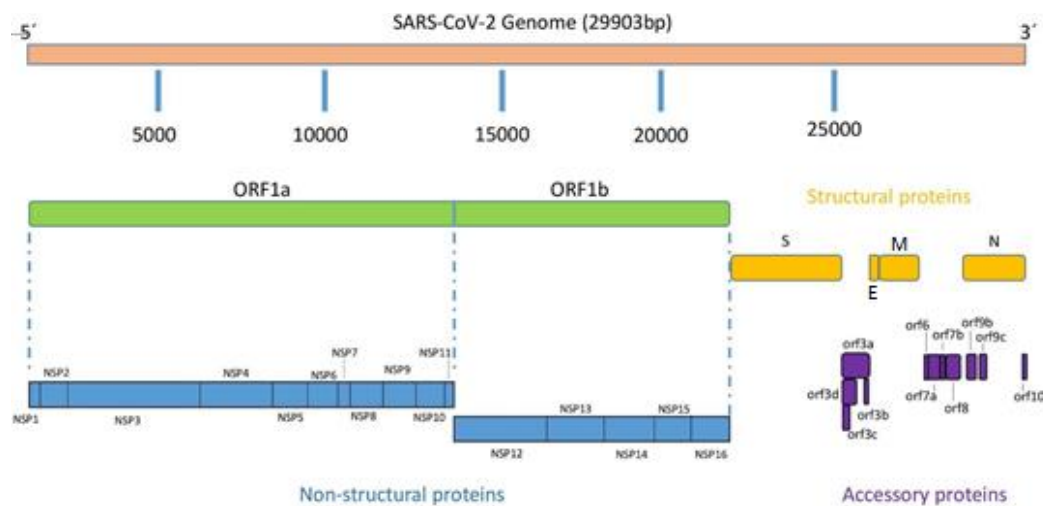


Figure 1.2. Genome organization of SARS-CoV-2 non-structural, structural and accessory proteins. (Adapted from Redondo, Zaldivar-Lopez, Garrido & Montoya, 2021)

1.1.3 Nonstructural and accessory proteins of SARS-CoV-2

Understanding the role of nonstructural and accessory proteins may be essential to prevent pathogenesis of the SARS-CoV-2 infection.

Although the functions of the ORF3c, ORF3d and ORF7b accessory proteins are unknown, ORF3a, ORF8 and ORF9c are suggested as highly pathogenic accessory proteins. On the one hand, the largest accessory protein ORF3a, which is found in the internal membrane of the virus, acts as an ion channel and leads to NLRP3 inflammasome activation and IL-1 β secretion (K. L. Siu et al., 2019). Moreover, it causes activation of apoptotic pathways by initiating cytochrome c release and caspase-9 activation (Ren et al., 2020). On the other hand, ORF8 not only interferes with surface expression of the MHC Class I molecules in order to prevent antigen presentation but also intercedes by activating IL-17 pathway during infection, eventually leading to a cytokine storm (Lin et al., 2021; Zhang et al., n.d.).

Moreover, while ORF10 doesn't have a role in viral replication, transmission or SARS-CoV-2 infection pathways, ORF3b, ORF6, ORF7a and ORF9b are able to interfere with IFN activation pathways ((Redondo et al., 2021) and the references therein).

Nonstructural proteins (nsps) are highly conserved among in coronaviruses. They have a wide range of roles in the replication machinery and are formed as a result of proteolytic cleavage of the two polyproteins (pp1a and pp1ab) encoded by ORF1a/b (Rohaim et al., 2021). Their functions are summarized in Table 1.1 (Y. Chen et al., 2020; M. Li et al., 2021; Snijder et al., 2016; M. Y. Wang et al., 2020; Yadav et al., 2021; H. Yang & Rao, 2021).

Table 1.1. Functions of the SARS-CoV-2 nonstructural proteins.

Proteins	Functions
nsp1	degrade host mRNA and harbor replication complex to membrane
nsp2	arrest host cell functions, initiate apoptosis
nsp3	role in viral replication, cleave full pp1a/b, initiate ER rearrangement
nsp4	initiate ER rearrangement, harbor replication complex to membrane
nsp5	cleavage of full pp1a/b & maturation of nsps
nsp6	initiate ER rearrangement, vesicle formation, IFN antagonist
nsp7	Have role in RNA-dependent RNA polymerase complex
nsp8	Have role in RNA-dependent RNA polymerase complex
nsp9	RNA production & processing
nsp10	Modification & proof-reading of viral RNA
nsp11	Unknown
nsp12	Have role in RNA-dependent RNA polymerase complex
nsp13	Part of replication-transcription complex (RTC)
nsp14	Proof-reading and capping of viral RNA
nsp15	Unclear role in viral replication & processing, interferon antagonist
nsp16	Modification of 5'cap & proof-reading of viral RNA

1.1.4 Structural proteins of SARS-CoV-2

Size of the SARS-CoV-2 virion ranges between 60 to 140 nm in diameter, which is structurally formed from the Membrane (M), Nucleocapsid (N), Envelope (E) and Spike (S) proteins (N. Zhu et al., 2020). The lipid bilayer, that is derived from host cells, surrounds the nucleocapsid encircling viral RNA. Membrane glycoproteins and envelope proteins are embedded in this lipid bilayer (Kumar et al., 2020). Additionally, Spike glycoproteins are found on the surface and mediate host cell invasion, so undoubtedly it has a pivotal role for SARS-CoV-2 infection. (Figure 1.3)

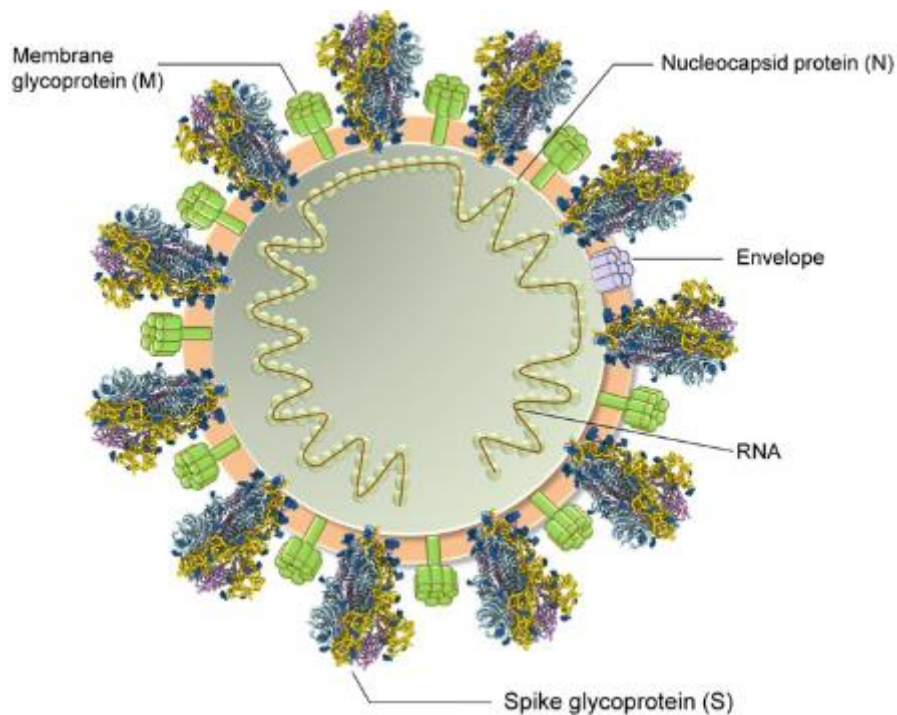


Figure 1.3. Model of SARS-CoV-2 virion structure with an emphasis on four structural proteins (S, M, E, N) (Adapted from (Kumar, Nyodu, Maurya et al. 2020).

1.1.4.1 Spike Glycoprotein

The spike glycoprotein is a trimeric fusion glycoprotein consisting of monomers of 180-200 kDa in size. Spike form a crown-like structure on the virion surface and are camouflaged by polysaccharides to escape from immune surveillance (Huang et al., 2020). Each spike protein is composed of S1 and S2 subunits (Hatmal et al., 2020). While the S1 subunit has a signal peptide, an extracellular N-terminal domain, a receptor binding domain (RBD), the S2 subunit consists of heptad repeats (HR1/2), a fusion peptide (FP), transmembrane (TM) and cytoplasmic (CT) domains (Mariano et al., 2020)(Figure 1.4). The RBD is located outwards and provides interaction with the host receptor, ACE2 (angiotensin converting enzyme 2) thereby facilitating viral entry into host cells. Thus, the S1 subunit provides cell attachment, whilst the S2 subunit enables fusion of the virus.

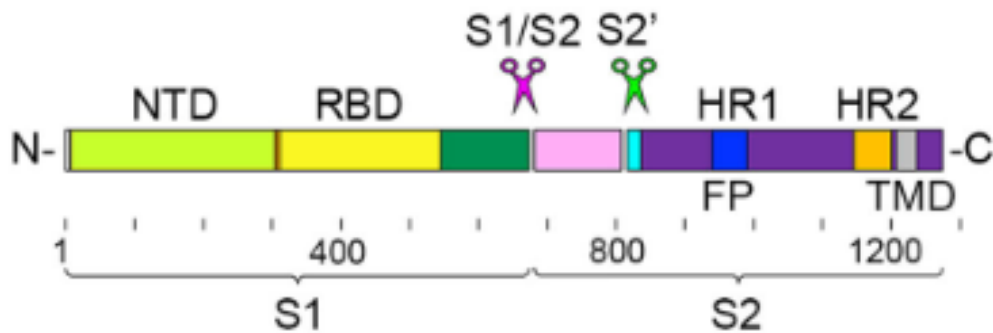


Figure 1.4. SARS-CoV-2- Spike protein structural domains and cleavage sites (Adapted from Takeda, 2021).

The S1 subunit is separated from S2 at the furin cleavage site (PRRARS'V), which provides a cleavage spot for host furin protease (Hoffmann et al., 2020). Moreover, this dissociation of the S1 subunit mediates priming of the Spike protein by host serine protease, TMPRSS2 (transmembrane protease serine 2) (Iwata-Yoshikawa et al., 2019). This results in the conformational change of S2, as six helical bundles with the help of two heptad repeats, leading to close proximity between the target cell membrane and the virion (Huang et al., 2020). (Figure 1.4)

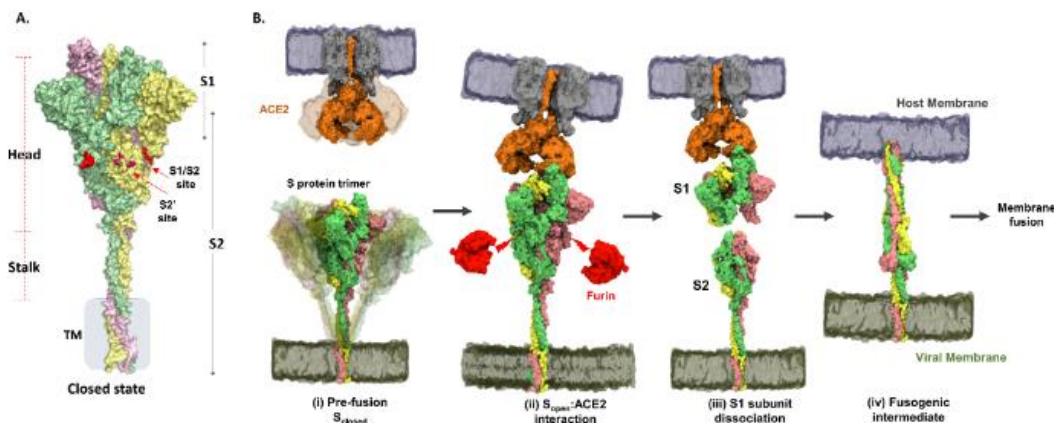


Figure 1.4. Model depicting the conformations of S1/S2 domains in pre-fusion and post-fusion forms of SARS-CoV-2 Spike protein during viral entry (Adapted from Raghuvamsi, Tulsian, Samsudin, Qian et al., 2021)

1.1.4.2 Nucleocapsid protein (N) of SARS-CoV-2

The Nucleocapsid protein is an abundantly expressed protein in host cells during the early stages of infection. The N terminal domain (NTD) and a C terminal domain (CTD) are linked together through highly phosphorylated serine rich linker region which is involved in regulation and self-association of the protein((Bai et al., 2021) and the references therein). The main role of the N protein is encapsulation of the viral genome. While NTD binds to the viral genome, the CTD mediates not only nucleocapsid formation but also enhances the interaction between the viral genome and the NTD region (Satarker & Nampoothiri, 2020). Moreover, Nucleocapsid binding to viral RNA prevents viral genome aggregation and host immune recognition (Bai et al., 2021). Indeed, after Spike glycoprotein, the N protein is another critical element in SARS-CoV-2 assembly.

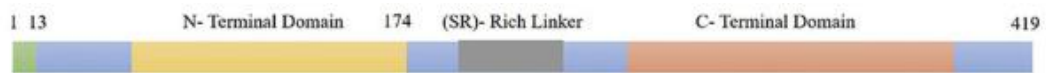


Figure 1.5. SARS-CoV-2 Nucleocapsid protein encoding gene (Adapted from Satarker & Nampoothiri, 2020).

1.1.4.3 Membrane (M) and Envelope (E) Proteins of SARS-CoV-2

Compared to spike and nucleocapsid, the Membrane and Envelope structural proteins of SARS-CoV-2 were found to be highly conserved among variants throughout the pandemic (Troyano-Hernández et al., 2021). Both are essential components for viral assembly and budding. Studies suggest that M and E co-expression is indispensable for virion and Virus Like Particle (VLP) production (Schoeman & Fielding, 2019).

The Envelope protein is the smallest protein of SARS-CoV-2 with a size of 8-12 kDa, and it is an integral membrane protein (Satarker & Nampoothiri, 2020). Through Golgi targeted elements in its N terminus, it directs the assembly and release

of virion structure through membrane scission in the ERGIC (ER-Golgi Intermediate Compartment) (Alsaadi & Jones, 2019).

Notably, membrane proteins are abundantly found in the viral membrane, and interact with all other structural proteins as a major organizer of the SARS-CoV-2 assembly (Bianchi et al., 2020). This N-linked glycosylated protein interacts with Spike to provide Spike incorporation to the virion as well as with Nucleocapsid to stabilize genomic information into the virion and Envelope for the release of the virion. Noteworthy, their interaction through ERGIC pathways and Spike retention, provided by expression of M & E proteins, is substantial for fully equipped virion formation and its secretion (Boson et al., 2021).

1.2 COVID-19 Disease

Coronavirus disease 2019 (COVID-19) is a respiratory disease resulting from SARS-CoV-2 infection and causes mild to severe symptoms. Like SARS-CoV, the virus infects humans through the human angiotensin converting enzyme (hACE2), mainly found on epithelial cells in the respiratory tract (Lebeau et al., 2020). High replication capacity of the virus results in invasion of upper airway and alveolar epithelial cells in the lungs. This mediates a strong immune response leading to cytokine storm, followed by acute respiratory distress syndrome and alveolar damage. Therefore, severe cases with respiratory failure require ventilation supply in intensive care units. However, older patients with these symptoms or individuals with specific chronic diseases have a risk of developing multi-organ and heart failure, eventually causing death. On the other hand, younger people develop milder symptoms such as fatigue, cough, chest pain, loss of smell and taste. Moreover, one third of infected people recover from the disease without any symptoms. Even though there are no symptoms, all infected individuals spread the virus through liquid droplets due to the increased viral load ((Allegra et al., 2020; Sah et al., n.d.; Satarker & Nampoothiri, 2020; Tangid et al., 2020) and references therein).

1.2.1 SARS-CoV-2 Entry and Replication of the Virus

Internalization of the virus is initiated right after the interaction between the receptor binding domain of viral Spike proteins and ACE2 receptors of the host cells (Figure 1.4). Viral fusion is initiated with Spike proteins' cleavage by TMPRSS2, which is followed by HR1- HR2 interaction-mediated conformational change to the post-fusion state (C. Yang et al., 2021). This conformational change eventually leads to virus entry, and to the release of the viral genome into the cytoplasm (V'kovski et al., 2021). As a result of evasion of host cell translation machinery and synthesis of nonstructural proteins that have a role in viral polymerase machinery (Table 1.1), viral genome replication is carried out through RNA dependent RNA polymerase, while translation of subgenomicRNAs perpetuate (Lebeau et al., 2020). The newly synthesized viral genome and structural proteins of the virus are assembled through the ER-Golgi intermediate compartment (ERGIC) and released as a virion by exocytosis (Bourgonje et al., 2020) (Figure 1.6).

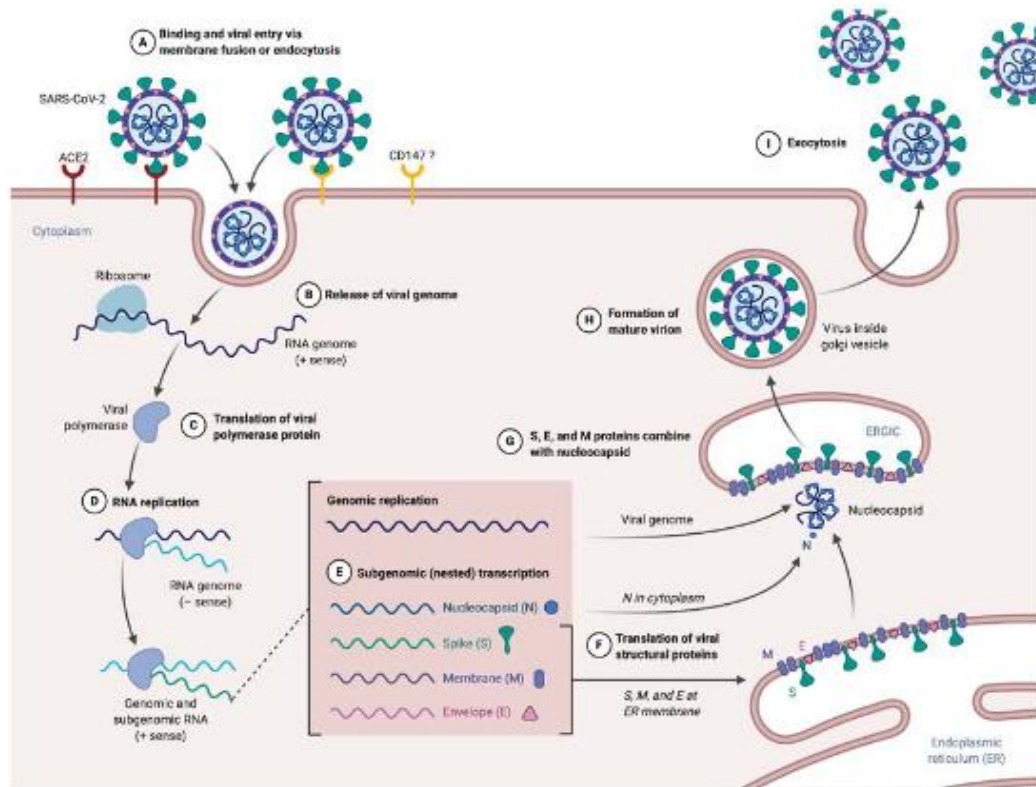


Figure 1.6. SARS-CoV-2 entry into target cell and virion exocytosis after viral genome processing (Adapted from Lebeau, Vagner, Frumence & Gasque, 2020).

1.2.2 Immune Response to COVID-19 disease

Initially, rapid responses to the pathogen and its toxin are generated by innate immune mechanisms with the help of host effector cells. These cells express pattern recognition receptors that can identify evolutionarily conserved molecular patterns of invading pathogens, which are normally not found in the host. In case the innate immune system is unable to eliminate the pathogen, the adaptive immune system is activated. T and B lymphocytes, effector cells of the adaptive immune response, harbor antigen-specific receptors, that are generated by random reshuffling of germ-line gene elements (Medzhitov & Janeway, 1997; Murphy et al., n.d.). This arbitrarily generated repertoire is complemented with clonal expansion of T and B

cells, leading to highly-specific cell-mediated and humoral immune responses through the recognition of target antigens (Murphy et al., n.d.). Furthermore, the adaptive immune system is able to generate memory T and B cells, providing accelerated clearance of the pathogen upon re-exposure. Ultimately, adaptive and innate immune mechanisms in synch, create a synergistic and effective host defense, albeit their distinct features from each other (Chaplin, 2010).

Although both innate and adaptive immune cells fight against infection, in severe COVID-19 cases, dysregulated immune responses with increased inflammation and excessive cytokine production is observed. While cytokine production provides an antiviral immune response, overproduction of proinflammatory cytokines causes septic shock and increases immunopathogenicity of the disease (Bourgonje et al., 2020). Herein, both innate and adaptive immune responses in COVID-19 will be briefly mentioned.

1.2.2.1 Innate Immunity to SARS-CoV-2

When a pathogen infects the host, an immediate response is initiated by the innate immunity through signaling cascades that are activated upon stimulation of pattern recognition receptors (PRRs). SARS-CoV-2 viral RNAs are recognized by either endosomal (TLR3, TLR7) or cytosolic (RIG-1) receptors as pathogen associated molecular patterns (PAMPs), which initiate an antiviral immune response through NF- κ B and IRF3 pathways, leading to induction of type I/III interferons and proinflammatory cytokines/ chemokines (Prompetchara et al., 2020). The initial innate immune response is generated by alveolar macrophages and monocytes. Parallel to leukocyte recruitment to the alveolar microenvironment, substantial levels of proinflammatory cytokines/chemokines (IL-6, IL-8, IL-1 β , CXCL10, TNF- α) and interferons are produced (Channappanavar & Perlman, 2017). However, in mild cases, cytokine secretion is progressively decreased with the clearance of infection, whilst continuous overproduction and cytokine storm are observed in severe cases

(Lebeau et al., 2020). This kind of cytokine response in severe cases creates a positive feedback loop for further infiltration of leukocytes, contributing to disease severity. For example, IL-8 and IL-17 overproduction causes attraction and activation of numerous neutrophils that are capable of inducing excessive NET (neutrophil extracellular traps) formation, followed by apoptotic cell death and tissue damage in alveoli, eventually causing respiratory failure (Paludan & Mogensen, 2022).

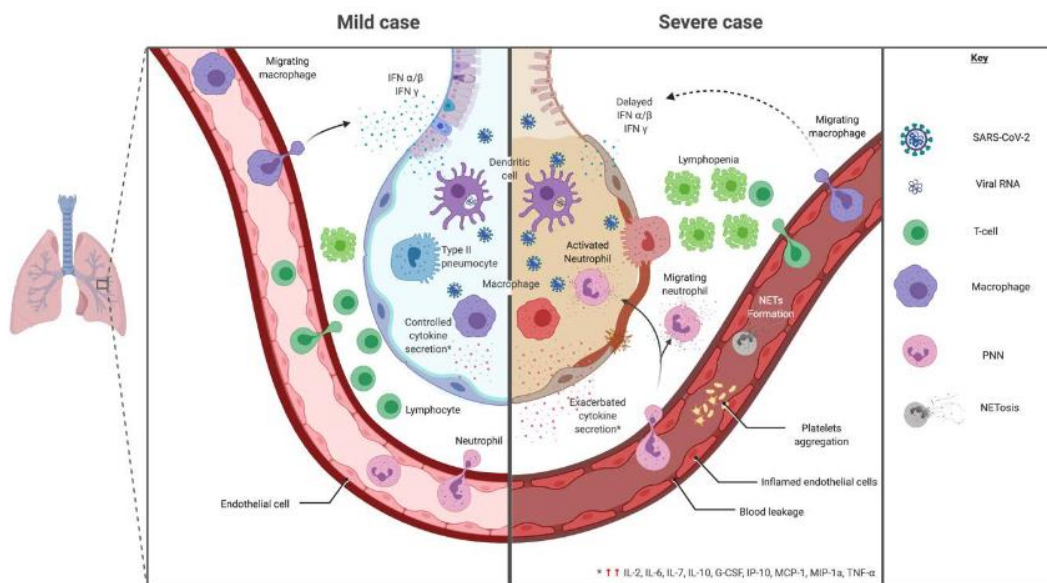


Figure 1.7. Immune response in alveoli against SARS-CoV-2 infection during mild and severe cases (Lebeau, Vagner, Frumence & Gasque, 2020).

1.2.2.2 Adaptive Immunity to SARS-CoV-2

Following the introduction of non-specific responses against infection or after vaccination, adaptive immune cells are primed and antigen-specific responses ensue through CD4⁺ T helper cells, CD8⁺ cytotoxic T cells and B cells. Even though the adaptive immune system responds 6-10 days after infection due to naïve cell proliferation and differentiation, it provides a strong and targeted response that not only eliminates viral infection but also prevents possible damage that can result from

re-infection through memory cell formation (Murphy et al., n.d.). During SARS-CoV-2 infection, it is suggested that adaptive immune responses have remarkable importance in the resolution of the infection due to the role of T cells on neutralizing antibody production. Therefore, the severity of the cases in elderly patients has been attributed to the reduced population of naïve T cells (Rydyznski Moderbacher et al., 2020). Notably, the depletion of lymphocytes, including CD4+ and CD8+ T cells, is predominantly observed in severe cases (Z. Chen & John Wherry, 2020).

After the proteasomal degradation of the viral proteins in antigen presenting cells (APCs), such as dendritic cells, the foreign peptides are presented to helper and cytotoxic T cells through MHC molecules. Clearance of the infected cells by cytotoxic T cells is initiated with viral antigen presentation on MHC Class I molecules and subsequently finalized through IFN- γ , perforin and granzymes A, B and K secretion by CD8+ T cells (Grifoni et al., 2020; Rydyznski Moderbacher et al., 2020). On the other hand, T helper cells have various roles during infection. Like cytotoxic T cells, they also have prominent roles in specific antiviral immune responses against SARS-CoV-2 infection through predominant differentiation to Type 1 T helper cells (Th1), which are capable of producing the cytokines IFN- γ , IL-2, TNF- α and thereby recruit other immune cells (Grifoni et al., 2020). At the same time, IL-22 secretion by CD4+ T cells suggests their involvement in lung tissue repair (Sette & Crotty, 2021). Furthermore, they enhance the immune responses of cytotoxic T cells and neutralizing antibody production (RBD IgG) by B cells, supporting long term humoral immunity (Grifoni et al., 2020; Sette et al., 2008; Sette & Crotty, 2021).

B cell maturation through recognition of mainly Spike and Nucleocapsid proteins of SARS-CoV-2 and presentation of their epitopes on MHC-II is followed by antibody production and plasma cell formation (Sette & Crotty, 2021; Weiskopf et al., 2020). Then, the antigen-MHC-II complex is recognized by T helper cells together with co-stimulation, this interaction triggers B cell activation and proliferation of effector B cells. While some of these activated B cells differentiate into memory B cells, others

become plasmablasts and long-lived plasma cells and release antibodies that are capable of recognizing the antigens to prevent further infection and/or re-infection.

Circulating antibodies against the RBD of the Spike protein are detected 10-15 days later and peak at 24-59 days post-infection or vaccination (K. Wang et al., 2021). These antibodies are essential in virus neutralization by blocking cell entry and interfering with ACE2 receptor binding, and therefore are named as neutralizing antibodies (NAbs) (Shi et al., 2020). While the titer of the neutralizing antibodies varies in individuals, vaccine-induced neutralizing antibody levels are inversely correlated with the severity of infection (Chmielewska et al., 2021). Consequently, NAbs are hypothesized as key adaptive immunity mediators for viral clearance and protection from infection. Therefore, vaccine-elicited neutralizing antibody levels are assumed as gold standard for the determination of vaccine efficacy (F. Wu, Wang, et al., 2020).

1.3 Vaccine platforms against SARS-CoV-2

With the high transmissibility rate and increasing deaths, effective vaccine formulations for controlling the pandemic became urgent. Protective immune responses are achieved with vaccines formulated with specific antigen targeting and immune stimulatory adjuvants. Adjuvants provide danger signal to dendritic cells supporting DC activation and causing antigen uptake and its presentation to T cells (both CD4+ & CD8+). As a result of CD4+ T cell activation, B cell development and proliferation is promoted, which is followed by antibody production. These antibodies specifically recognize the formulated antigens that are administered within the vaccine. Even though underlying protective mechanisms are suggested to be centralized around increased neutralizing antibody production through vaccination, whole immune responses are also shaped with memory B and CD8+ T cells (Figure 1.8) (Murphy et al., n.d.; Pollard & Bijker, 2021).

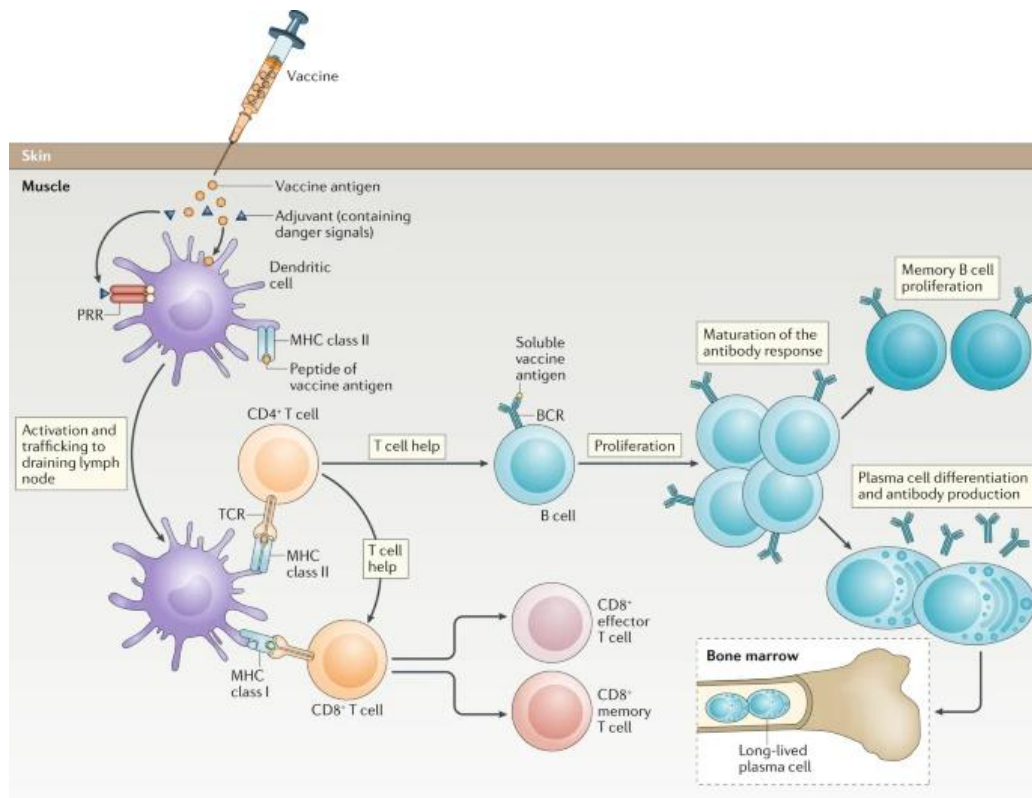


Figure 1.8. The underlying mechanism of immunization through vaccination (Adapted from (Pollard & Bijker, 2021)).

While most vaccine candidates against SARS-CoV-2 are inspired from the antigenicity of Spike protein and its RBD region which provide neutralizing antibody and T cell responses in patients, there are vaccine candidates that contain other structural, nonstructural and/or accessory protein antigens due to their role in directing CD4⁺ T cell and CD8⁺ T cell responses (Grifoni et al., 2020; Ni et al., 2020a; J. Yang et al., 2020).

In the following sections, vaccine platforms based on inactivated virus, protein subunits, virus like particle (VLP), nucleic acid, adenoviral vector, will be briefly mentioned.

1.3.1 mRNA based vaccines

mRNA vaccines represent one of the most technologically advanced and innovative vaccine development platforms. Spike protein encoding synthetic mRNA strands are encapsulated in lipid nanoparticles, which can be taken into cells through endocytosis and provoke anti-viral responses (M. Y. Wang et al., 2020). After providing mRNA access into the recipient cell cytoplasm, translation of the encoding protein is initiated. Vaccine candidates of Moderna (mRNA-1273) and BioNTech (BNT162b1& BNT162b2) utilize this technology (Walsh et al., 2020). The BNT162b1 mRNA vaccine was designed to produce the RBD domain of Spike protein in the recipient cells as antigen. Efficacy of the vaccine is dependent on high level neutralizing antibody production against RBD, since neutralizing antibodies in the sera of the recipient prevent viral entry as well as replication (J. Yang et al., 2020). On the other hand, BNT162b2 and mRNA-1273 vaccines encode for the prefusion stabilized Spike protein for eliciting neutralizing antibody response. Both mRNA platforms' clinical trials suggest that high efficacy is provided through significant neutralizing levels and a Th1-skewed response with reduced re-infection and symptoms against the authentic virus (Baden et al., 2021; Polack et al., 2020).

1.3.2 DNA vaccines

DNA vaccine strategies are based on inserting the genes of target proteins into plasmid DNA. These plasmid DNAs have also mammalian promoters which drive the expression of the genes in the recipient cells. However, this strategy needs a successful delivery system to provide access of the gene into the recipient nucleus and facilitate antigen expression without being subject to DNase degradation (Kyriakidis et al., 2021). Inovio Pharmaceuticals and Zydus Cadila are producers of the INO-4800 and ZyCoV-D, respectively. They develop Spike DNA based vaccines and are working on electroporation-based delivery route through the use of patented devices (Andrade et al., 2021; Dey et al., 2021). However, since DNA based vaccines

possess genotoxicity risks due to their potential of genome integration, they are seen as an alternative to other vaccines in low-income countries.

1.3.3 Inactivated vaccines

The most traditional method in vaccine development is by inactivating the virus. This strategy is based on creating a non-infectious form of the authentic virus through chemical and physical methods, so the platform necessitates Biosafety level 3 laboratories (Dong et al., 2020). It provides a wide range of antigenic content to the immune system as it contains multiple proteins of the virus similar to the original virus. However, there is the possibility of unsuccessful induction of immune responses after the inactivation step (Kyriakidis et al., 2021). Sinovac's CoronaVac, with its favorable immunogenicity is one of the most widely used vaccines in the world including in our country (Zhang & Zeng, 2020).

1.3.4 Vector Based vaccines

This strategy is mainly based on carrying the target genes by using replication deficient viruses and harnessing their infection capacity. In addition, replication competent counterparts are also available, but were not preferred during the COVID-19 pandemic because of their safety issues (WHO, 2022).

This platform, generally use adenoviruses or pox viruses. Paradoxically, this type of vaccine immunogenicity is higher due to the viral carrier, but accuracy in targeting is lower because of the heterogeneity in antigenic content ((Dong et al., 2020) and the references therein). During the Covid-19 pandemic, CanSino (Ad5-nCoV), Johnson& Johnson (JNJ-78436735/Ad26.COV) and Oxford University/AstraZeneca vaccine (AZD1222) candidates concentrated on the development of a codon optimized full-length Spike gene of SARS-CoV-2 carried by adenoviruses from different serotypes (Kyriakidis et al., 2021). While Phase1/2 clinical trials of the

CanSino vaccine indicated low levels of neutralizing antibody production because of pre-existing immunity against the carrier adenoviruses (F. C. Zhu et al., 2020), clinical trials of AstraZeneca and Johnson & Johnson resulted in efficient protection with sufficient neutralizing antibody titers and T cell responses (Logunov et al., 2021; Voysey et al., 2021). However, phase 3 clinical trials of both Ad26.COV and AZD1222 were canceled due to severe adverse effects in some volunteers, but then the studies resumed because of tolerability in the majority of volunteers (Logunov et al., 2021).

1.3.5 Protein Based Vaccines

In this platform, viral proteins are produced by using expression systems such as insect, yeast, bacterial, mammalian or plant cells (Dai et al., 2018). Then, secreted and purified antigens are formulated with appropriate adjuvants that activate the immune system. There are plenty of vaccine platforms using recombinant Spike protein, RBD region of the Spike protein or all structural proteins by forming Virus Like Particle (VLP) (WHO, 2022).

Novavax (NVX-CoV2373) is one example of the subunit vaccine employing prefusion stabilized Spike protein expressed using the baculovirus-Sf9 system. Phase1/2 clinical trials revealed high neutralizing antibody eliciting capacity with a Th1 skewed T cell response and mild side effects (Keech et al., 2020).

Immunity against the whole virus is only partially provided in previously mentioned platforms including subunit vaccines, except for the inactivated virus and VLP platforms. Similar to the inactivated virus platform, VLP based vaccines provide inclusive antigenic content and immunogenicity owing to their morphological homology with the authentic virus. However, VLP vaccines are more advantageous than the inactivated virus platform due to the absence of viral nucleic acids and lower toxicity (Nooraei et al., 2021). Moreover, it accomplishes strong T cell responses in addition to achieving high neutralizing antibody capacity. In combination with a

potent adjuvant, this vaccine strategy has the potential to induce an even more robust adaptive response than the one observed in Covid-19 convalescents (Ward et al., 2020).

1.4 Emergence of SARS-CoV-2 Variants of Concern

Through the rapid spread and circulation of SARS-CoV-2 across the world, evolution and accumulation of mutations in the viral genome has become inevitable. Therefore, we have come across with the emergence of new variants causing variations in transmissibility and severity of the infection, despite high immunization rates in developed countries.

B.1.1.7 (Alpha) and B.1.351 (Beta) variant emergence in the UK and South Africa, on December 2020 was followed by the emergence of P.1 (Gamma) and B.1.617.2 (Delta) lineages in Brazil and India, which were recognized as Variants of Concern (VOC) by US Centers for Disease Control and Prevention (Tao et al., 2021). This classification is based on elevated competence in transmissibility and severity of variants with respect to pre-existing variants. Nonetheless, immune evasion is observed in this group of variants due to mutations at the receptor binding domain (RBD) of the Spike protein, causing irresponsiveness to neutralizing antibodies that were generated by vaccination or infection. Therefore, mutations in the Spike protein are under high consideration (Figure 1.9).

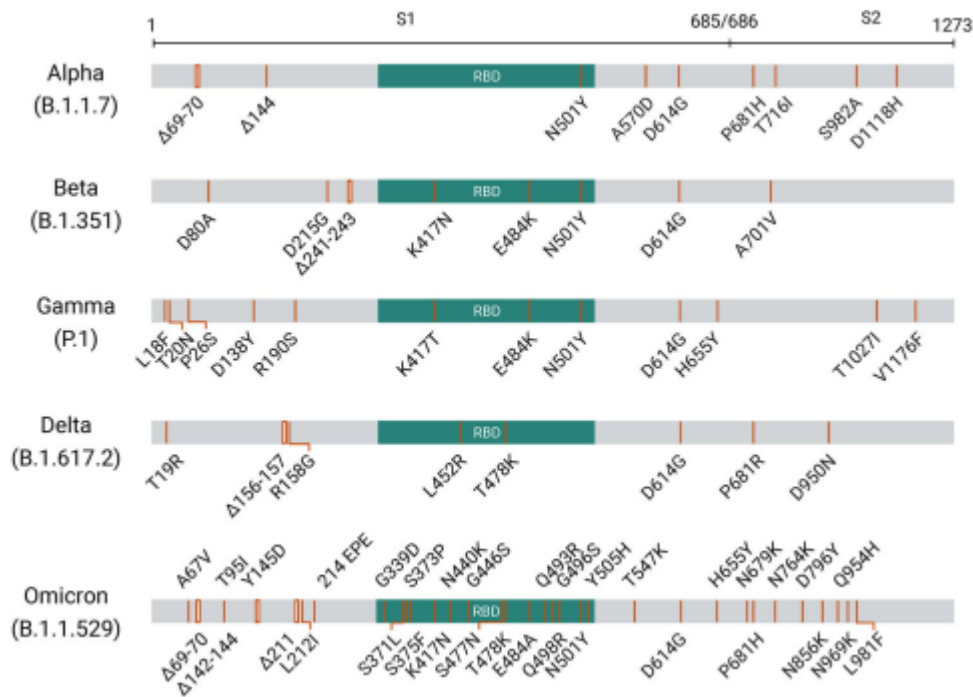


Figure 1.9. Spike protein Mutations in Emerging SARS-CoV-2 Variants of Concern (Adapted from He X., Hong W., Pan X., Lu G. & Wei X., 2021).

The B.1.1.7 variant contains mutations in most of the viral proteins including Spike. Near the occupation of the missense mutations in the Spike protein, the N501Y and D614G substitutions at the receptor binding domain were under high consideration since they led to enhanced interactions between RBD and the ACE2 receptor on host cells. Furthermore, these mutations augmented viral replication ability and increased Spike expression on the virus, resulting in elevation of infectivity and transmission (Santos & Passos, n.d.; Tao et al., 2021). 50% more mortality and transmissibility than pre-existing lineages was observed with the emergence of the B.1.1.7 variant (Volz, Mishra, et al., 2021). Furthermore, B.1.351 and P.1 variants share the K417N, E484K, N501Y mutations in RBD, with five Spike N terminal domain mutations (Garcia-Beltran et al., 2021). These three RBD mutations, together with the dominant role of the E484K mutation, result in 48% reduced susceptibility to neutralizing antibodies in these variants (Abdool Karim & de Oliveira, 2021).

Substantial reduction in vaccine efficacy and increased mortality were assessed with these variants (Abu-Raddad et al., 2021).

On a different note, the B.1.617.2 variant has emerged with the D614G and the following specific mutations: L452R, T478K at RBD and P681R at the furin cleavage site, causing enhanced fusion of the virus through easier S1/S2 cleavage (Saito et al., n.d.). It displaced the dominance of other variants resulting from L452R substitution which significantly raised its transmissibility, reduced neutralizing efficacy and thereby fostered pathogenicity (Deng et al., 2021; Hester Allen et al., n.d.). Then, the B.1.617.2.1 (Delta plus) sub-lineage emerged with a K417N substitution in Spike, near the mutations identified in the B.1.617.2 variant, causing binding affinity augmentation to the ACE2 receptor (Mullen et al., 2022).

Recently, a new variant B.1.1.529 (Omicron) was detected on November 26 with the highest number of mutations in the whole genome including fifteen mutations on RBD; G339D, S371L, S373P, S375F, K417N, N440K, G446S, S477N, T478K, E484A, Q493R, G496S, Q498R, N501Y, Y505H, and P681H at the furin cleavage site (Cele et al., n.d.). It rapidly became dominant worldwide with the shortest case doubling time when compared to other characterized variants so far, which is 1.2 days, and therefore was categorized as a VOC (He et al., 2021). Even though, the importance of the mutations, pathogenicity and its neutralizing antibody escape level of this variant are still under investigation, overlapping mutations with other variants in VOC suggests boosted pathogenicity and immune evasion (Cele et al., n.d.; Wilhelm et al., n.d.).

Only partial protection to reinfection against novel variants among vaccinated people with other authorized vaccines points out the necessity of vaccines that can elicit broad and/or variant specific neutralizing activity.

1.5 Aim of the Study

Several variants and lineages with a wide range of mutations has emerged since the beginning of the pandemic. However, due to significant changes in virulence, some variants were grouped as Variants of Concern (VOC) after December 2020. While there are lots of missense mutations, several mutations on the Spike gene in VOC directly affected the course of the pandemic. Increased immune evasion and decreased efficacy of vaccines over VOC, determined as a result of neutralizing antibody irresponsiveness, necessitates the development of variant specific vaccines. In this study, we aimed to utilize Virus Like Particle (VLP) based antigen production for the B.1.1.7 and B.1.617.2.1 variants in order to eliminate immune evasion and provide higher protection. In this context, we cloned variant specific Spike proteins and the Envelope (E) gene into pViro2 expression vector. To achieve VLP production, we also cloned the genes encoding the Membrane (M) and Nucleocapsid (N) structural proteins into the pViro1 vector. Following to transfection of the expressing vectors to the Hek293 suspension cells, purification of secreted VLPs, characterization of the purified products, DNA and protein contents were determined in preclinical stage of the study. The VLP products were adjuvanted with a K type CpG ODN and Alhydrogel for clinical trials. Finally, neutralizing antibody levels of vaccinated volunteers were analyzed through pseudotyped virus neutralization assay.

CHAPTER 2

MATERIALS & METHODS

2.1 Materials

2.1.1 HEK293 Suspension Cell line and HEK293-FT-hACE 2 Adherent Cell line

Hek293 human embryonic kidney cells which were adapted to suspension culture was purchased from Florabio (İzmir, Turkey). This cell line was used in order to produce Virus Like Particles, since these cells were optimized to achieve high growth rate and production performance in the transfection medium employed in this thesis.

Hek293FT-hACE 2 adherent cells, selected using 1 mg/ml final concentration of puromycin, were donated by Tolga Sütü (Bogazici University, Turkey). The cells stably overexpress human angiotensin I converting enzyme 2 (ACE2), through transduction with LeGo-ACE2-iT2puro vector. This cell line was used for pseudovirus neutralization assays, allowing us to determine SARS-CoV-2-Spike protein specific neutralizing antibody titers in tested human and mice serum samples.

2.1.2 Cell Culture Media, Buffers and Solutions

Serum/animal protein free growth and transfection medium for HEK293 suspension cells (Orchid293 CD Transfection Medium) was purchased from Florabio, İzmir, Turkey. The medium was supplemented with 400 mg L-glutamine per liter (Sigma,

Canada). Suspension cells were cultured under 8% CO₂ at 37°C in shake flasks by shaking at 130 rpm reciprocally.

For transfection of plasmids, PEIpro transfection reagent (PolyPlus, France) was used.

Hek293FT-hACE 2 adherent cells were cultured in Dulbecco's modified essential medium (DMEM) (Biological Industries, BI, Cromwell, USA) supplemented with 2.5% HEPES buffer, 1% non-essential amino acids, 10% Fetal Bovine Serum, 1% sodium pyruvate, 1% penicillin and streptomycin (BI, Cromwell, USA), 1mg/ml puromycin (Sigma-Aldrich, USA) for continuity of selection, and they were incubated at 37°C with 5% CO₂ in T75 flasks (Sarstedt, Germany). Cells were passaged every 3 days by diluting 1 ml of 3x 10⁶ cells in 12 ml of fresh medium.

Molecular biology & cell culture grade water and phosphate buffer saline were purchased from Biological Industries (Israel).

2.1.3 Bacteria Strain and Bacterial Culture Media

NEB Stable *E.coli* competent cells were used in this study (New England Biolabs, UK). They were cultured in Low Salt LB medium, composed of Tryptone (Sigma Aldrich, USA), Yeast Extract (Serva, Germany), NaCl (Isolab, Germany), or in Low Salt LB Agar plates which additionally contained 1% Agar (Merck, Germany).

For antibiotic selection after transformation of plasmid constructs, Hygromycin B Gold (Invivogen, CA, USA) was added into media at a working concentration of 100 µg/ml.

2.1.4 Plasmids, Enzymes and Related Reagents

pVitro1-hygro-mcs and pVitro2-hygro-mcs dual mammalian expression plasmids (Invivogen, France) were used in cloning and expression of SARS-CoV-2 structural

proteins. Both plasmids contain two different promoter sites which enabled us to express S, M, E and N genes in mammalian cells. Since we harnessed BamHI, BglII cut sites that are found in multiple cloning sites of both plasmids, we used High Fidelity-BamHI and BglII restriction enzymes (NEB, UK). Moreover, ScaI, HF-HindIII and ApaLI restriction enzymes (NEB, UK) were also used in order to confirm cloning directions of genes. In order to achieve high activity of the restriction enzymes, CutSmart or NEB3.1 Buffers (Massachusetts, USA) were used during digestion. T4 DNA Ligase and its buffer, which were used in the ligation process, were purchased from NEB, UK.

pcDNA 3.1(+) eGFP (Addgene, USA) green fluorescent expressing plasmid was used to track PEIpro mediated transfection of the HEK293ft suspension cells.

LeGO-G2 (GFP), pMDLg/pRRE and pRSV-Rev, pCMV-Spike Δ 19(D614G) plasmids, which were used for pseudovirus production, were gifts from Tolga Sütü (Bogazici University, Turkey).

NucleoSpin Plasmid, Mini kit was used for plasmid DNA isolation from pelleted bacteria, and NucleoSpin Gel & PCR Clean-up, Mini kit was used for extraction of plasmids from the gel (Macherey- Nagel, Düren, Nordrhein-Westfalen). BioDrop (Biochrom, UK) was used for the quantitation of DNA.

Agarose powder was obtained from Sigma, USA. Molecular Biology Grade 10X Tris-Acetate-EDTA (TAE) buffer and Tween 20 detergent were purchased from Thermo Fisher Scientific (USA). 10 mg/ml ethidium bromide (Invitrogen, CA, USA) was added into 1%(w/v) agarose-1X TAE buffer mix. 6X Gel Loading dye, Purple and 1kb DNA Ladder were bought from NEB, UK.

2.1.5 Solutions and tools of VLP purification

Microfiltration was performed with 0.22 μ m Filtropur S filters (Sarstedt, Germany), to remove remaining cells and other unwanted remnants after VLP harvest. In

addition, Denarase treatment was carried out using 200 U/ml Denarase (c-LEcta, Germany) for elimination of host cell-derived nucleic acids.

For purification of VLPs, fast protein liquid chromatography on a prepacked Hi-Screen Capto Core 400 column (Cytiva, USA) was conducted using the ÄKTA go (Cytiva, USA) technology.

Moreover, Sartocan® Slice 200 Hydrosart® 100kDA and stainless-steel holder, Sartocan Slice 200 Holder, were acquired from Sartorius Stedim Biotech GmbH, Germany for ultrafiltration and diafiltration of the VLP containing samples collected from the Capto Core flow through.

2-propanol and ethanol with a concentration of $\geq 95\%$ (Sigma, USA) and DPBS (Biological Industries, USA) were used during cleaning steps of Capto Core and Sartocan slices.

2.1.6 Protein analyses tools for purified and concentrated VLP samples

2.1.6.1 Device and tools for Nanoparticle analyses

The measurement of VLP particle size was based on tunable resistive pulse sensing method using qNano Gold (IZON S/N 601A) device (Izon Science LTD, New Zealand), along with coating solution (IZON Training Kit, TK5-091), nanopores (NP80, NP100, NP150) and calibration particles (CPC100, IZON Reagent Kit, RK3-167).

2.1.6.2 Solutions, instruments and antibodies for SDS-PAGE & Western-blotting, Dot Blotting& micro BCA

4–20% Mini-PROTEAN TGX Stain-Free Precast polyacrylamide gels and Mini-PROTEAN® Tetra cell apparatus were from Bio-Rad,USA. Gels were

electrophoresed in 1:10 diluted 10X Tris/Tricine/SDS buffer, which was also obtained from Bio-Rad, USA. PageRuler Prestained 10 to 250 kDa Protein Ladder was bought from Thermo Scientific, Lithuania.

Transfer of the proteins from gel to nitrocellulose 0.25 μm or PVDF 0.2 μm transfer membrane (Thermo Scientific, USA) was executed in Transfer buffer composed of 10X Tris Glycine Buffer (Bio-Rad, USA), 100% methanol (Sigma, USA), ddH₂O at a ratio of 1:2:7, respectively. Equipment for wet transfer was Wet/Tank Blotting System (Bio-Rad, USA).

Bovine Serum Albumin (Roche, Switzerland) was dissolved in PBST, and used in blocking of the membrane. (Appendix B).

HRP-conjugated His-tag antibodies were used to detect C terminus histidine tagged Spike, Envelope and Membrane proteins. Moreover, Nucleocapsid primary antibodies were coupled with anti-mouse secondary antibodies for the detection of Nucleocapsid protein. The properties of antibodies used in immunoblotting are summarized in Table 2.1

Table 2.1. Antibodies used in western and dot blots.

Antibody	HRP-conjugation	Company	Dilution	Catalog #
His-tag	YES	CST, USA	1:10.000	2365S
Nucleocapsid primary	NO	ProSci, USA	1:1000	35-579
Anti-mouse IgG	YES	CST, USA	1:5000	7076S
Spike 1	NO	ProSci, USA	1:500	9083
Anti-rabbit IgG	YES	CST, USA	1:1500	7074S

ECL™ Prime HRP Reagent (Cytiva,USA) allowed us to reveal proteins with almost 1pg level sensitivity under Amersham Imager 600 device (Cytiva,USA) or Bio-Rad

Gel Doc XR+ Imager (Biorad, USA) through emitting signals with enzyme activation.

Pierce™ micro BCA protein assay kit (Thermo Fisher Scientific, USA) was used to quantify VLP protein amount.

2.1.7 DNA amount determination with Picogreen Assay

Host cell derived residual DNA in purified VLP samples was assessed by Quant-iT™ PicoGreen™ dsDNA Assay Kit (Thermo Fisher Scientific, USA). Kit contained all components that are needed: 20X TE buffer, Quant-iT™ PicoGreen® dsDNA reagent and Lambda DNA standard. Fluorescence readings were recorded on a SpectraMax iD5 multi-mode plate reader (Molecular Devices, USA).

2.1.8 Serums and reagents used in neutralization assay

Human serum samples were collected from the volunteers of Phase2 Clinical trial, and four the BALB/c mice sera were included in pseudovirus neutralization assay. For transduction of pseudovirus to mammalian cells, polybrene infection/transfection reagent was purchased from Merck Millipore, USA. Pseudovirus infection was visualized under FLoid™ Cell Imaging Station (Thermo Fisher Scientific, USA) and quantitated on a Novocyte flow cytometer.

2.2 Methods

2.2.1 Cloning of SARS-CoV-2 Spike, Membrane, Nucleocapsid and Envelope expressing plasmids

2.2.1.1 Sequences of the proteins & expressing vectors and cloning strategy

Human codon optimized versions of gene fragments of SARS-CoV-2 structural proteins, Spike (S), Envelope(E) (NCBI Refseq: YP_009724392.1), Membrane(M) (NCBI Refseq: YP_009724393.1) and Nucleocapsid(N) (NCBI Refseq: YP_009724397.2) tagged with 6Xhistidine at C terminus, were purchased from Integrated DNA Technologies, Inc. (California, USA). Two Spike variant genes were designed for Delta (B.1.617.2) and Alpha (B.1.1.7) variants of concern. For the Alpha variant, we designed the sequence according to two amino acid deletions at 69-70 of Wild Type (hexaprolin stable version) Spike gene, and N501Y & D614G amino acid substitutions. For the Delta variant, we designed the sequence with D614G, K417N, P681R, T19R, D950N, T478K, L452R, G142D, E156G amino acid substitutions and deletions of 157th and 158th amino acids (Appendix A). Also, Spike gene was separated with the addition of NheI restriction enzyme cut site and synthesized as two fragments (S1 and S2).

We utilized pVITRO1 dual expression vector for N and M proteins, and pVITRO2 dual expression vector for S and E in order to express the genes inside mammalian cells (Appendix A). Both vectors possess BamHI and BglII cut sites at their multiple cloning sites. Therefore, we added BamHI restriction sites to both ends of the Spike and Membrane gene sequences, and BglII restriction sites to both ends of the Envelope and Nucleocapsid gene sequences. Then, we cloned the Spike and Envelope genes into pVITRO2 vector under human ferritin heavy chain (hFerH) promoter and human ferritin light chain (hFerL) promoter, respectively. In addition,

Membrane and Nucleocapsid gene sequences were cloned in pVitro1 vector under rat elongation factor 1 alpha (rEF1) and mouse elongation factor 1 alpha (mEF1) promoters, respectively.

2.2.1.2 Transformation of the genes and ligated plasmids

Gene fragments (S,M,N,E) and/or ligation products which were expected to become pVitro1 M+N and pVitro2 hexapS+E were transformed into Neb Stable *E. Coli* competent cells for propagation and isolation of plasmid constructs. Competent cells were prepared by CaCl₂ method. After thawing of competent cells on ice, they were mixed with plasmid DNA in amounts of 100 pg-100 ng. Once the 30-minute incubation of plasmid-competent cell mixture on ice was completed, the heat shock procedure was introduced with an exact 1 minute incubation in a 42°C water bath, followed by incubation on ice for 3 minutes. Then, the mixture was diluted with 900 µl Low Salt Lb medium and incubated in an incubator at 37°C for 80 minutes or a shaker at 37°C for 1 hour. Following centrifugation at 3000 rpm for 10 minutes, the pellet was resuspended in 100 µl of low salt LB medium and 50-100 µl was spread on agar plates. The inoculated plates were incubated in an incubator at 37°C for 16-18 hours.

2.2.1.3 Plasmid DNA isolation

16-18 hours after the transformation, a single colony was selected and inoculated from the plates into 10 ml Low Salt LB medium supplemented with Hygromycin B Gold selection antibiotic. After 18-20 hours of incubation in a shaker at 37°C & 180 rpm, bacteria were pelleted and the plasmid DNA isolation was conducted using the NucleoSpin Plasmid, Mini kit (Macherey- Nagel, Düren, Nordrhein-Westfalen) according to the Manufacturer's instructions. Following purification, plasmid DNA concentration and purity were determined using Biodrop.

2.2.1.4 Restriction enzyme digestion, Gel elution and Ligation

In order to achieve successful ligation, digestion of gene fragments and vectors with suitable restriction enzymes is needed. In accordance with our design which is explained in section 2.2.1.1, BamHI and BglII restriction enzymes were used so that we could get cleaved DNA fragments and compatible ends in vectors. Restriction enzyme digestion was conducted with 1µg DNA, 1 µl restriction enzyme, 1X restriction enzyme buffer (CutSmart or Neb3.1) and completed to a final volume (20-30 ul) using molecular biology grade water. After vortexing and spinning down, the mixture was incubated at 37°C for 1 hour.

At the end of restriction enzyme digestion, loading dye was added into mixtures to achieve 1X final concentration. Then, all samples and the 1kb ladder were applied to the wells of an 1% agarose gel and electrophoresis was carried out at 120 Volt for 1 hour. Separated digested and undigested fragments were visualized under a UV transilluminator and extraction of digested plasmids at their expected band sizes (1100 bp for S1 fragment, 2800 bp for S2 fragment, 300 bp for Envelope, 700 bp for Membrane and 1200 bp for nucleocapsid) from the gel was conducted with the NucleoSpin Gel and PCR Clean-up, Mini kit (Macherey- Nagel, Düren, Nordrhein-Westfalen). Concentration and purity of the desired fragments were assessed using Biodrop and samples with an A260/A280 ratio of 1.7-2.0 were subjected to ligation.

Ligation volume of the fragments and vectors were calculated according to vector & insert fragment lengths and 1:3-vector:insert ratio using the Neb Ligation Calculator tool. Then, ligation mix was prepared by the addition of 1 µl T4 ligase and 1X T4 ligase buffer into calculated volumes of vector and insert, and total volume was completed with molecular biology grade water. Ligation was carried through incubation at room temperature for 2 hours. Then, the ligation product was transformed to competent NebStable *E.coli* cells. Single colonies, that grew under hygromycin B gold antibiotic selection, were considered to uptake ligation products

successfully and therefore were inoculated in low salt LB with 1:1000 hygromycin B gold. Next, plasmid isolation was performed.

2.2.1.5 Agarose Gel Electrophoresis and Next Generation Sequencing

For the separation of digested fragment from undigested ones and confirmation of the transformation and ligation, we performed agarose gel electrophoresis. 1% agarose gel was prepared by adding 1.4g agarose powder into 1X TAE (10X TAE is diluted with distilled water) and dissolving in microwave oven to achieve a homogeneous solution. After cooling the mixture, 5-6 μl Ethidium Bromide (10 $\mu\text{g}/\mu\text{l}$) (Invitrogen, CA, USA), the fluorescent dye that can detect DNA and RNA, was added. Maximum loading volume into wells was 30 μl , and the gel is conducted was electrophoresed on a runVIEW (Clever Scientific, UK) agarose gel electrophoresis system at 120 V for 1 hour in 1X TAE buffer. At the end of the running, bands were visualized under a UV transilluminator.

Further verification of the end products, which are expected to be pVITRO1 M+N, pVITRO2-Alpha- hexapS+E and pVITRO2-Delta- hexapS+E were performed by sending the plasmid constructs to Intergen for Next Generation Sequencing (Appendix A).

2.2.2 Transient Transfection of HEK293 Suspension Cells

HEK293 suspension adapted cell line was transiently transfected with cloned constructs with using the PEIpro transfection reagent (Polyplus, France). Transfection protocol was initiated when the cell density reached around $1.3 \times 10^6/\text{mL}$, which corresponds to the logarithmic growth phase. Cells were centrifuged at 100g for 5 minutes and resuspended in Orchid293 CD transfection medium, DNA and PEIpro were mixed at a ratio of 1 μg DNA: 2 μl transfection reagent according to the manufacturer's manual. The molar ratio of pVITRO2 hexapS+E (delta variant

or alpha variant) to pVITro1 M+N plasmids was optimized as 1.22:1.0. Based on this ratio, 1 µg plasmid DNA per 10⁶ cells was diluted in 5% of the final volume of Orchid293 CD TFM. PEIpro was also diluted in the same amount of Orchid293 CD TFM. Next, PEIpro-TFM mix was added onto DNA-TFM mix and the tube was vortexed, immediately. After completion of 15-minute complexation time for the PEIpro-DNA reagent, the mix was added onto cells dropwise. Then, the cells were left for 48h incubation with the transfection mixture at 37°C, 8% CO₂ and 130 rpm reciprocal shaking, at the end of incubation medium was replaced with fresh medium.

2.2.3 Virus Like Particle Purification

2.2.3.1 First clarification of harvest and removal of host cell-derived nucleic acids

After incubation of the cells in the transfection mixture for 96-120 hours, VLP harvest was initiated. Briefly, supernatant was collected, and residual cellular material was removed by a 10-minute centrifugation step at 500g. Supernatant was then filtered with a Filtropur S 0.22 µm microfilter (Sarstedt, Germany), for further clarification of the supernatant.

Next, 200 U/ml of Denarase (c-LEcta, Germany) was added onto the harvest, and incubated for 2 hours at 37°C in order to digest host cell-derived nucleic acids.

2.2.3.2 Fast Protein Liquid Chromatography System for VLP purification

ÄKTA go fast protein liquid chromatography (Cytiva, USA) technology was utilized using prepacked Hi-Screen Capto Core 400 column (Cytiva, USA) to obtain high purity VLPs at large operational volumes. Hi-Screen Capto Core 400 column was

preferred because of its dual functionality in a single resin: simultaneous size exclusion and ion-exchange chromatography. The column material excludes molecules larger than 400 kDa from entering the pores thanks to inactive shell part, while small impurities enter and bind the core with high efficiency. The approach is briefly summarized below:

Hi-Screen Capto Core 400 column was equilibrated with 5 column volumes of DPBS at a flow rate 1.2 ml/min, in line with the manufacturer's recommendation. As soon as equilibration was completed, sample was applied and the column flow through containing the VLP was collected. Following washing with 4-10 column volumes of DPBS. Bound impurities were eluted with 2M NaCl supplemented 50 mM HEPES buffer. These impurities are molecules smaller than 400 kDa that have entered the beads, such as, host cell proteins and nucleic acid fragments. Lastly, cleaning in place (CIP) procedure was carried out to regenerate the column. For this, the column was inverted and then incubated with 2 CV of 1M NaOH and 30% isopropanol for 30 minutes and then washed with 5 CV of distilled water at a 0.3 ml/min flow rate. Then, the column was in 20% ethanol until next use (Appendix B). All protein content measurements during the VLP purification steps were monitored using the A280 values of the collected fractions. (Detailed information in Emre Mert İpekoğlu MSc thesis.)

2.2.3.3 Tangential Flow Filtration of VLPs

Final purification step of the VLP product was based on Tangential Flow Filtration method. TFF not only further removes contaminants of lower molecular weight but also aids concentration and diafiltration of the product into DPBS. Sartocan® Slice 200 Hydrosart® 100kDA (Sartorius, Germany), a stabilized cellulose based membrane was chosen based on the GMP requirements of Food and Drug Administration for its non-fiber releasing feature.

The VLP samples purified through the Capto Core column were placed in the feed reservoir and pumped through the membrane. While VLPs return to the feed reservoir as retentate without passing through the membrane, smaller unwanted impurities pass through the membrane and are collected in a different flask (Figure 2.1)

During these steps, membrane pressure tracking is important for creating significant pressure for the continuity of the filtration which should not exceed the suggested limits. Therefore, we conducted all steps with a constant transmembrane pressure of 0.5 bars. During running, feed rate was as adjusted to 300 ml/min, and the feed pressure was kept at 0.95 bar. After 5X volume reduction, diafiltration into DPBS was initiated until the volume reached the original volume. Then, 5 X volume reduction was repeated.

Cleaning of the membrane was conducted with 1M, 50°C NaOH for 30 minutes, and filter was kept in 20% EtOH solution at +4 °C until next use.

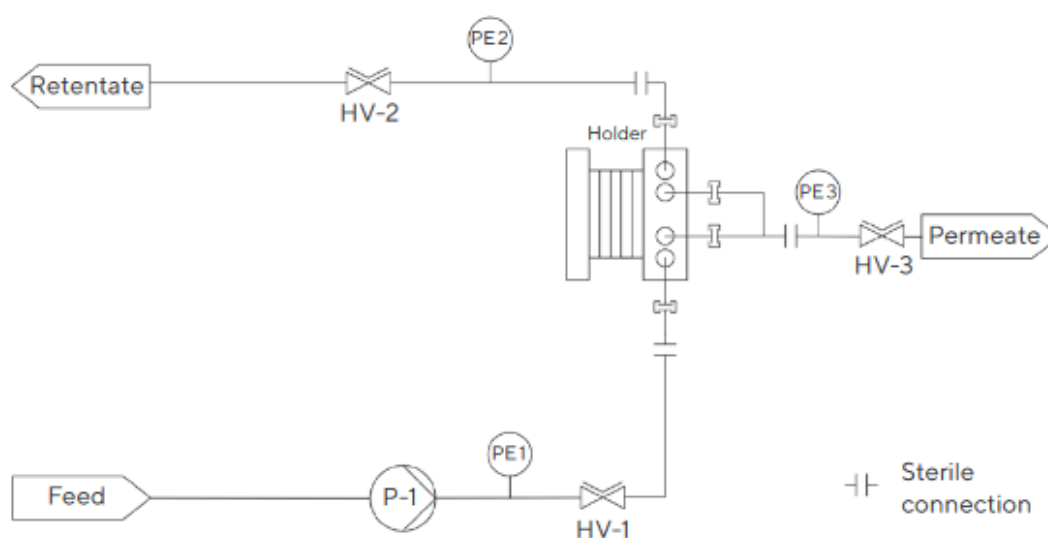


Figure 2.1. Diagram of Tangential Flow System

2.2.4 Characterization and Quantification of VLPs

2.2.4.1 Nanoparticle Analysis with Tunable Resistive Pulse Sensing

For the tunable-resistive pulse sensing (TRPS) measurements, qNano Gold (IZON S/N 601A) device was used, and the analyses were conducted via IZON Control Suite 3.4.2.48 software (IZON Science LTD). The working principle of TRPS is based on temporary disruptions in baseline current generation during the passage of particles through the nanopore. While electrolyte ions movement between electrodes creates a current through the nanopore, particles that enter the pore causes attenuation of the current and blockade signal. The application software then extrapolates particle dimensions and frequency of these measurements in order to determine the size of the particles in suspension and gives size distribution of the particles in a histogram plot.

Operation begins with the preparation of the fluid cell by wetting with sterile DPBS and stretching the nanopores to 47 mm according to the manufacturer's instructions. After removing the DPBS and stretching the nanopore by winding the stretch adjustment wheel clockwise, the software is turned on, and the stretch is calibrated. Then, pore openness is verified under 20 mbar pressure for 2 minutes after loading 75 μ l and 35 μ l DPBS to lower and upper fluid cells, respectively. Prior to determining the baseline current, nanopore coating carried out with Izon coating solution to avoid the performance decline of the pores in long runs by reducing the non-specific binding of proteins. During the coating, DPBS in the fluid cell is replaced with the same amount of coating solution, and 20 mbar pressure is applied for 10 minutes at this time. The coating solution is substituted with DPBS and at 20 mbar pressure for 10 minutes in order to remove excess coating solution. Then, baseline current is determined by loading the electrolyte solution and obtaining the stable current value, after which, the system is ready for sample loading.

Before beginning the relative particle size recording, the sample is loaded, and pressure is applied until a stable current is achieved. Then, recording is continued till the particle count exceeds 500, and the rate is over 100. Also, calibration particles, which are diluted in DPBS, are loaded and recorded under the same pressure, voltage and pore stretch. Thus, data is processed according to the recordings of calibration particle reading.

At the end of the readings, nanopore, upper and lower fluid cells are washed with double distilled water.

2.2.4.2 SDS-PAGE, Western and Dot Blotting for the Characterization of VLPs

Spike, Envelope, Membrane and Nucleocapsid protein content of VLPs were analyzed by SDS-PAGE/ Immunoblotting as described below. Purified VLP samples were mixed with 4X Laemmli Buffer (Loading Dye) (Appendix B) to 1X final concentration. Next, the mixture was vortexed and boiled at 70 °C for 20 minutes and 90 °C for 10 minutes to denature proteins before loading. 18-24 µl samples and 4 µl PageRuler Prestained 10 to 250 kDa Protein Ladder were introduced into wells of a 4–20% Mini-PROTEAN TGX Stain-Free Precast Gel is followed by running of the gel at 100 Vs in 1X Running buffer on a Mini-PROTEAN® Tetra cell apparatus (Bio-Rad,USA).

PVDF 0.2 µm transfer membrane was preferred rather than nitrocellulose because of its higher adsorption rate of proteins. Therefore, near the end of the SDS-PAGE, PVDF membrane was activated with 100% methanol and washed with 1X Transfer buffer before the process. When SDS-PAGE was completed, gel was removed from the cassette and placed in a wet transfer stack as illustrated in Figure 2.2.

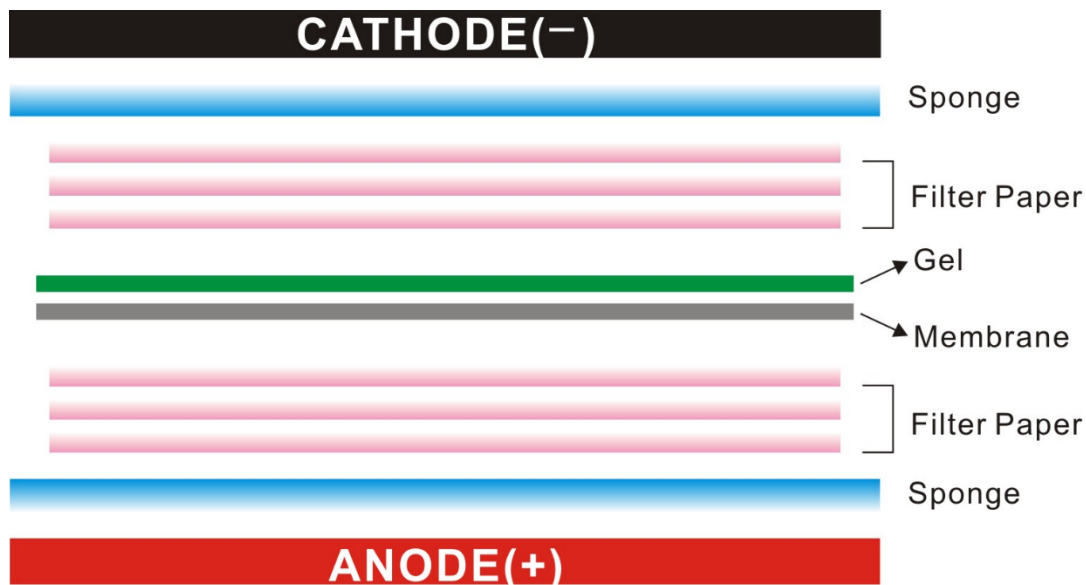


Figure 2.2. Western blot transfer stack for transfer of proteins form gel to membrane.

Order of the gel and membrane in the transfer stack is determined according to the current, which is from (-) to (+). Consequently, gel should be placed at cathode site, while membrane should be positioned at anode site to meet the protein movement from gel to PVDF.

All components in the transfer stack were wetted with a pre-cold transfer buffer. Bubbles were removed for equal distribution of the current onto all proteins in the gel without any disruption. Then, transfer was carried out with the Wet/Tank Blotting System (Bio-Rad, USA) at 0.25 A for 1 hour.

Following the completion of transfer, the membrane was blocked in 0.5% BSA in PBST for 1 hour to reduce non-specific binding of antibodies. After washing with 1X PBST three times for five minutes, incubation in Hrp-conjugated His-tag or Nucleocapsid primary antibodies was carried out for an hour at 1:10.000 or 1:1000 dilutions, respectively. For detection of nucleocapsid protein, an additional step of incubation with an HRP-anti-mouse secondary antibody for 1 hour was included since the primary nucleocapsid specific antibody was not enzyme conjugated. Excess antibodies were removed by washing three times as above. To visualize protein

bands, ECL™ Prime HRP Reagent (Cytiva) substrate was added onto the membrane according to manufacturer's instructions and the membrane was imaged on an Amersham Imager 600 device (Cytiva).

On the other hand, determination of VLP secretion in different days into culture supernatant were analyzed through dot blotting. 10 µl of Supernatants from samples collected on days 2,4 and 5 were applied onto nitrocellulose membranes. Following drying, membranes were blocked in 5% blocking buffer for 1 hour and washed 3X with PBST for 5 minutes. Probing and incubation in secondary antibodies were achieved as described above. Same ECL™ Prime HRP Reagent (Cytiva) substrate was used to develop dots, and membranes were imaged on BioRad Gel Doc XR+ imager (Bio-rad, USA).

All incubation steps were carried out on a shaker at room temperature.

2.2.4.3 VLP protein content determination with micro BCA

Pierce™ micro BCA protein assay kit was used for VLP protein content determination.

Briefly, albumin standards were prepared using 2-fold dilutions starting with 200µg/ml to 0.625 µg/ml. Samples and standards were mixed with the working solution of the kit at 37 °C for 2 hours as described in the manufacturer's technical protocol sheet.

Protein concentrations were then determined according to absorbance readings at 562 nm based on the BSA standard calibration curve.

2.2.5 Determination of residual DNA amount in purified VLPs with the PicoGreen Assay

Presence of the residual DNA in vaccines is considered as a risk factor because of DNA's pathogenic potential. Accordingly, residual DNA amount in vaccines should be limited to not exceed a dose of 10 ng/dose. To quantitate the residual DNA amount in purified VLPs, Quant-iT™ PicoGreen™ dsDNA Assay Kit was employed.

Briefly, Lambda DNA standards were prepared, starting with 1000 ng/ml DNA and serially diluting four-fold to the low standard of 0.24 ng/ml. All samples and calibration standards were prepared as duplicates and loaded into wells of a Costar black plate. Then, PicoGreen reagent was diluted 1:200 with Quant-iT™ PicoGreen® dsDNA reagent in 1X TE buffer. Following 4 minutes incubation at room temperature, fluorescence intensities were determined at 490-525 nm using a SpectraMax multimodal plate reader.

2.2.6 Pseudovirus Neutralization Assay

Assessment of neutralizing antibody-inducing potential of a candidate SARS-CoV-2 vaccine is of utmost importance in evaluating its immunoprotective activity. Most serum virus neutralization assays for detection and quantitation of serum neutralizing antibodies are based on inhibition of authentic virus infectivity in cell culture in the presence of neutralizing antibodies. However, in the case of SARS-CoV-2, such an assay can only be performed in a BSL3 laboratory. To bypass the need for such BSL3 facilities, neutralization assays based on pseudotyped virus expressing the SARS-CoV-2 Spike protein can be adopted and carried out in BSL2 laboratory. Simply put, a pseudotyped virus is a replication-defective virus particle with the envelope protein (such as Spike), originating from another virus. The following section describes our strategy to generate the SARS-CoV-2 Spike protein expressing pseudotyped virus carrying the GFP gene to be used as a reporter in infection experiments.

2.2.6.1 SARS-CoV-2 Spike Protein expressing Pseudotyped virus Production

Pseudotyped production was optimized by combining the SARS-CoV-2 Spike protein with GFP-encoding lentivirus system. The LeGO-G2 (GFP), pMDLg/pRRE and pRSV-Rev plasmids constituted the main components of the GFP expressing lentiviral system, whereas, the pCMV-Spike Δ 19(D614G) plasmid encodes the spike protein of SARS-CoV-2 to enable infection of human ACE2 receptor expressing cells. The pCMV-Spike Δ 19(D614G), lacks the endoplasmic reticulum retention signal and contains D614G point mutation in receptor binding domain of Spike protein. This strategy was previously reported to increase the transmissibility and infectivity of the pseudotyped SARS-CoV-2 (Pamukcu et al., 2020; Volz, Hill, et al., 2021)

Briefly, plasmids were transfected to Hek293ft adherent cells at a confluency of $\geq 90\%$, according to amounts given in Table 2.2. Prior to transfection, plasmids were expanded as given detailed in Section 2.2.2. 100ng of each plasmid was transformed into competent *E.coli* cells, in which were then transferred into liquid LB growth medium and Ampicillin selection medium. Once the plasmid isolation was completed, plasmid amounts and purity were measured with Biodrop.

Table 2.2. Plasmid amounts used for pseudotyped virus production.

Amount for 1XT75 transfection	Plasmids
7.5 μ g	LeGO-G2
3.75 μ g	pMDLg/pRRE
2.25 μ g	pRSV-Rev
0.5 μ g	pCMV-Spike Δ 19(D614G)

Transfection was conducted with the help of PEIpro reagent. Complexation medium is prepared using the same procedure as described in section 2.2.2. Plasmids/PEI-pro

complexes were introduced dropwise onto Hek293ft adherent cells in 10% regular DMEM medium (Appendix B).

Following 16-18 hours of transfection, the medium was replaced with a fresh 10% regular DMEM medium. 48 hours later, cells were centrifuged at 300g for 5 minutes to remove debris, followed by the filtration through 0.45 μm filters. The as such prepared pseudotyped virus in the culture supernatants were stored at $-80\text{ }^{\circ}\text{C}$ (Figure 2.3).

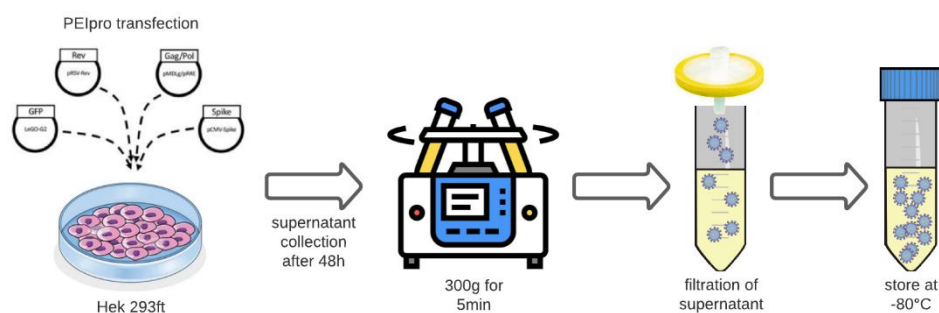


Figure 2.3. Pseudotyped virus production scheme starting with transfection of the Hek293ft cells to the cryopreservation of the pseudoviruses at -80°C .

Following pseudotyped virus isolation, collected products were applied onto a nitrocellulose membrane for dot blot analysis as described in Section 2.2.4 with only differences in primary (S1) and secondary (HRP conjugated anti-rabbit IgG) antibodies.

2.2.6.2 Pseudotyped virus Neutralization Assay

HEK293-FT-hACE 2 adherent cells were seeded in wells of 96 well flat bottom plates at a density of 20.000 cells per well in 100 μ l fresh DMEM and incubated under 5% CO₂ at 37 °C. Human serum samples from naïve (negative control), COVID-19 convalescent (positive control) or SARS-CoV-2 vaccinated individuals were inactivated by incubation at 56 °C for 30 minutes, together with the Balb/c serum samples. Possible aggregates were removed via brief spin at highest speed of an Eppendorf centrifuge. Then, serum samples were serially two-fold diluted in a 96 well master plate with FBS-free fresh DMEM, and serially diluted 2-fold until 1:128. The final volume of diluted serum samples in each well was 50 μ l. Then, 50 μ l of thawed pseudotyped virus was added onto each well, and pseudovirus-serum mixtures were incubated at 37 °C for 1.5 hour to achieve neutralization of the pseudoviruses with available neutralization antibodies in the serum.

Near the end of pseudovirus-serum incubation, polybrene was added onto each well of HEK293-FT-hACE 2 cells, to a final concentration of 0.08%. As soon as incubation was completed, pseudovirus-serum mixtures were transferred from the master plate onto cells. Next, the mixture is centrifuged at 1000g, 32 °C for one hour, followed by the incubation at 37 °C for 24 hours. (Figure 2.4). At the end of incubation, GFP expression of cells was visualized on a Fluid imaging station and GFP expression amount was quantitated by flow cytometry.

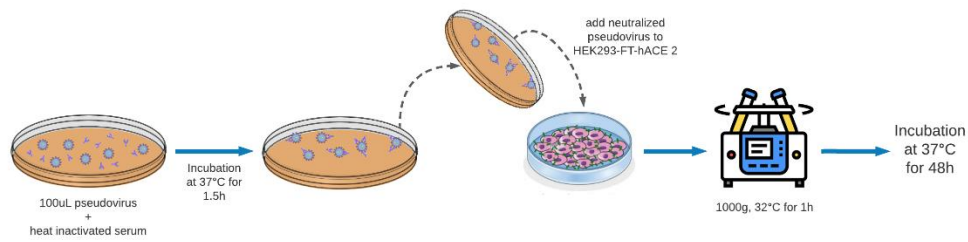


Figure 2.4. Summary of Pseudotyped Virus Neutralization Protocol

2.2.7 Statistical Analysis

Statistical analyses and graphical representations were conducted by using GraphPad Prism 9 software. VLP secretion rates into the culture supernatant on different days were compared statistically by Kruskal-Wallis test followed by Dunn's Multiple comparison test while densities of the spike bands in immunoblot were statistically analyzed with ordinary one-way ANOVA. (*:p<0.05, **:p<0.01, ***:p<0.001)

2.3 Ethical Statement

The 12 volunteer samples were part of the approved and ongoing Phase 2 clinical trial (*NCT04962893*; A Randomized, Placebo-controlled, Phase II Study to Assess the Safety, Efficacy, and Immunogenicity of Virus-like Particle (VLP) Vaccine for the Prevention of COVID-19 in Healthy Adults Aged 18 Years and Older) sponsored by The Scientific and Technological Research Council of Turkey and approved by TITCK.

CHAPTER 3

RESULTS & DISCUSSION

At the end of 2019, a novel coronavirus, since then named as SARS-CoV-2 has emerged and had infected more than seventy thousand and had killed over eighteen hundred people when the epidemic was at its fiftieth day. The viral infection was quickly identified to cause an acute respiratory disease called as COVID-19, resulting in fever, dyspnea, cough, chest discomfort in affected patients, some of which progress to multi organ failure, resulting in death. Then, on 11 March 2020, World Health Organization declared the outbreak as a global pandemic (Shereen et al., 2020).

Based on sequence analysis of its genome, SARS-CoV-2 has 79.5% genomic homology with SARS-CoV, and its genome organization is consistent with viruses in betacoronavirus genus and Sarbecovirus subgenus. Therefore, SARS-CoV-2 is placed under Sarbecovirus subgenus together with SARS-CoV and bat SARS related coronaviruses in the phylogenetic tree (Hu et al., 2021).

SARS-CoV-2 genome has four structural genes encoding Spike(S), Membrane(M), Envelope (E), and Nucleocapsid (N), eleven accessory protein coding genes (ORF3a, ORF3b, ORF3c, ORF3d, ORF6, ORF7a, ORF7b, ORF8, ORF9b, ORF9c and ORF10); and sixteen nonstructural proteins are encoded by Open Reading Frame 1a and ORF1ab(X. Li et al., 2021; Mariano et al., 2020). While nonstructural proteins play various roles in viral transcription and replication, methylation and ER membrane modification (Table 1.1), structural proteins are involved in virion formation, assembly of virus particles, translocation to ER, and are fundamental to viral pathogenesis (M. Li et al., 2021; Mariano et al., 2020; Yadav et al., 2021; H. Yang & Rao, 2021). Therefore, structural proteins are considered as attractive

vaccine targets due to their higher immunogenic potential. SARS-CoV-2 infects the host type-II pneumocytes and unciliated epithelial cells through binding to ACE2 (angiotensin-converting enzyme) receptors (Bourgonje et al., 2020). Receptor binding domain (RBD) of the Spike protein binds to host cells' ACE2 receptors and this initial binding initiates a series of conformational changes in the spike protein, culminating in fusion of viral envelope with the host cell membrane, which is necessary for the release of viral genome into the host cell cytoplasm (Shang et al., 2020). Since, spike protein establish the first contact with the host cells, most of the SARS-CoV-2 vaccine development platforms target spike protein or its receptor binding domain in order to prevent host cell ACE2 – virus RBD attachment by interfering with antibodies that can neutralize the virus (Dong et al., 2020; Krammer, 2020; Kyriakidis et al., 2021; M. Y. Wang et al., 2020). However, emergence of the Alpha (B.1.1.7), Delta (B.1.617.2), Gamma (P.1), and Beta (B.1.351) and lately, the Omicron (B.1.1.529) variants, with mutations in the Spike and its RBD, caused concern on the neutralizing potential of antibodies induced with vaccines targeting the S and/or the RBD domain of the authentic virus (Gobeil et al., n.d.; Harvey et al., 2021; Petersen et al., 2022). Since Spike protein is under evolutionary pressure to escape neutralizing antibodies, the frequency of mutations in this protein is considerably higher than the other structural proteins of SARS-CoV-2 (Pereson et al., 2021). Therefore, incorporation of other structural proteins as antigens in vaccine design can potentially broaden the breadth of T-cell responses, limit dependence solely on neutralizing antibodies and contribute to protection. Even though inactivated virus vaccines such as CoronaVac target all structural proteins of the virus, its effectiveness against variants were significantly reduced compared to the wild type virus (X. N. Li et al., 2021), with the induced antibodies capable of only partially neutralize the variants (Melo-González et al., 2021). This suggests that variant-specific vaccines could be an attractive alternative in combatting spread of SARS-CoV-2.

Virus Like Particle (VLP) vaccine platform generates particles, mimicking the authentic virus structure without having the viral genome. A VLP vaccine composed of not only S but also M, N and E proteins of the virus, broadens the spectrum of antigenic epitopes, especially with respect to the T cell epitopes, stimulating both the humoral and cellular response (Ghorbani et al., 2020). Furthermore, some studies suggest that N protein specific T cells might have role in supporting neutralizing antibodies (Ni et al., 2020b). Besides these advantages of the VLP technology, it has also ability to quickly adapt the platform to emerging variants of SARS-CoV-2 with minimal effort.

Herein, we aimed to design Spike antigen in line with the emergence of Delta plus (B.1.617.2.1) and Alpha (B.1.1.7) variants of concern, and prepared the vaccines against these variants by harnessing the technology we used our previous Virus Like Particle vaccine for the wild type virus. Furthermore, based on experiments on non-human primates demonstrating the protective potential of neutralizing antibodies (Krammer, 2020), we tried to evaluate the neutralizing activity of the sera of 12 volunteers 49 days after immunization with Alpha-VLPs and (n=4) BALB/c receiving Delta plus-VLP as a third booster which were adjuvanted with Alhydrogel and K type CpG ODN. For this, a SARS-CoV-2 Spike pseudotyped neutralization assay was established.

2.4 Cloning of Alpha (B.1.1.7) and Delta (B.1.617.2.1) Variant expressing genes and Confirmation of Structural Protein Expression Vectors

Wild type N, M, E proteins with mutated Spike glycoprotein genes of SARS-CoV-2 were cloned into mammalian dual expression vectors for subsequent production of VLP. Human codon optimized Membrane glycoprotein (M) and Nucleocapsid (N) expressing genes were cloned into pVITro1 dual expression vector at the site of BamHI and BglII restriction enzymes. HexaProline(6p) Spike (S) expressing gene, which has six proline substitution, was cloned into pVITro2 dual expression vector at

the BamHI site together with Envelope protein expressing gene at the BglII site(Yilmaz et al., 2021). Spike, Membrane and Envelope proteins expressing genes were tagged with 6X histidine tag at their C terminus. No His-tag was present in the Nucleocapsid gene sequence (Yilmaz et al., 2021). Following the emergence of variants with mutations in the spike gene (Li et al., 2021), we aimed to modify the 6P-Spike proteins of our VLP product according to the mutations defined for Delta plus (B.1.617.2.1) and Alpha (B.1.1.7) variants (Planas et al., 2021). For this, we utilized previously designed pVitro1 (M+N) plasmid without any modification and the pVitro2 (E) construct where the wild type Spike gene was replaced with the Alpha variant Spike mutations or the Delta plus variant spike mutations as indicated in Figure 3.1.

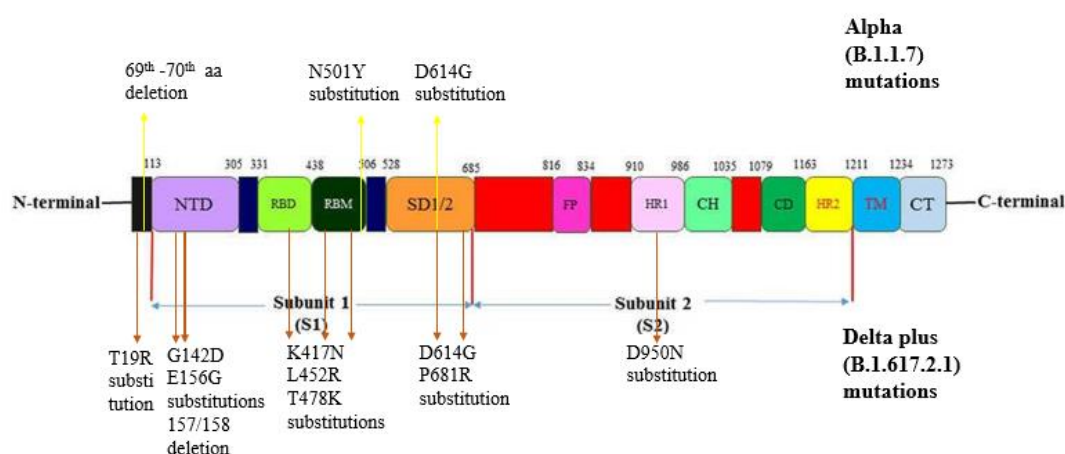
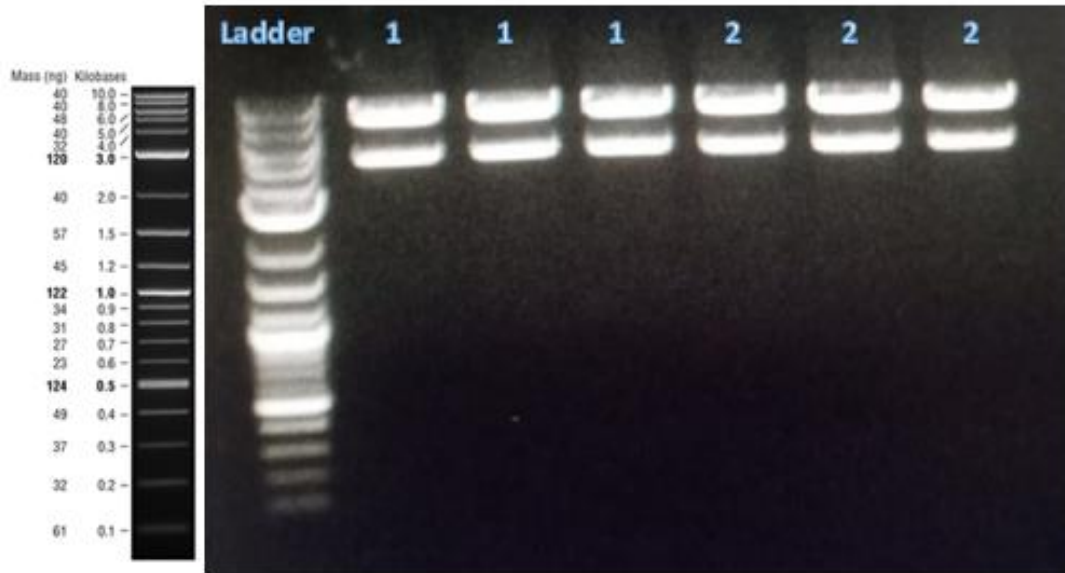


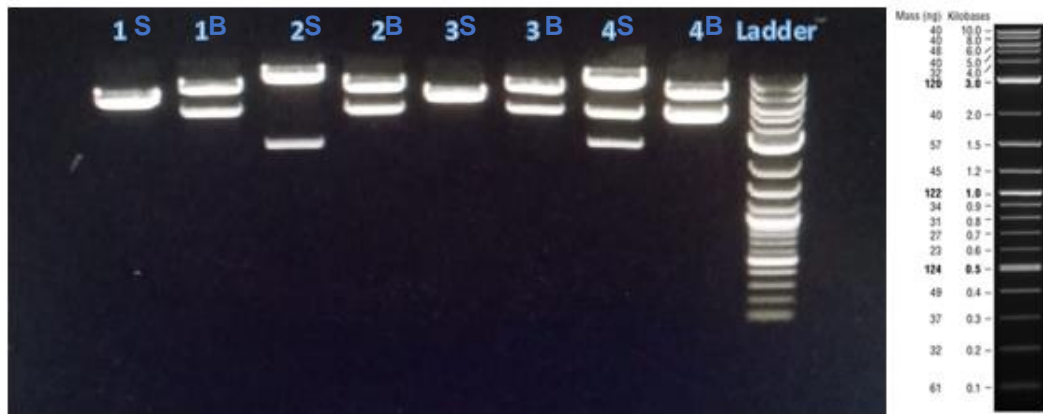
Figure 3.1. Schematic Representation of Spike Gene Design with the Inclusion of Mutations that were found in Alpha and Delta plus Variants (Adapted from Mohammadi et al., 2021)

After the transformation and isolation of mutated Spike constructs which were synthesized by Integrated DNA Technologies and were received in pBRIDT plasmids (Appendix A), ligation was conducted with the pVitro2 (E) vectors at the BamHI restriction enzyme cut site. Transformation of ligated product was followed by colony selection and plasmid DNA isolation (Section 2.2.1). In order to evaluate the success of the cloning and verify that the insert was in the right direction, isolated

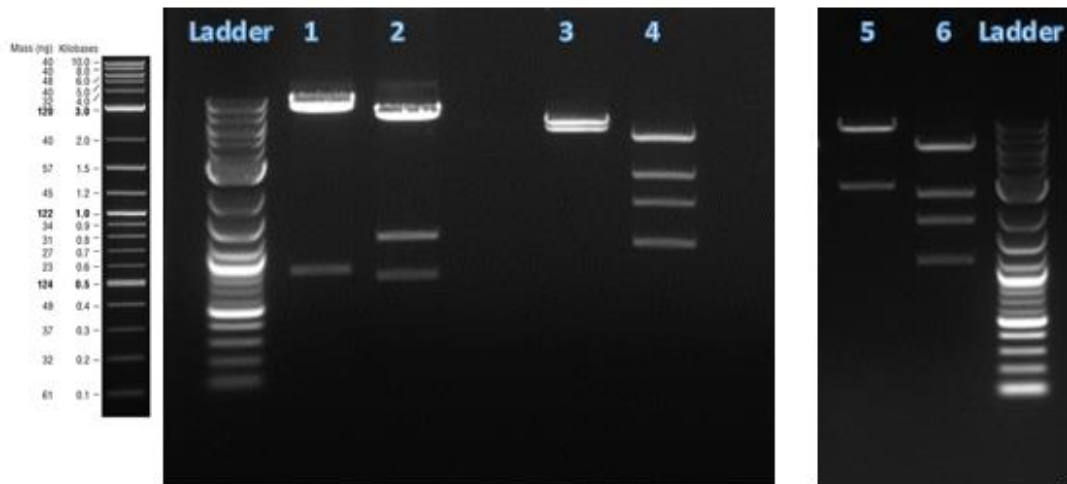
plasmids were digested with different restriction enzymes, and digested plasmids were run on an agarose gel (Fig 3.2).



a.



b.



c.

Figure 3.2. Confirmation of isolated plasmid constructs digested with various restriction enzymes.

1-1.5 µg plasmid isolates were treated with 1 µl restriction enzyme, 1X restriction enzyme buffer at 37 °C for 1 hour. At the end of restriction enzyme digestion, loading dye was added to a final 1X concentration. Then, all samples and the 1kb ladder were loaded onto an agarose gel (1% w/v), and electrophoresed at 120V for 1 hour. The gel was visualized under UV Transilluminator.

- a. BamHI restriction enzyme digestion of pVtro2 WT-S- 6P+E in triplicate lanes labelled with 1, BamHI restriction enzyme digestion of pVtro2 Alpha-S-6P+E in triplicate lanes labelled with 2.
- b. ScaI restriction enzyme digestion of isolated plasmids from four different colonies potentially harboring pVtro2 Delta-S-6P+E. Lanes labelled with 1S,2S,3S,4S, and BamHI digested bands of the same colonies were labelled with 1B,2B,3B,4B.
- c. BamHI and HindIII digestion of pVtro1 M+N constructs in lanes 1 and 2, respectively. Further digestion of the pVtro2 Alpha-S-6P+E and pVtro2 Delta-S-6P+E products were conducted with ApaII and HindIII restriction enzymes in lanes labelled with 3,4,5,6, in the following order: pVtro2 Alpha-S-6P+E digestion with ApaII, pVtro2 Alpha-S6P+E HindIII, pVtro2 Delta-S-6P+E digestion with ApaII, pVtro2 Delta-S6P+E HindIII.

To verify the pVtro2 plasmid with the Alpha Spike gene insert, we digested the isolated plasmid with BamHI (Figure 3.2.a.). Lane 2, demonstrates fragments located between the 6-8 kb and 3-4kb bands of DNA ladder, respectively, which coincides

with the expected 6015 and 3396 bp digests following successful enzymatic cleavage. Moreover, these bands were at the same molecular weights with the bands seen in lane 1, which corresponds to the BamHI digested Wuhan pVITRO2- 6p-S+E construct that was previously verified with next generation sequencing (MSc thesis of Emre Mert İpekoğlu). Since both constructs share BamHI cut site in the same region and their sequences are almost identical (except for 4 amino acid change that does not affect the restriction enzyme digestion), we concluded that Spike gene of Alpha variant was inserted into the vector. We further digested this construct with ApaLI and HindIII restriction enzymes to verify the direction of insert (Fig 3.2.c). We expected to observe two bands with 5061 and 4950 bp, and four bands with 4362,2857,1717,1075 bp following digestion with ApaLI and HindIII, respectively, and confirm their presence in lanes 3 and lane 4 (Figure 3.2.c.). Therefore, we decided that Alpha variant Spike was successfully cloned into the vector in the right direction. Had the insertion failed, we would have observed only three bands in lane 4, and if the insert was in reverse direction, only two bands would be visible in lane 3.

Verification of Delta plus variant Spike gene insertion into pVITRO2 vector was carried out as described above. Plasmids from four possible colonies were isolated and digested with ScaI and BamHI (Figure 3.2.b). Figure 3.2.b shows that all four colonies were positive for Delta plus variant Spike gene (BamHI digested fragments in lanes 1B,2B,3B and 4B) (Figure 3.2.b). Since ScaI restriction enzyme cuts the plasmid within the Spike gene, we confirmed the direction of the insert using this enzyme. Lane 2S shows two fragments corresponding to 8197 and 2447 bp, validating that the insert was in the correct direction. Using this plasmid, further diagnostic digestion with ApaLI and HindIII generated two bands with 8063, 2581 bp, four bands with 5434,2435,1717,1058 bp, respectively, in lanes 5 and 6 (Figure 3.2.c), validating the correct direction of the insert.

Previously used pVITRO1 (M+N) plasmid construct was also digested with BamHI and HindIII restriction enzymes in order to verify the purity before proceeding to

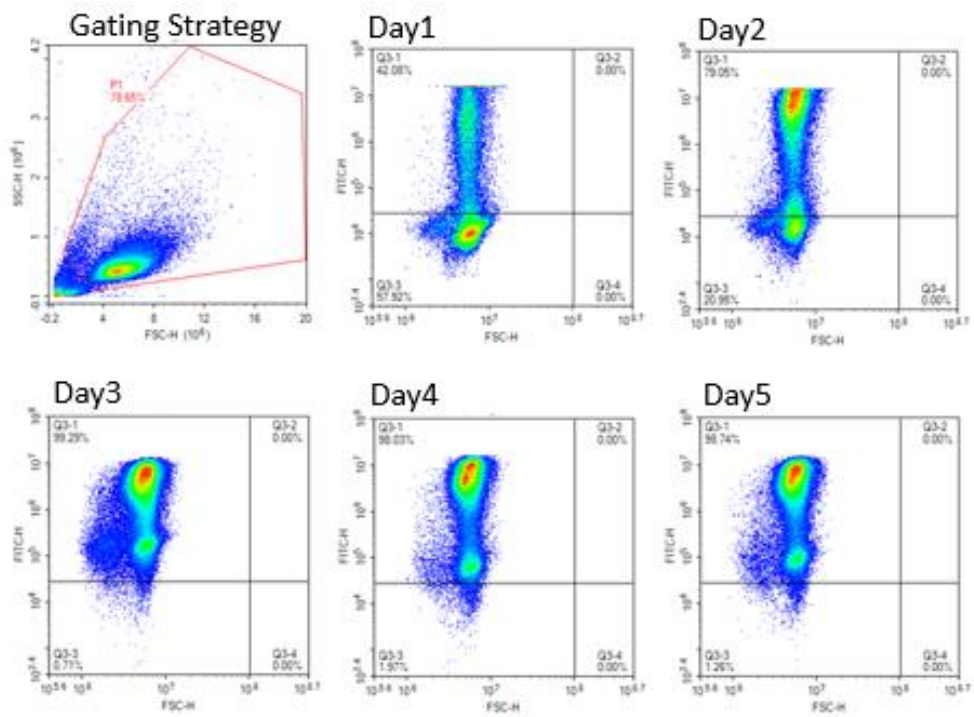
transfection. We observed fragments (lane 1 and 2 ;Figure 3.2.c) at their expected molecular weights.

Collectively, these results demonstrate successful cloning of variant Spike genes into the pVITRO2 vector. Cloned plasmids were also assessed by Next Generation Sequencing based quality control to confirm the sequence (Appendix A).

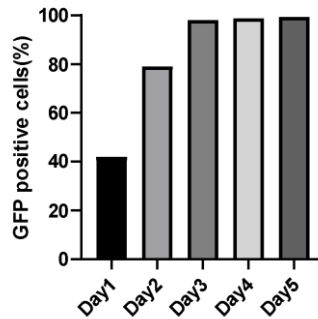
2.5 Optimization of PEIpro Mediated Transfection of HEK293 Suspension Cells Using Green Fluorescence Protein Expressing Plasmid

To determine the transfection efficiency, HEK293 suspension cells were transduced with pcDNA3.1 (+) eGFP plasmid/PEIpro complexes as described in Section 2.2.2. Previous studies conducted in our laboratory guided us to use DNA to PEIpro ratio as 1 µg: 2µl for transfection. Following transfection, GFP expression was followed for 5 consecutive days (Figure 3.3).

As can be seen in Figure 3.3.a and 3.3.b, GFP positive cell percentages increased daily and reached the maximum level on day 3. However, highest yield in GFP production was observed on day five since cells continued to proliferate without losing GFP expression. Based on these results, subsequent VLP production experiments were also carried out using a DNA:PEIpro ratio of 1:2.



a.



b.

Figure 3.3. Flow Cytometric Analysis of GFP expression following transfection of Hek293 suspension cells.

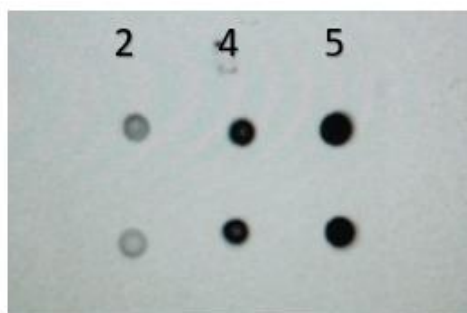
Percentages of GFP expressing cells after pcDNA3.1(+) eGFP transfection were assessed, following gating of viable cells. GFP expression percentage was determined using the signal detected on the FITC channel.

2.6 Transient Transfection of HEK293 Suspension Cells Generates Virus Like Particles in the Culture Supernatant

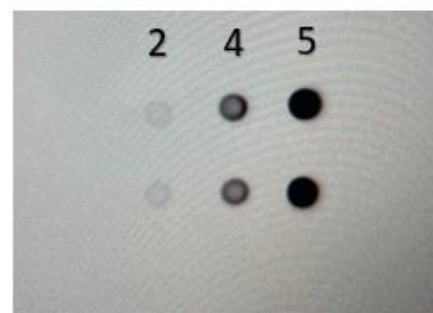
Co-expressed viral structural proteins can self-assemble into nano particles known as Virus Like Particles (Arevalo et al., 2016). We harnessed this self-assembly property and delivered our constructs into the mammalian expression system to generate our VLP based vaccine.

2.6.1 Virus Like Particle Accumulation Rates in the Culture Supernatant on 2, 4 and 5 Days After Transfection

Transfection of the structural protein expression plasmids to HEK293 suspension cells is followed by Virus Like Particle production. To increase production yield and manufacture the maximum amount of VLP in a single batch, we monitored relative accumulation rates of VLP products on different days following transfection. For this, samples from the supernatant were taken on day 2, 4 and 5 after transfection, and dot blot analysis was performed (Figure 3.4).



a.



b.

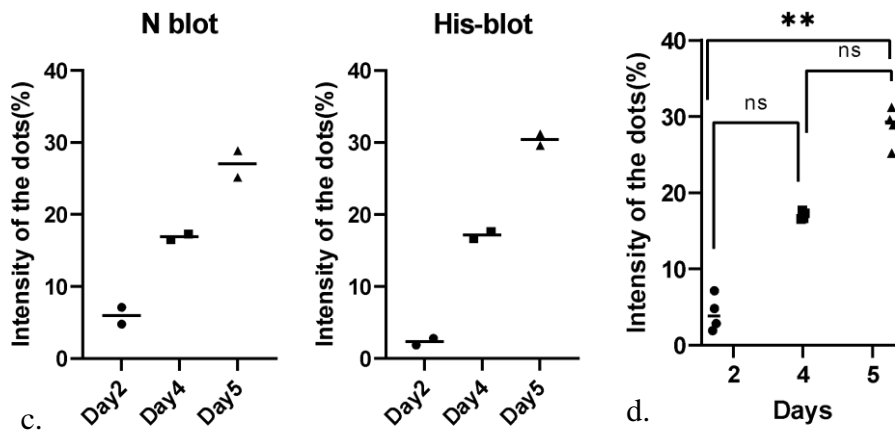


Figure 3.4. Determination of VLP Secretion Rate into the Culture Supernatant on Different Days through Dot Blot Analysis.

10 μ l of Supernatants from samples collected on days 2,4 and 5 were applied onto nitrocellulose membranes. Following drying, membranes were blocked in 5% blocking buffer for 1 hour and washed 3X with PBST for 5 minutes. Probing was achieved with primary His-tag or Nucleocapsid antibodies for 1 hour. Following washing, Nucleocapsid membrane was probed with a secondary antibody. Membranes were developed with the substrate and imaged on BioRad Gel Doc XR+ imager.

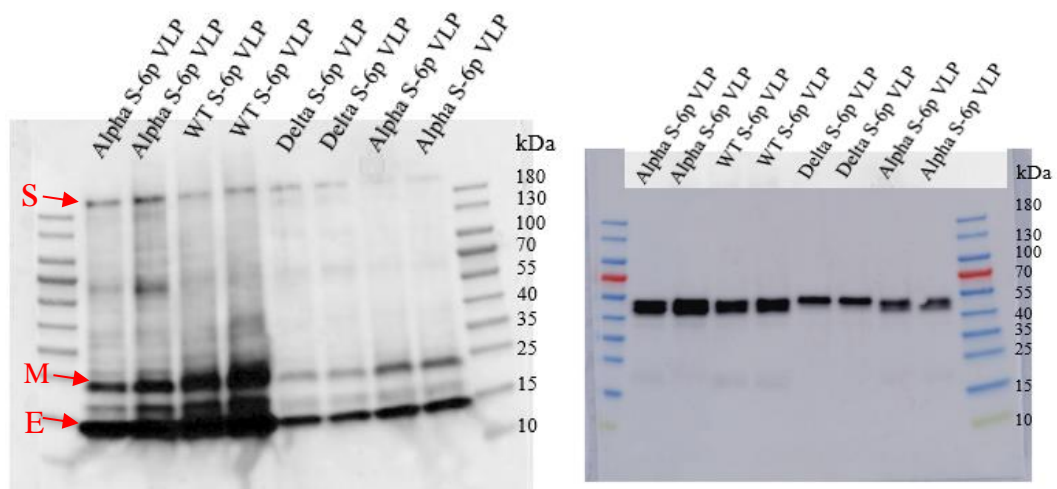
Intensity of the dots were determined by ImageJ, and dot densities for all days were compared with each other statistically by Kruskal-Wallis test followed by Dunn's Multiple comparison test (*:p<0.05, **:p<0.01, ***:p<0.001).

Verification of VLP presence and rough estimation of its amount in culture supernatant was conducted by taking samples 2, 4 and 5 days after the transfection. Samples were then applied in duplicates on two different nitrocellulose membranes which were subsequently incubated with Nucleocapsid antibodies (Figure 3.4.a) or His-tag antibodies (Figure 3.4.b). Therefore, we expected to observe the relative accumulation amount of Nucleocapsid protein and His-tagged-Membrane, Envelope and Spike proteins of SARS-CoV-2 as of indicators of VLP accumulation on different days of sampling.

According to dot blot analysis presented in Figure 3.4.a and Figure 3.4.b, we observed increasing levels of secreted proteins starting from day 2 to day 5. Dot blots were also subjected to semi-quantitative densitometric analysis in order to determine the percent changes of dot intensities among different days (Figure 3.4.c). Data presented, in Figure 3.4.c, indicate not only the percent increase of the accumulated proteins in the supernatant with each passing day, but also demonstrates that of His-tagged (S, E, M) and Nucleocapsid signal intensities increased in parallel. Therefore, when we combined percent intensities of the dots from His-& Nucleocapsid-tagged proteins in a single graph, we observed highest protein expression on day 5 (Figure 3.4.d). Signal intensities were significantly higher in samples collected on day 5 with respect to those collected on day 2 (Figure 3.4.d). Taken together day 5 was chosen as the optimum harvest day based on both the VLP yields and the viability VLP producing cells (Appendix D).

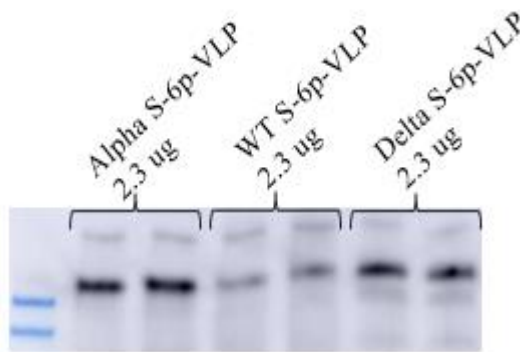
2.6.2 Characterization of Purified VLPs

Co-expression of four structural proteins is essential for assembly of the proteins and their release as intact VLPs (Y. L. Siu et al., 2008). Following VLP production and purification (Section 2.2.3), VLPs that were engineered with 6-proline mutations incorporating Spike genes from WT or the Alpha and Delta plus variants were characterized through immuno-blotting. His-tag and Nucleocapsid antibodies were used in immunoblots in Figures 3.5.a & Figure 3.5.b, respectively.

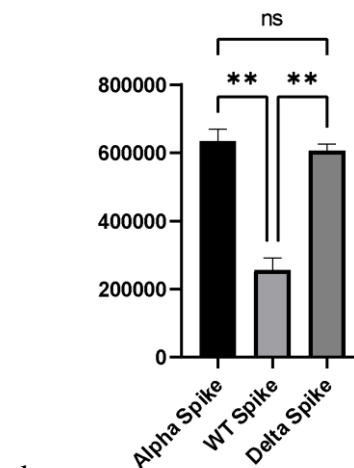


a.

b.



c.



d.

Figure 3.5. Verification of expression of the four structural proteins in purified VLPs incorporating the WT, Alpha- or Delta- 6p-VLP Spikes (a,b) and comparison of their Spike expression rates in gels loaded with equal protein amounts of VLPs (c,d).

25 μ g of each sample was loaded into the wells of 4–20% Mini-PROTEAN TGX Stain-Free Precast Gels. Following SDS-PAGE, proteins were transferred onto PVDF membranes using wet transfer. At the end of the transfer, both gels were blocked in 5% BSA. Before the incubation in primary His-tag (a,c) or Nucleocapsid (b) antibodies, appropriate washing steps were applied. Incubation of the membrane (b) with secondary antibodies was followed by imaging of the membranes under an Amersham Imager 600 device.

Densitometric analysis of the Spike bands was conducted by using ImageLab Software. Densities of the Spike bands from the three groups were statistically analysed with ordinary one-way ANOVA test (*:p<0.05, **:p<0.01, ***:p<0.001).

All VLPs expressed comparable levels of the 4 structural proteins (Figure 3.5.a/b). Moreover, molecular weight dependent localization of the protein bands were at their expected size.

In parallel experiments, equal concentration of VLPs were applied to gels and then probed for His-tag to enable comparative Spike quantitation in different VLPs (Figure 3.5.c). Densitometric analysis of the Spike bands were achieved by using ImageLab Software (Figure 3.5.d).

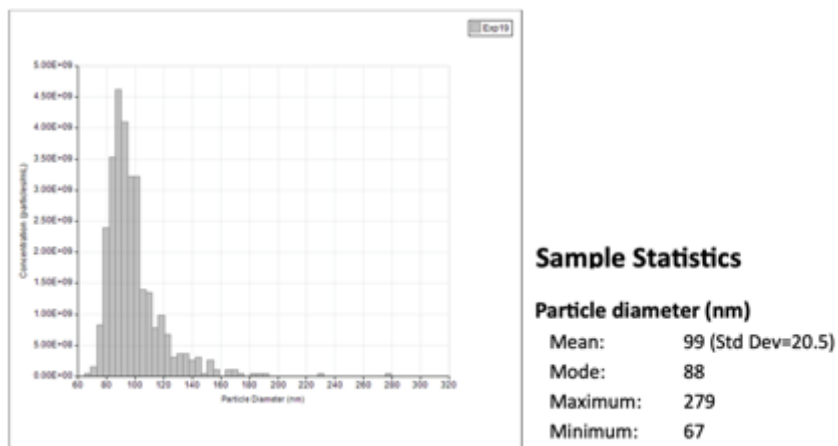
We detected a significant increase in density of the Spike proteins in Alpha & Delta plus variant VLPs compared to their Wild type counterpart (Figure 3.5.d). This increase in Spike amount in VLP products might be elucidated by the mutations in variants. Mutations in both variants play various roles in Spike incorporation and stability. Specifically, documented role of D614G substitution, which increases Spike expression in all variants of concern (Tao et al., 2021), possibly contributes to significant increase in Spike expression in variant but not WT VLPs.

Collectively, our data validated the presence of all four structural proteins in the final VLP product of both Alpha and Delta plus variant adjusted constructs. Therefore, VLPs expressing Delta plus or Alpha variant Spike were successfully produced with higher variant spike expression rates than WT spike containing VLPs.

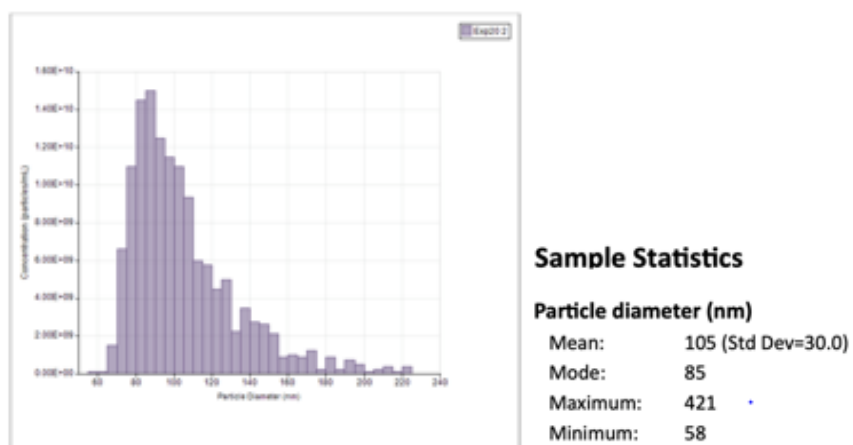
2.7 Size Distributions of the Alpha- and Delta-6p-VLPs

SARS-CoV-2 is a spherical virion whose size ranges between 60 to 140 nm in diameter (N. Zhu et al., 2020). To test the size distribution of our VLPs products we analyzed the particles using tunable-resistive pulse sensing (TRPS) measurements

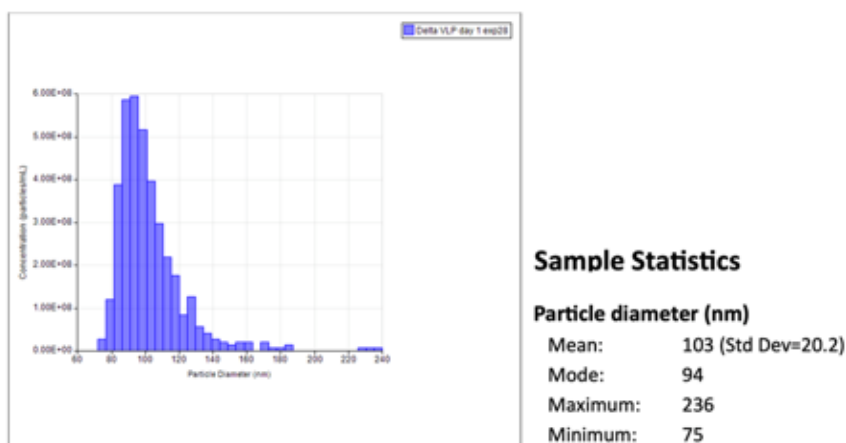
(given in detail in Section 2.2.4.1). Distribution of the particle sizes of purified VLPs are presented in histogram plots in Figure 3.6.



a.



b.



c.

Figure 3.6. Size distributions of the Alpha-6p-VLP (a), WT-6p-VLP (b) and Delta-6p-VLPs (c).

Particle size measurements were recorded on a qNano Gold device. Prior to loading the sample, baseline current was determined through electrolyte application. Size distribution of the samples were recorded and displayed in histogram plot format together with sample statistics.

Size distribution of the Alpha-6p-VLP, WT-6p-VLP and Delta-6p-VLPs were 99 ± 20 nm, 105 ± 30 nm and 103 ± 20 nm in diameter, respectively. These results are similar to the reported size distribution of the authentic virus, indicating that the purified VLPs were indeed duplicating the virion morphology.

Altogether, our data suggest that incorporation of all structural proteins genes for expression in HEK293 cells, produce similar sized VLP irrespective of the spike variant they expressed.

2.8 Protein and DNA contents of Alpha-S and Delta-S-6p-VLPs

Prior to preclinical immunization studies, for dose calculations and assessment of safety of the VLP antigen candidate, it was imperative to determine the protein and

DNA content of the VLPs. For this, microBCA assay (Section 2.2.4.3) and PicoGreen assays (Section 2.2.5) were performed (Table 3.1).

Table 3.1. Protein and DNA contents of Alpha-, Delta- and WT-6p-VLPs.

	Protein amount(μ g/ml)	DNA amount (ng/ml)
Alpha-6p-VLP	133.9	6.5
WT-6p-VLP	204.9	46.63
Delta-6p-VLP	86.43	40.41

Even though there are microbial expression systems for recombinant protein production with the advantage of high yield, low cost and easy to control production process, we utilized a mammalian expression system since mammalian cells are more efficient in producing multi-subunit high molecular weight and post-translational modifications. However, protein production yield is lower, controlling the process is harder, and batch-to-batch variations are likely (J. Zhu, 2012). Consistent with this, the protein and DNA content of VLPs ranged between 86-134 μ g/ml and 6.5-47 ng/ml respectively, for the indicated VLPs (Table 3.1). Nevertheless, both the protein content and the residual host DNA content were found to be within acceptable limits (upper limit of 10 ng/dose of DNA) to formulate the antigens and test their immunogenicity in mice.

Based on these results, both the Alpha-6p VLP and Delta-6p-VLPs were then formulated with vaccine adjuvants (alum/CpG ODN) and tested later for immunogenicity in mice to assess their potential as variant-specific vaccines. Antigen contents of these vaccines were calculated according to the protein quantities given in Table 3.1.

Next, we extended our research to assess the neutralizing antibody titers induced by our VLP vaccine formulations. For this, neutralizing antibody titers in sera of VLP vaccine volunteers and mice that have received the Alpha-6p-VLP or Delta-6p-VLP formulations, respectively, were analyzed through a pseudotyped virus neutralization assay.

2.9 Establishment of Pseudotyped Virus Neutralization Assay

Protective immunity against SARS-CoV-2 largely depends on neutralizing antibody levels which block ACE2-RBD interaction and thereby prevent infection (Suthar et al., 2020). However, with the emergence of new SARS-CoV-2 variants of concern (VOC), the ability of Wuhan spike-targeting vaccines to generate neutralizing antibodies against the VOCs has been compromised. Therefore, to address the neutralizing antibody eliciting capacity of variant specific VLP vaccines (Alpha (B.1.1.7) and Delta plus (B.1.617.2.1) variants) we developed a pseudotyped virus neutralization assay.

2.9.1 Spike Bearing Pseudotyped Virus Production

Because of the limitations in live virus usage in non BSL-3 laboratories, we first produced pseudotyped viruses, enabling neutralizing antibody binding to the expressed spike. For this, we used a lentiviral system, which carried a Green Fluorescent Protein reporter gene together with a D614G mutant of the Spike protein. The D614G mutation is not only found in both B.1.17 and B.1.617.2.1 variants, but it also contributes to the overall stability of the pseudoviruses (Pamukcu et al., 2020). Replication incompetent SARS-CoV-2 Spike bearing pseudoviruses were generated through transfection of the related plasmids into HEK293 adherent cells. Pseudoviruses were then collected from the supernatant (given in detail in Section 2.2.6.1). Then, we confirmed the presence of the Spike protein in isolated pseudoviruses by performing dot blot analysis using S1 domain specific antibodies (Figure 3.7).

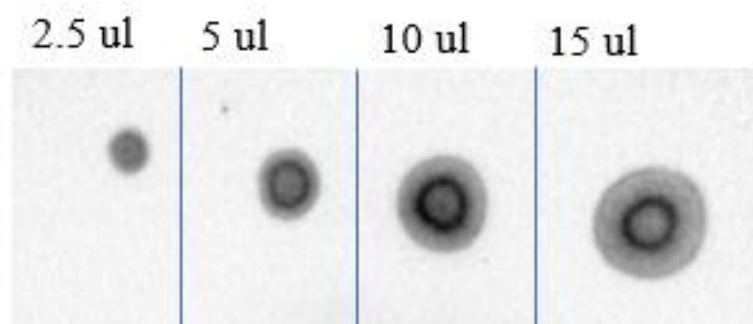


Figure 3.7. Confirmation of Spike protein expression in isolated Pseudotyped Viruses via Dot Blot Analysis.

Following pseudotyped virus isolation, 2.5, 5, 10 or 15 μ l of Supernatants were applied onto a nitrocellulose membrane and probed for S1 expression. The membrane was imaged by BioRad Gel Doc XR+ imager.

3.6.2 Evaluation of Neutralizing Activity of the Sera Taken from Volunteers Vaccinated with Alpha- S-6p-VLP and Mice Vaccinated with Deltaplus-S-6p-VLP

Next, we aimed to analyze the titers of neutralizing antibodies in sera of four Balb/c that have received a Delta plus-S-6P-VLP as a third booster and twelve volunteers that have received the Alpha-S- 6P- VLP vaccine during the approved Phase 2 study. Negative and positive controls were also included (data on controls were given in Appendix E). To achieve this, sera collected on day 49 post-vaccination were serially diluted and incubated with pseudoviruses. Each diluted serum-pseudovirus mixture was then added onto human ACE2 (hACE2) overexpressing HEK293-FT cells (given in detail in Section 2.2.6.2). The neutralizing activity of sera were determined through the GFP expression level in the ACE2 expressing cells. Decreased GFP expression is attributed to the blocking of the interaction between ACE2- Spike by the neutralizing antibodies. However, before proceeding in neutralization assay, we

confirmed the efficiency of the interaction between ACE2 and Spike bearing pseudoviruses, which directs GFP expression (Figure 3.8).

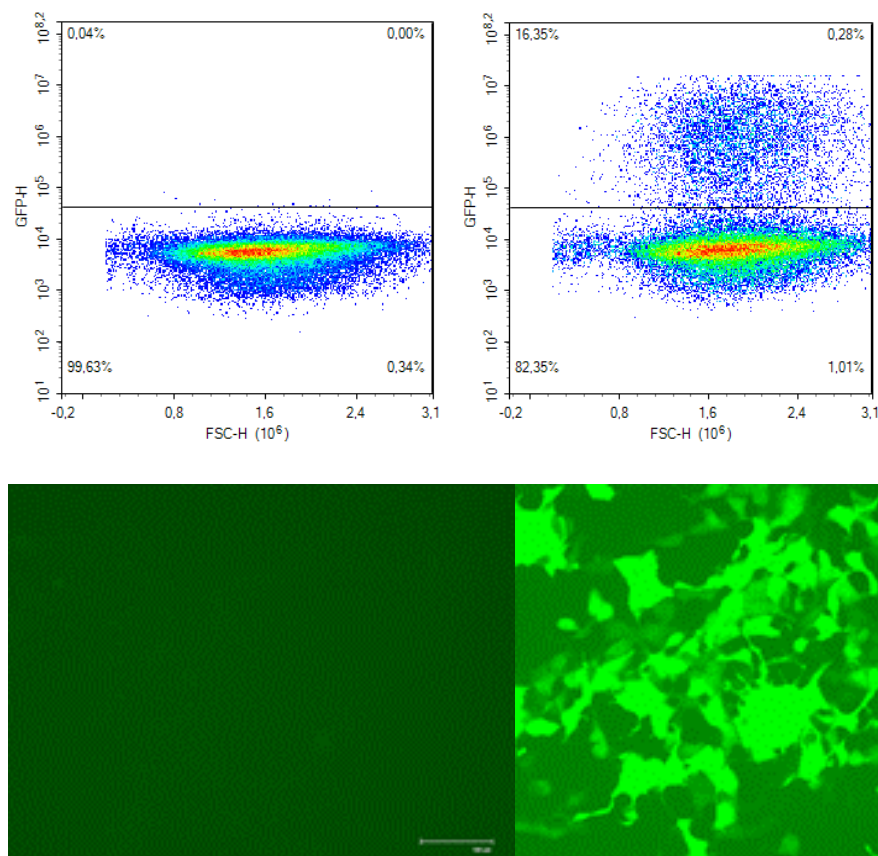


Figure 3.8. GFP expression levels of hACE2 expressing HEK293FT cells infected with/out pseudoviruses in the absence of neutralizing antibodies.

Upper panel represents the GFP expression of the target cell line in flow cytometry following incubation without (left) or with pseudoviruses (right). Lower panel represents corresponding fluorescence microscopy images.

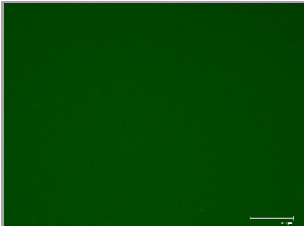
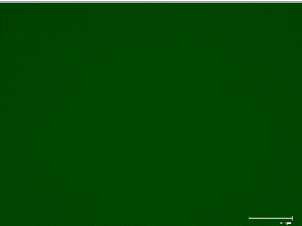
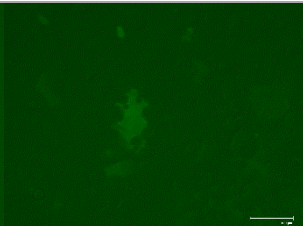
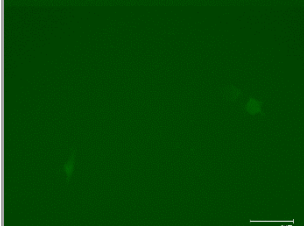
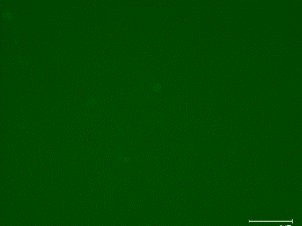
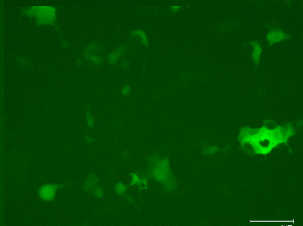
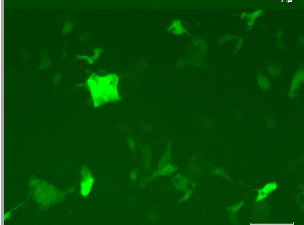

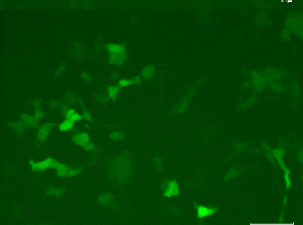
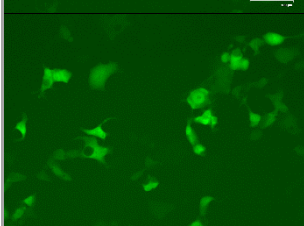
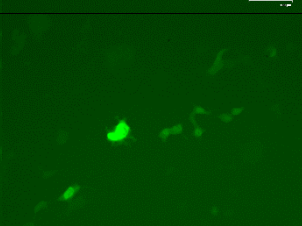
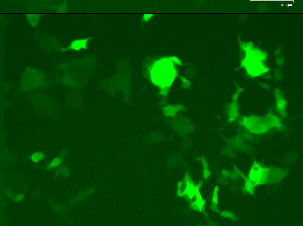
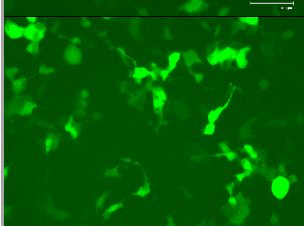
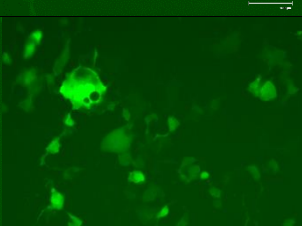
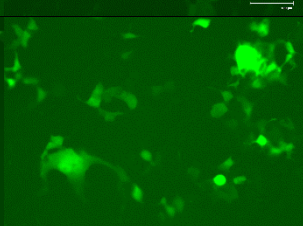
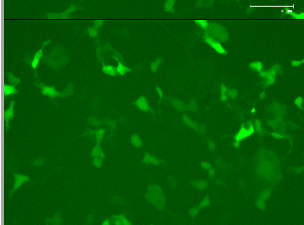
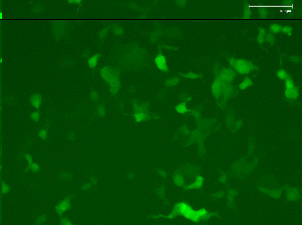
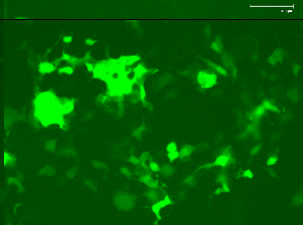
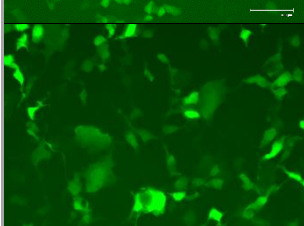
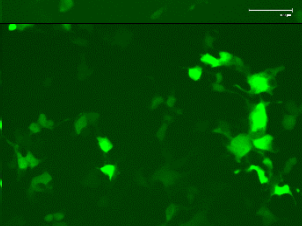
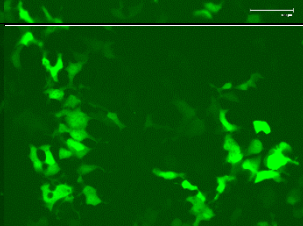
20,000 cells were plated and centrifuged with 100 ul Null DMEM (left) or 50 ul Null DMEM+ 50 ul pseudotyped virus suspension (right) for 1 hour at 1000g, 32°C. After 48 hours of incubation at 37 °C, GFP expression of the cells were visualized on FLOID™ Cell Imaging Station and quantified by flow cytometry.

Having confirmed that ACE2-Pseudotype virus interaction led to GFP expression in cells through Fluorescence Microscopy and Flow Cytometry, we proceeded to assess

the neutralizing antibody titers in sera of vaccinated volunteers. Signal obtained from 'pseudovirus only' positive controls served as a reference for normalization of mean fluorescent intensities resulting from GFP expression in the neutralization assay.

Figure 3.9 presents neutralizing antibody levels in serially diluted sera of mice receiving Deltaplus-S-6p-VLP as a third booster (n=4) in comparison to sera from BioNTech and SinoVac vaccinated volunteers. Moreover, neutralization rates, which are based on reduction in mean fluorescent intensity in the diluted sera of each sample were based on flow cytometry results (Appendix F) and were represented in separate graphs. In parallel experiments, neutralizing activities of sera from twelve Alpha-S-6p-VLP vaccinated volunteers was carried out with the same procedure as described above (Figure 3.10).

			1:2
			1:4
			1:8
			1:16
			1:32
			1:64
			1:128
Deltap-S-6p-VLP-V1	Deltap-S-6p-VLP-V2	Deltap-S-6p-VLP-V3	BN DF

			1:2
			1:4
			1:8
			1:16
			1:32
			1:64
			1:128
Deltap-S-6p-VLP-V4	BioNTech	SinoVac	BN DF

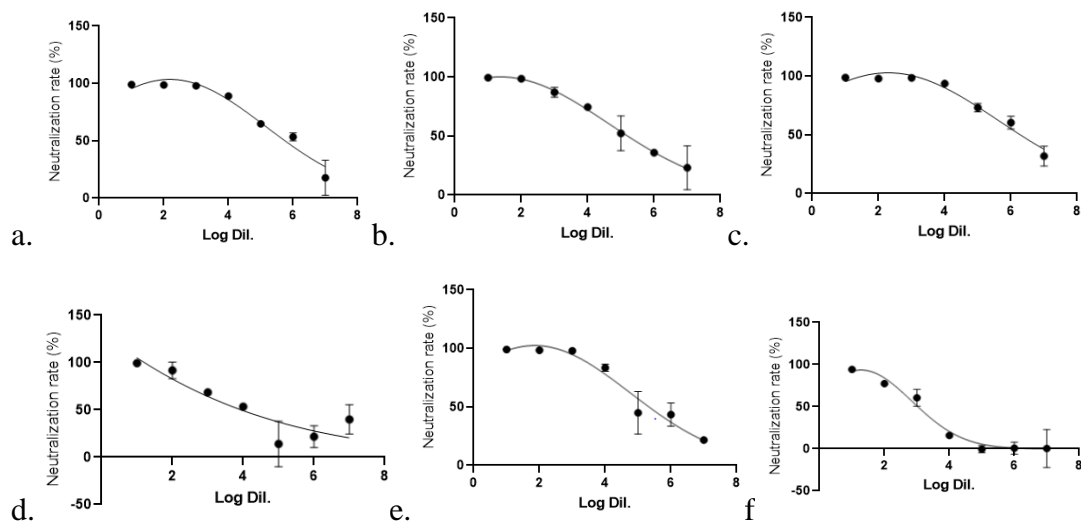


Figure 3.9. Fluorescent Microscopy Images and Neutralization Activity Analysis from the Sera of Deltap-S-6p-VLP, BioNTech and SinoVac Vaccinated Mice/Volunteers (DF: dilution factor, BN: Balb/c number).

Serum samples were serially diluted with FBS-free fresh DMEM to 50 ul final volume. Then, 50 ul of pseudovirus solution was added onto diluted sera, and the mixtures were left for incubation at 37 °C for 1.5 hour to enable binding of available neutralizing antibodies in the sera to the Spike epitopes on the pseudoviruses. The incubated mixtures were then added onto HEK293-FT-hACE2 cells together with the polybrene (.08%), followed by centrifugation at 1000g, 32 °C for one hour. Plates were incubated at 37 °C for 48 hours. At the end of 48h incubation, cells were imaged on a FLoid™ Cell Imaging Station and GFP expressions were quantified using Flow Cytometry. The assay was performed in duplicate.

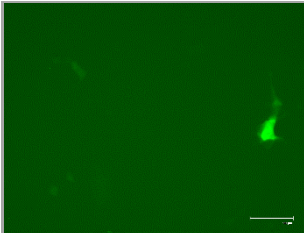
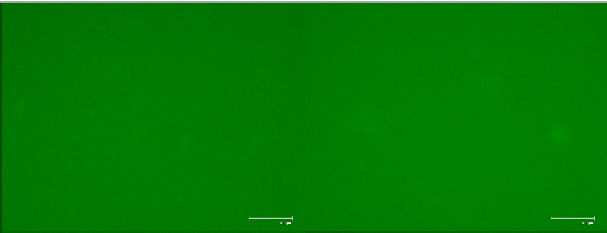

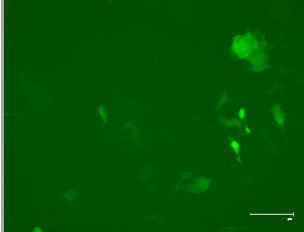
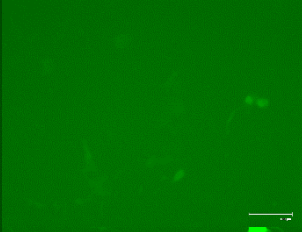
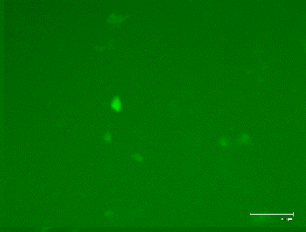
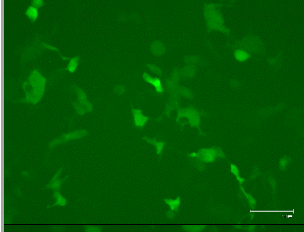
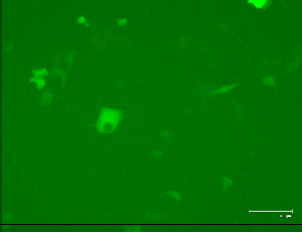
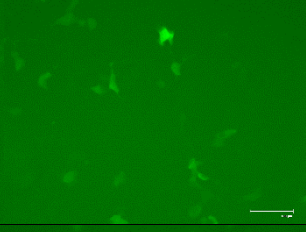
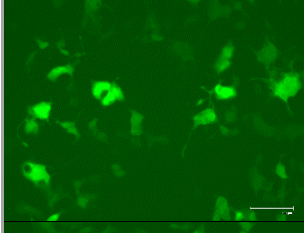
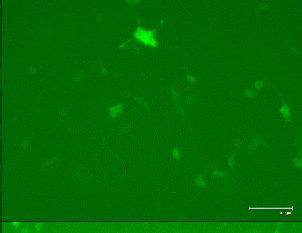
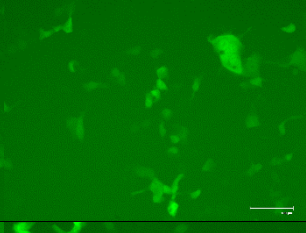
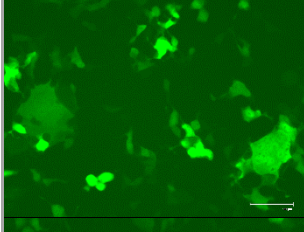
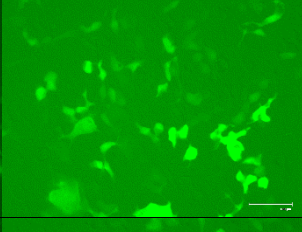
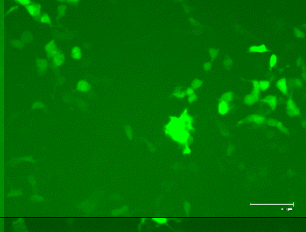
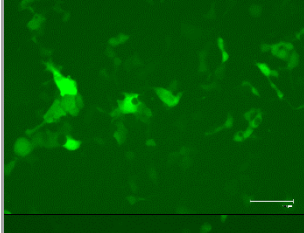
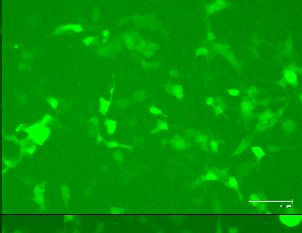
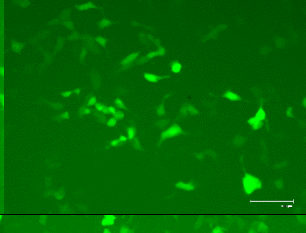
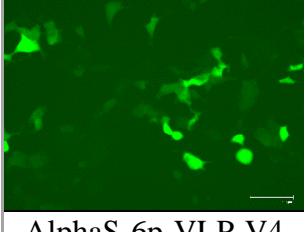
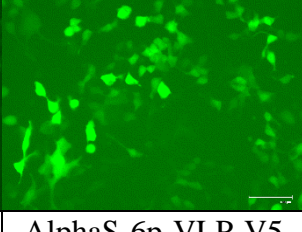
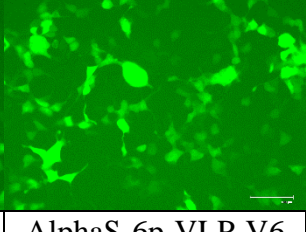
In the upper panel, each column represents FLoid™ images of an individual according to dilutions of the sera indicated at right marginst.

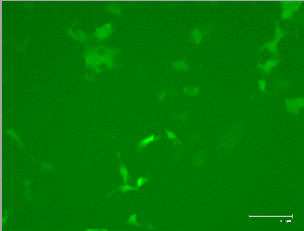
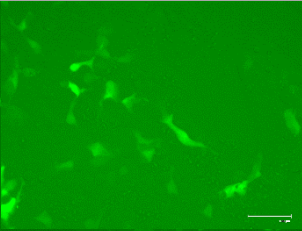
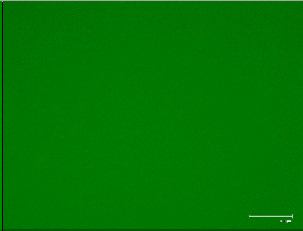
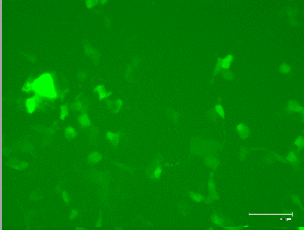
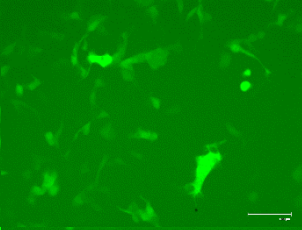
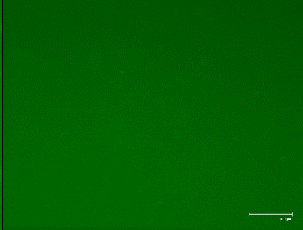
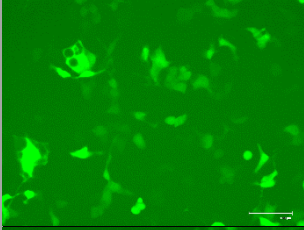
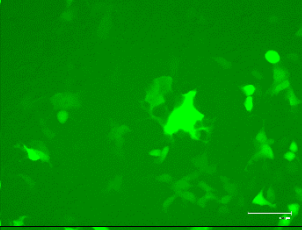
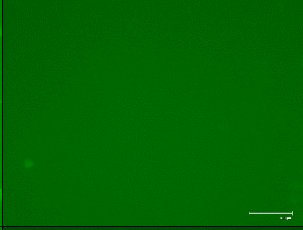
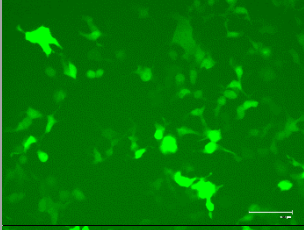
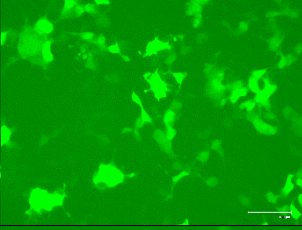
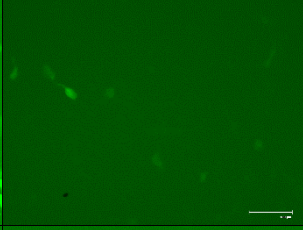
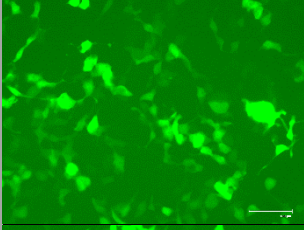
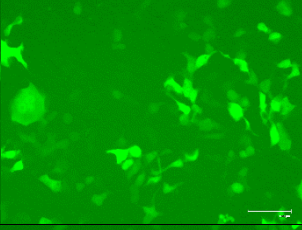
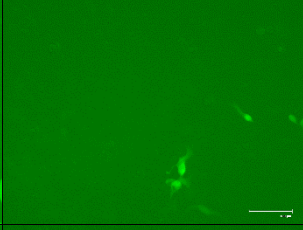
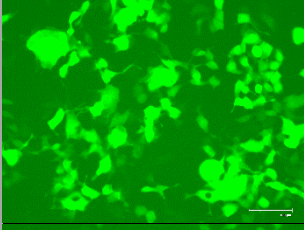
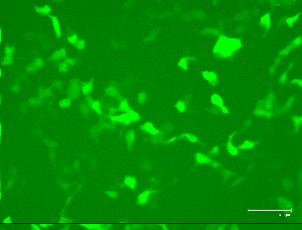
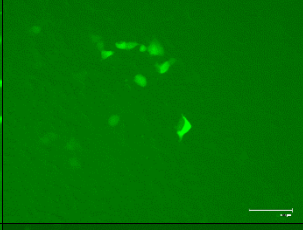
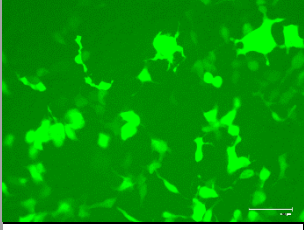
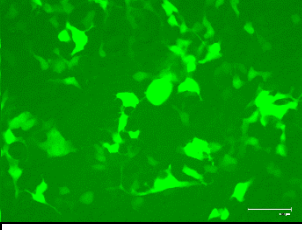
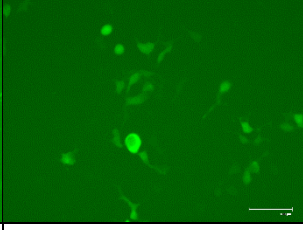
Graphs in the lower panel depict the changes in neutralization rate according to log dilutions of the sera from (a) to (f) in the following order: Deltap-S-6p-VLP-V1, Deltap-S-6p-VLP-V2, Deltap-S-6p-VLP-V3, Deltap-S-6p-VLP-V4, BioNTech, SinoVac.

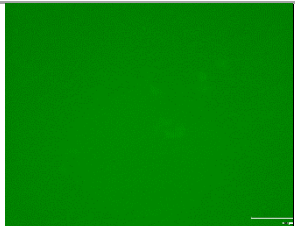
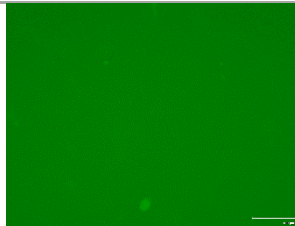
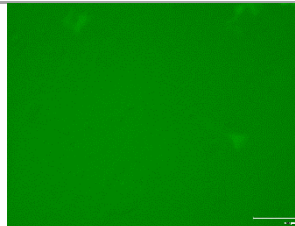
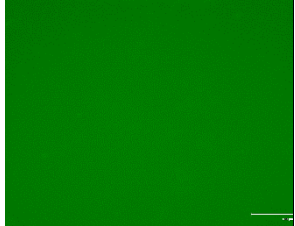
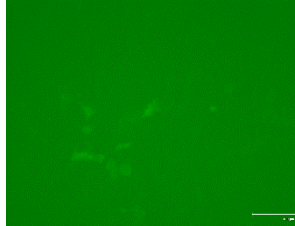
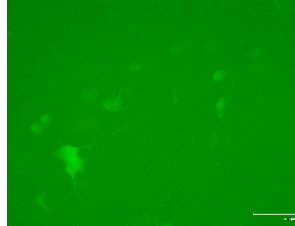
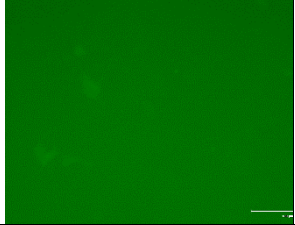
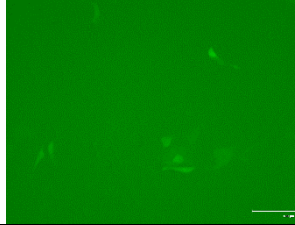
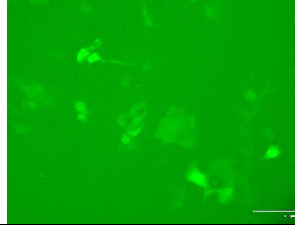
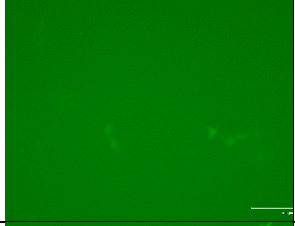
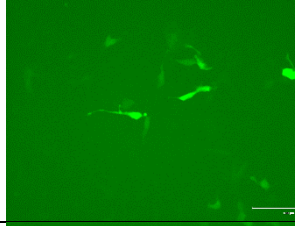
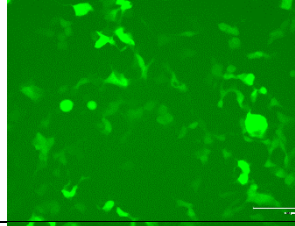
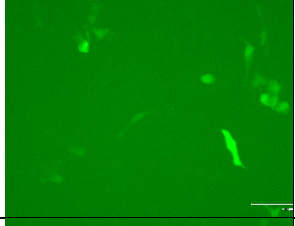
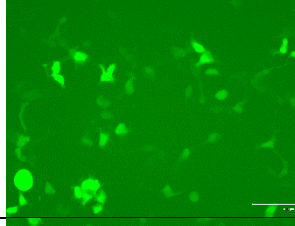
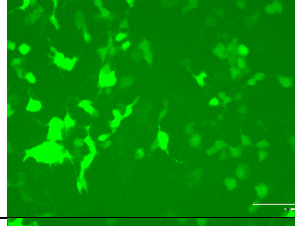
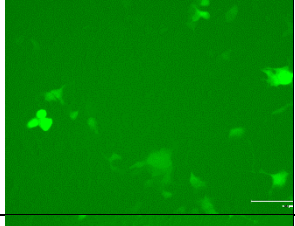
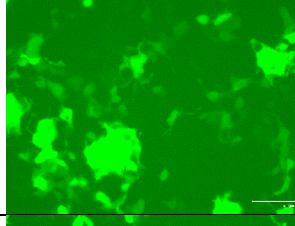
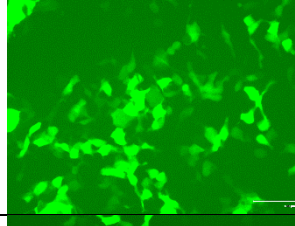
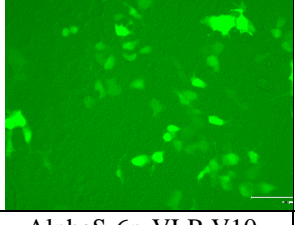
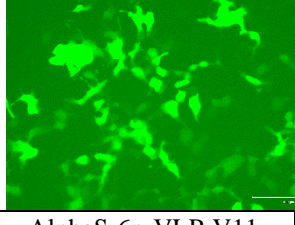
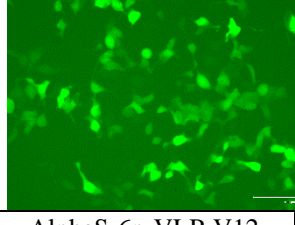
All mice boosted with the Deltaplus-S-6p-VLPs had neutralizing antibodies to the pseudotyped virus at a titer of at least 1:8 (Figure 3.9a, b, c), which was comparable to the titer generated in a BioNTech (Figure 3.9e) vaccinated individual. Although our sample size is too small to conduct statistical analyses between different

vaccines, nevertheless, serum obtained from a SinoVac vaccinated individual displayed the least amount of neutralizing antibody titers (Figure 3.9f).

			1:2
			1:4
			1:8
			1:16
			1:32
			1:64
			1:128
AlphaS-6p-VLP-V1	AlphaS-6p-VLP-V2	AlphaS-6p-VLP-V3	VN DF

			1:2
			1:4
			1:8
			1:16
			1:32
			1:64
			1:128
AlphaS-6p-VLP-V4	AlphaS-6p-VLP-V5	AlphaS-6p-VLP-V6	VN DF

			1:2
			1:4
			1:8
			1:16
			1:32
			1:64
			1:128
AlphaS-6p-VLP-V7	AlphaS-6p-VLP-V8	AlphaS-6p-VLP-V9	VN DF

			1:2
			1:4
			1:8
			1:16
			1:32
			1:64
			1:128
AlphaS-6p-VLP-V10	AlphaS-6p-VLP-V11	AlphaS-6p-VLP-V12	VN DF

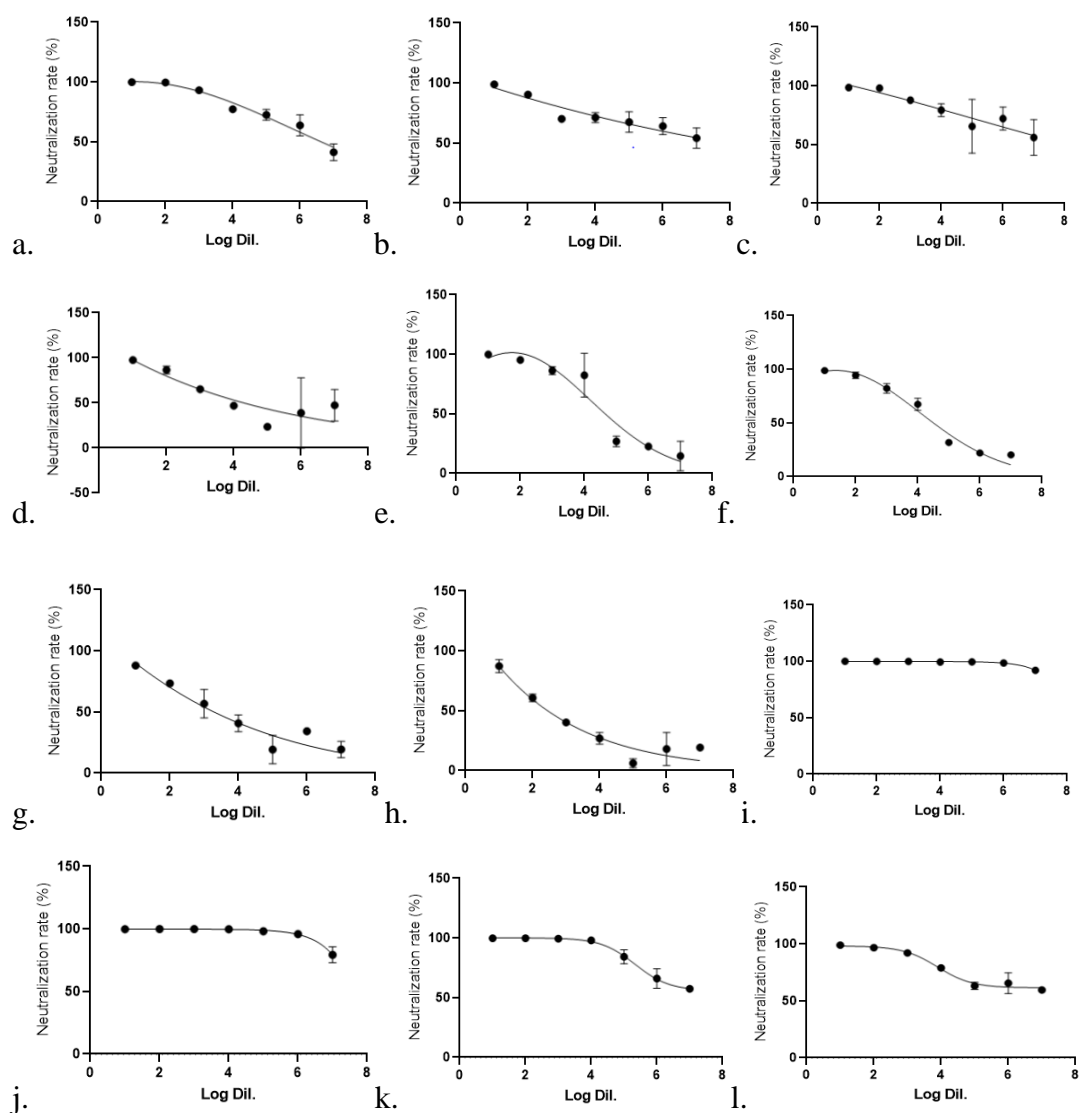


Figure 3.10. Fluorescent Microscopy Images and Neutralization Activity Analysis from the Sera of Alpha-S-6p-VLP Vaccinated Volunteers (DF: dilution factor, VN: volunteer number).

Neutralization assay, images and GFP expressions in the cells were performed as described in the legend of the Figure 3.9, and the assay was performed in duplicate.

In the upper panel, each column represents FLoid™ images of an individual according to dilutions of the sera indicated at right marginst.

Graphs in the lower panel show the changes in neutralization rate according to log dilutions of the sera from (a) to (l) in the following order of the increasing numbers of the Alpha-S-6p-VLP vaccinated volunteers from one to twelve: V1 to V12.

All volunteers vaccinated with Alpha-S-6p-VLP also had substantial levels of neutralizing antibodies and there were no non-responders (Figure 3.10).

Taken together, our results suggest that pseudotyped viruses bearing the SARS-CoV-2 Spike with the D614G mutation, could be generated and proved to be a valuable tool in assessment of neutralizing antibody titers in vaccinated volunteers and mice. Furthermore, despite limited sample size, preliminary results indicate that sera from Alpha-S- & Deltaplus-S- 6P- VLP vaccinated volunteers or mice contained neutralizing antibodies against the pseudotyped virus.

Collectively, our strategy to produce variant specific VLPs as vaccine antigens against the B.1.1.7 and B.1.617.2.1 variants of interest particularly since these could generate neutralizing antibodies against the mutated Spike epitopes, indicating their potential utility as protective vaccines. The adaptability to emerging variants with minimal effort is an advantage of the VLP platform and might prove to be of benefit in development of vaccines against rapidly mutating infectious agents. Moreover, it is noteworthy that pseudotyped virus neutralization assay is a valuable laboratory tool in evaluation of vaccine induced Nab levels and could be established in non BSL-3 laboratories, broadening the capability of laboratories throughout the country to perform neutralization assay.

CHAPTER 4

CONCLUSION

Previous studies from our laboratory on Virus Like Particle based vaccine production strategy against SARS-CoV-2, demonstrated the immunoprotective effects of VLPs when formulated with CpG ODN plus Alum. These VLPs consist of M, N, E proteins of the authentic virus and prefusion stabilized Spike protein with its six proline substitutions (Yilmaz et al., 2021). Since late 2020, with the emergence of several variants of concern (VOC) and declining efficacy of the currently applied vaccines against the variants (especially against Alpha (B.1.1.7) and Delta (B.1.617.2) variants), necessity to develop variant specific vaccines arose. Therefore, in this thesis, we intended to produce variant-specific VLP based vaccines against the Alpha (B.1.1.7) and sublineage of Delta (B.1.617.2.1) variants. The design of Spike antigen was based on the mutations carried on Delta plus (B.1.617.2.1) or the Alpha (B.1.1.7) variant of concern together with hexaproline stabilization. Alpha or Delta plus variant Spike protein expression genes were cloned into pVITRO2 vector together with the Envelope protein expression gene. Meanwhile, Membrane glycoprotein plus Nucleocapsid genes were cloned into the pVITRO1. Success of clonings were verified by restriction enzyme digestions and next generation sequencing. The plasmid constructs were transfected to Hek293 suspension cells with an optimized DNA:PEIpro ratio of 1:2. Purification of the VLP products were performed five days after the transfection, which was determined by tracking the rates of secretion of VLPs into supernatant on different days. Then, expression of the four structural proteins in purified VLPs harboring the Alpha or the Delta plus variant Spike were verified through immunoblotting. Furthermore, nanoparticulate nature of both products were tested by tunable-resistive pulse sensing (TRPS) measurements. These measurements demonstrated similarity of size distribution of the purified

VLPs with the SARS-CoV-2 virion, which is in the range of 60-140 nm in diameter (Bar-On et al., 2020). Moreover, to investigate the effects of the mutations on Spike incorporation efficiency into VLPs, we quantitated spike protein amounts among Alpha-, Deltaplus- and WT- 6p-VLPs using VLPs containing equal concentrations of protein. Our results revealed that Spike expression significantly increased in both variant Spike expressing VLPs in contrast to WT VLPs. The increased spike incorporation of variant spikes into VLPs might have stem from the D614G substitution, in which was previously reported to increase stability and expression of the Spike (Volz, Hill, et al., 2021). However, the contributions of other mutations found in Alpha and Delta plus variants to spike fitness cannot be excluded.

In summary, we concluded that Alpha-6p-VLPs and Deltaplus-6p-VLPs were successfully produced at their expected size range. Then, we analyzed protein and DNA contents in the final products to understand whether the VLPs conformed with acceptable protein/DNA limits for formulation with the adjuvants prior to preclinical immunization studies. As a result of this analysis and the assessment of their variant specific vaccine potential through immunization experiments on mice, volunteers received the Alpha-6p-VLP as part of the phase 2 clinical studies. 4 mice received Delta plus-6p-VLP vaccine as a third booster. Vaccine induced neutralizing antibody levels, generally peak at 24-59 days of post-vaccination (K. Wang et al., 2021). Therefore, we aimed to explore the neutralizing antibody eliciting capacities of these products in order to assess their protective abilities. Accordingly, we collected sera from the volunteers and mice 49 days post-vaccination and established a pseudotyped virus based neutralization assay. For this, replication incompetent Spike protein expressing lentiviral pseudovirus system carrying a GFP reporter gene was generated.

The neutralization experiments were conducted with serially diluted sera from the volunteers/mice and GFP expressions in target cells were normalized to positive controls. These experiments demonstrated significant decrease in GFP expressions in all volunteers from both vaccination groups. The reduction in GFP expression

correlated with reduction in pseudotyped virus infection resulting from neutralizing activity in the sera. Therefore, both Delta-6p-VLPs and Alpha-6p-VLPs containing vaccines actively elicited neutralizing antibody production which intervened with ACE2-SARS-CoV-2 Spike interaction. Collectively, we concluded that both variant specific VLP products are immunoprotective against the variants of concern and can be utilized as variant specific vaccine candidates capable of eliciting NAbs. Unquestionably, more experiments have to be performed regarding the mutations and neutralizing levels, in large number of volunteers. Moreover, pseudotyped virus neutralization assay expands the capability of non-BSL3 laboratories to carry out neutralization assays to measure not only the efficacy of the vaccines but also the durability of the vaccine induced neutralizing antibodies.

REFERENCES

- Abdool Karim, S. S., & de Oliveira, T. (2021). New SARS-CoV-2 Variants — Clinical, Public Health, and Vaccine Implications. *New England Journal of Medicine*, 384(19), 1866–1868. <https://doi.org/10.1056/nejmc2100362>
- Abu-Raddad, L. J., Chemaitelly, H., & Butt, A. A. (2021). Effectiveness of the BNT162b2 Covid-19 Vaccine against the B.1.1.7 and B.1.351 Variants. *New England Journal of Medicine*, 385(2), 187–189. <https://doi.org/10.1056/nejmc2104974>
- Allegra, A., di Gioacchino, M., Tonacci, A., Musolino, C., & Gangemi, S. (2020). Immunopathology of SARS-CoV-2 infection: Immune cells and mediators, prognostic factors, and immune-therapeutic implications. In *International Journal of Molecular Sciences* (Vol. 21, Issue 13, pp. 1–19). MDPI AG. <https://doi.org/10.3390/ijms21134782>
- Alsaadi, E. A. J., & Jones, I. M. (2019). Membrane binding proteins of coronaviruses. In *Future Virology* (Vol. 14, Issue 4, pp. 275–286). Future Medicine Ltd. <https://doi.org/10.2217/fvl-2018-0144>
- Andrade, V. M., Christensen-Quick, A., Agnes, J., Tur, J., Reed, C., Kalia, R., Marrero, I., Elwood, D., Schultheis, K., Purwar, M., Reuschel, E., McMullan, T., Pezzoli, P., Kraynyak, K., Sylvester, A., Mammen, M. P., Tebas, P., Kim, J. J., Weiner, D. B., ... Broderick, K. E. (2021). INO-4800 DNA vaccine induces neutralizing antibodies and T cell activity against global SARS-CoV-2 variants. *New England Journal of Medicine*, 121. <https://doi.org/10.1038/s41541-021-00384-7>
- Arevalo, M. T., Wong, T. M., & Ross, T. M. (2016). Expression and purification of virus-like particles for vaccination. *Journal of Visualized Experiments*, 2016(112). <https://doi.org/10.3791/54041>
- Baden, L. R., el Sahly, H. M., Essink, B., Kotloff, K., Frey, S., Novak, R., Diemert, D., Spector, S. A., Rouphael, N., Creech, C. B., McGettigan, J., Khetan, S., Segall, N.,

- Solis, J., Brosz, A., Fierro, C., Schwartz, H., Neuzil, K., Corey, L., ... Zaks, T. (2021). Efficacy and Safety of the mRNA-1273 SARS-CoV-2 Vaccine. *New England Journal of Medicine*, 384(5), 403–416. <https://doi.org/10.1056/nejmoa2035389>
- Bai, Z., Cao, Y., Liu, W., & Li, J. (2021). The sars-cov-2 nucleocapsid protein and its role in viral structure, biological functions, and a potential target for drug or vaccine mitigation. In *Viruses* (Vol. 13, Issue 6). MDPI AG. <https://doi.org/10.3390/v13061115>
- Bar-On, Y. M., Flamholz, A., Phillips, R., & Milo, R. (2020). Sars-cov-2 (Covid-19) by the numbers. *ELife*, 9. <https://doi.org/10.7554/eLife.57309>
- Bianchi, M., Benvenuto, D., Giovanetti, M., Angeletti, S., Ciccozzi, M., & Pascarella, S. (2020). Sars-CoV-2 Envelope and Membrane Proteins: Structural Differences Linked to Virus Characteristics? *BioMed Research International*, 2020. <https://doi.org/10.1155/2020/4389089>
- Boson, B., Legros, V., Zhou, B., Siret, E., Mathieu, C., Cosset, F. L., Lavillette, D., & Denolly, S. (2021). The SARS-CoV-2 envelope and membrane proteins modulate maturation and retention of the spike protein, allowing assembly of virus-like particles. *Journal of Biological Chemistry*, 296. <https://doi.org/10.1074/jbc.RA120.016175>
- Bourgonje, A. R., Abdulle, A. E., Timens, W., Hillebrands, J. L., Navis, G. J., Gordijn, S. J., Bolling, M. C., Dijkstra, G., Voors, A. A., Osterhaus, A. D. M. E., van der Voort, P. H. J., Mulder, D. J., & van Goor, H. (2020). Angiotensin-converting enzyme 2 (ACE2), SARS-CoV-2 and the pathophysiology of coronavirus disease 2019 (COVID-19). In *Journal of Pathology* (Vol. 251, Issue 3, pp. 228–248). John Wiley and Sons Ltd. <https://doi.org/10.1002/path.5471>
- Cele, S., Jackson, L., Khoury, D. S., Khan, K., Moyo-Gwete, T., Tegally, H., Emmanuel San, J., Cromer, D., Scheepers, C., Amoako, D., Karim, F., Bernstein, M., Lustig,

- G., Archary, D., Smith, M., Ganga, Y., Jule, Z., Reedoy, K., Hwa, S.-H., ... Sigal, A. (n.d.). SARS-CoV-2 Omicron has extensive but incomplete escape of Pfizer BNT162b2 elicited neutralization and requires ACE2 for infection. *Richard J. Lessells*, 11, 12. <https://doi.org/10.1101/2021.12.08.21267417>
- Channappanavar, R., & Perlman, S. (2017). Pathogenic human coronavirus infections: causes and consequences of cytokine storm and immunopathology. *Springer*, 39, 529–539. <https://doi.org/10.1007/s00281-017-0629-x>
- Chaplin, D. D. (2010). Overview of the immune response. *Journal of Allergy and Clinical Immunology*, 125(2 SUPPL. 2). <https://doi.org/10.1016/j.jaci.2009.12.980>
- Chen, Y., Liu, Q., & Guo, D. (2020). Emerging coronaviruses: Genome structure, replication, and pathogenesis. In *Journal of Medical Virology* (Vol. 92, Issue 4, pp. 418–423). John Wiley and Sons Inc. <https://doi.org/10.1002/jmv.25681>
- Chen, Z., & John Wherry, E. (2020). T cell responses in patients with COVID-19. *Nature Reviews Immunology*, 20(9), 529–536. <https://doi.org/10.1038/s41577-020-0402-6>
- Chmielewska, A. M., Czarnota, A., Bieńkowska-Szewczyk, K., & Grzyb, K. (2021). Immune response against SARS-CoV-2 variants: the role of neutralization assays. *Npj Vaccines*. <https://doi.org/10.1038/s41541-021-00404-6>
- Dai, S., Wang, H., & Deng, F. (2018). Minireview Open Access Advances and challenges in enveloped virus-like particle (VLP)-based vaccines. In *J Immunol Sci* (Vol. 2, Issue 2).
- Deng, X., Garcia-Knight, M. A., Khalid, M. M., Servellita, V., Wang, C., Morris, M. K., Sotomayor-González, A., Glasner, D. R., Reyes, K. R., Gliwa, A. S., Reddy, N. P., Sanchez San Martin, C., Federman, S., Cheng, J., Balcerek, J., Taylor, J., Streithorst, J. A., Miller, S., Sreekumar, B., ... Chiu, C. Y. (2021). Transmission, infectivity, and neutralization of a spike L452R SARS-CoV-2 variant. *Cell*, 184(13), 3426-3437.e8. <https://doi.org/10.1016/J.CELL.2021.04.025>

- Dey, A., Chozhavel Rajanathan, T. M., Chandra, H., Pericherla, H. P. R., Kumar, S., Choonia, H. S., Bajpai, M., Singh, A. K., Sinha, A., Saini, G., Dalal, P., Vandriwala, S., Raheem, M. A., Divate, R. D., Navlani, N. L., Sharma, V., Parikh, A., Prasath, S., Sankar Rao, M., & Maithal, K. (2021). Immunogenic potential of DNA vaccine candidate, ZyCoV-D against SARS-CoV-2 in animal models. *Vaccine*, 39(30), 4108–4116. <https://doi.org/10.1016/j.vaccine.2021.05.098>
- Dong, Y., Dai, T., Wei, Y., Zhang, L., Zheng, M., & Zhou, F. (2020). A systematic review of SARS-CoV-2 vaccine candidates. In *Signal Transduction and Targeted Therapy* (Vol. 5, Issue 1). Springer Nature. <https://doi.org/10.1038/s41392-020-00352-y>
- Garcia-Beltran, W. F., Lam, E. C., St. Denis, K., Nitido, A. D., Garcia, Z. H., Hauser, B. M., Feldman, J., Pavlovic, M. N., Gregory, D. J., Poznansky, M. C., Sigal, A., Schmidt, A. G., Iafrate, A. J., Naranbhai, V., & Balazs, A. B. (2021). Multiple SARS-CoV-2 variants escape neutralization by vaccine-induced humoral immunity. *Cell*, 184(9), 2372-2383.e9. <https://doi.org/10.1016/j.cell.2021.03.013>
- Ghorbani, A., Zare, F., Sazegari, S., Afsharifar, A., Eskandari, M. H., & Pormohammad, A. (2020). Development of a novel platform of virus-like particle (VLP)-based vaccine against COVID-19 by exposing epitopes: an immunoinformatics approach. *New Microbes and New Infections*, 38. <https://doi.org/10.1016/j.nmni.2020.100786>
- Gobeil, P., Pillet, S., Boulay, I., Charland, N., Lorin, A., Cheng, M. P., Vinh, D. C., Boutet, P., van der Most, R., Roman, F., de Los, M., Ceregido Perez, A., D'aoust, M.-A., Landry, N., & Ward, B. J. (n.d.). *Durability and Cross-Reactivity of Immune Responses Induced by an AS03 Adjuvanted Plant-Based Recombinant Virus-Like Particle Vaccine for COVID-19*. <https://doi.org/10.1101/2021.08.04.21261507>
- Gorbalenya, A. E., Baker, S. C., Baric, R. S., de Groot, R. J., Drosten, C., Gulyaeva, A. A., Haagmans, B. L., Lauber, C., Leontovich, A. M., Neuman, B. W., Penzar, D., Perlman, S., Poon, L. L. M., Samborskiy, D. v., Sidorov, I. A., Sola, I., & Ziebuhr, J. (2020a). The species Severe acute respiratory syndrome-related coronavirus: classifying 2019-nCoV and naming it SARS-CoV-2. In *Nature Microbiology* (Vol.

5, Issue 4, pp. 536–544). *Nature Research*. <https://doi.org/10.1038/s41564-020-0695-z>

Gorbalenya, A. E., Baker, S. C., Baric, R. S., de Groot, R. J., Drosten, C., Gulyaeva, A. A., Haagmans, B. L., Lauber, C., Leontovich, A. M., Neuman, B. W., Penzar, D., Perlman, S., Poon, L. L. M., Samborskiy, D. v., Sidorov, I. A., Sola, I., & Ziebuhr, J. (2020b). The species Severe acute respiratory syndrome-related coronavirus: classifying 2019-nCoV and naming it SARS-CoV-2. In *Nature Microbiology* (Vol. 5, Issue 4, pp. 536–544). *Nature Research*. <https://doi.org/10.1038/s41564-020-0695-z>

Gordon, D. E., Jang, G. M., Bouhaddou, M., Xu, J., Obernier, K., White, K. M., O’Meara, M. J., Rezelj, V. v., Guo, J. Z., Swaney, D. L., Tummino, T. A., Hüttenhain, R., Kaake, R. M., Richards, A. L., Tutuncuoglu, B., Foussard, H., Batra, J., Haas, K., Modak, M., ... Krogan, N. J. (2020). A SARS-CoV-2 protein interaction map reveals targets for drug repurposing. *Nature*, 583(7816), 459–468. <https://doi.org/10.1038/s41586-020-2286-9>

Grifoni, A., Weiskopf, D., Ramirez, S. I., Mateus, J., Dan, J. M., Moderbacher, C. R., Rawlings, S. A., Sutherland, A., Premkumar, L., Jadi, R. S., Marrama, D., de Silva, A. M., Frazier, A., Carlin, A. F., Greenbaum, J. A., Peters, B., Krammer, F., Smith, D. M., Crotty, S., & Sette, A. (2020). Targets of T Cell Responses to SARS-CoV-2 Coronavirus in Humans with COVID-19 Disease and Unexposed Individuals. *Cell*, 181(7), 1489-1501.e15. <https://doi.org/10.1016/j.cell.2020.05.015>

Harvey, W. T., Carabelli, A. M., Jackson, B., Gupta, R. K., Thomson, E. C., Harrison, E. M., Ludden, C., Reeve, R., Rambaut, A., Peacock, S. J., & Robertson, D. L. (2021). SARS-CoV-2 variants, spike mutations and immune escape. In *Nature Reviews Microbiology* (Vol. 19, Issue 7, pp. 409–424). *Nature Research*. <https://doi.org/10.1038/s41579-021-00573-0>

Hatmal, M. M., Alshaer, W., Al-Hatamleh, M. A. I., Hatmal, M., Smadi, O., Taha, M. O., Oweida, A. J., Boer, J. C., Mohamud, R., & Plebanski, M. (2020). Comprehensive

Structural and Molecular Comparison of Spike Proteins of SARS-CoV-2, SARS-CoV and MERS-CoV, and Their Interactions with ACE2. In *Cells* (Vol. 9, Issue 12). NLM (Medline). <https://doi.org/10.3390/cells9122638>

He, X., Hong, W., Pan, X., Lu, G., & Wei, X. (2021). SARS-CoV-2 Omicron variant: Characteristics and prevention. *MedComm*, 2(4), 838–845. <https://doi.org/10.1002/mco2.110>

Hester Allen, A., Vusirikala, A., Flannagan, J., Twohig, K. A., Zaidi, A., Harris, R., Charlett, A., Dabrera, G., Kall, M., & Author affiliations, M. (n.d.). *Increased household transmission of COVID-19 cases associated with SARS-CoV-2 Variant of Concern B.1.617.2: a national case-control study.*

Hoffmann, M., Kleine-Weber, H., Schroeder, S., Krüger, N., Herrler, T., Erichsen, S., Schiergens, T. S., Herrler, G., Wu, N. H., Nitsche, A., Müller, M. A., Drosten, C., & Pöhlmann, S. (2020). SARS-CoV-2 Cell Entry Depends on ACE2 and TMPRSS2 and Is Blocked by a Clinically Proven Protease Inhibitor. *Cell*, 181(2), 271-280.e8. <https://doi.org/10.1016/j.cell.2020.02.052>

Hu, B., Guo, H., Zhou, P., & Shi, Z. L. (2021a). Characteristics of SARS-CoV-2 and COVID-19. In *Nature Reviews Microbiology* (Vol. 19, Issue 3, pp. 141–154). Nature Research. <https://doi.org/10.1038/s41579-020-00459-7>

Hu, B., Guo, H., Zhou, P., & Shi, Z. L. (2021b). Characteristics of SARS-CoV-2 and COVID-19. In *Nature Reviews Microbiology* (Vol. 19, Issue 3, pp. 141–154). Nature Research. <https://doi.org/10.1038/s41579-020-00459-7>

Huang, Y., Yang, C., Xu, X. feng, Xu, W., & Liu, S. wen. (2020). Structural and functional properties of SARS-CoV-2 spike protein: potential antiviral drug development for COVID-19. In *Acta Pharmacologica Sinica* (Vol. 41, Issue 9, pp. 1141–1149). Springer Nature. <https://doi.org/10.1038/s41401-020-0485-4>

Iwata-Yoshikawa, N., Okamura, T., Shimizu, Y., Hasegawa, H., Takeda, M., Nagata, N., & Gallagher, T. (2019). TMPRSS2 Contributes to Virus Spread and

- Immunopathology in the Airways of Murine Models after Coronavirus Infection. *Jvi.Asm.Org I Journal of Virology*, 93, 1815–1833. <https://doi.org/10.1128/JVI>
- Keech, C., Albert, G., Cho, I., Robertson, A., Reed, P., Neal, S., Plested, J. S., Zhu, M., Cloney-Clark, S., Zhou, H., Smith, G., Patel, N., Frieman, M. B., Haupt, R. E., Logue, J., McGrath, M., Weston, S., Piedra, P. A., Desai, C., ... Glenn, G. M. (2020). Phase 1–2 Trial of a SARS-CoV-2 Recombinant Spike Protein Nanoparticle Vaccine. *New England Journal of Medicine*, 383(24), 2320–2332. <https://doi.org/10.1056/nejmoa2026920>
- Keni, R., Alexander, A., Nayak, P. G., Mudgal, J., & Nandakumar, K. (2020). COVID-19: Emergence, Spread, Possible Treatments, and Global Burden. In *Frontiers in Public Health* (Vol. 8). Frontiers Media S.A. <https://doi.org/10.3389/fpubh.2020.00216>
- Krammer, F. (2020). SARS-CoV-2 vaccines in development. In *Nature* (Vol. 586, Issue 7830, pp. 516–527). Nature Research. <https://doi.org/10.1038/s41586-020-2798-3>
- Kumar, S., Nyodu, R., Maurya, V. K., & Saxena, S. K. (2020). *Morphology, Genome Organization, Replication, and Pathogenesis of Severe Acute Respiratory Syndrome Coronavirus 2 (SARS-CoV-2)* (pp. 23–31). https://doi.org/10.1007/978-981-15-4814-7_3
- Kyriakidis, N. C., López-Cortés, A., González, E. V., Grimaldos, A. B., & Prado, E. O. (2021). SARS-CoV-2 vaccines strategies: a comprehensive review of phase 3 candidates. In *npj Vaccines* (Vol. 6, Issue 1). Nature Research. <https://doi.org/10.1038/s41541-021-00292-w>
- Lebeau, G., Vagner, D., Frumence, É., Ah-Pine, F., Guillot, X., Nobécourt, E., Raffray, L., & Gasque, P. (2020). Molecular Sciences Deciphering SARS-CoV-2 Virologic and Immunologic Features. *International Journal of Molecular Sciences*. <https://doi.org/10.3390/ijms21165932>

- Li, J., Lai, S., Gao, G. F., & Shi, W. (2021). The emergence, genomic diversity and global spread of SARS-CoV-2. *Nature*, *600*(7889), 408–418. <https://doi.org/10.1038/s41586-021-04188-6>
- Li, M., Ye, G., Si, Y., Shen, Z., Liu, Z., Shi, Y., Xiao, S., Fu, Z. F., & Peng, G. (2021). *Structure of the multiple functional domains from coronavirus nonstructural protein 3*. <https://doi.org/10.1080/22221751.2020.1865840>
- Li, Q., Guan, X., Wu, P., Wang, X., Zhou, L., Tong, Y., Ren, R., Leung, K. S. M., Lau, E. H. Y., Wong, J. Y., Xing, X., Xiang, N., Wu, Y., Li, C., Chen, Q., Li, D., Liu, T., Zhao, J., Liu, M., ... Feng, Z. (2020). Early Transmission Dynamics in Wuhan, China, of Novel Coronavirus–Infected Pneumonia. *New England Journal of Medicine*, *382*(13), 1199–1207. <https://doi.org/10.1056/nejmoa2001316>
- Li, X., Hou, P., Ma, W., Wang, X., Wang, H., Yu, Z., Chang, H., Wang, T., Jin, S., Wang, X., Wang, W., Zhao, Y., Zhao, Y., Xu, C., Ma, X., Gao, Y., & He, H. (2021). SARS-CoV-2 ORF10 suppresses the antiviral innate immune response by degrading MAVS through mitophagy. *Cellular and Molecular Immunology*. <https://doi.org/10.1038/s41423-021-00807-4>
- Li, X. N., Huang, Y., Wang, W., Jing, Q. L., Zhang, C. H., Qin, P. Z., Guan, W. J., Gan, L., Li, Y. L., Liu, W. H., Dong, H., Miao, Y. T., Fan, S. J., Zhang, Z. bin, Zhang, D. M., & Zhong, N. S. (2021). Effectiveness of inactivated SARS-CoV-2 vaccines against the Delta variant infection in Guangzhou: a test-negative case–control real-world study. *Emerging Microbes and Infections*, *10*(1), 1751–1759. <https://doi.org/10.1080/22221751.2021.1969291>
- Li, X., Wang, W., Zhao, X., Zai, J., Zhao, Q., Li, Y., & Chaillon, A. (2020). Transmission dynamics and evolutionary history of 2019-nCoV. *Journal of Medical Virology*, *92*(5), 501–511. <https://doi.org/10.1002/jmv.25701>
- Lin, X., Fu, B., Yin, S., Li, Z., Liu, H., Zhang, H., Xing, N., Wang, Y., Xue, W., Xiong, Y., Zhang, S., Zhao, Q., Xu, S., Zhang, J., Wang, P., Nian, W., Wang, X., & Wu, H.

- (2021). ORF8 contributes to cytokine storm during SARS-CoV-2 infection by activating IL-17 pathway. *IScience*, 24(4). <https://doi.org/10.1016/j.isci.2021.102293>
- Logunov, D. Y., Dolzhikova, I. v., Shcheblyakov, D. v., Tukhvatulin, A. I., Zubkova, O. v., Dzharullaeva, A. S., Kovyrshina, A. v., Lubenets, N. L., Grousova, D. M., Erokhova, A. S., Botikov, A. G., Izhaeva, F. M., Popova, O., Ozharovskaya, T. A., Esmagambetov, I. B., Favorskaya, I. A., Zrelkin, D. I., Voronina, D. v., Shcherbinin, D. N., ... Gintsburg, A. L. (2021). Safety and efficacy of an rAd26 and rAd5 vector-based heterologous prime-boost COVID-19 vaccine: an interim analysis of a randomised controlled phase 3 trial in Russia. *The Lancet*, 397(10275), 671–681. [https://doi.org/10.1016/S0140-6736\(21\)00234-8](https://doi.org/10.1016/S0140-6736(21)00234-8)
- Lu, R., Zhao, X., Li, J., Niu, P., Yang, B., Wu, H., Wang, W., Song, H., Huang, B., Zhu, N., Bi, Y., Ma, X., Zhan, F., Wang, L., Hu, T., Zhou, H., Hu, Z., Zhou, W., Zhao, L., ... Tan, W. (2020). Genomic characterisation and epidemiology of 2019 novel coronavirus: implications for virus origins and receptor binding. *The Lancet*, 395(10224), 565–574. [https://doi.org/10.1016/S0140-6736\(20\)30251-8](https://doi.org/10.1016/S0140-6736(20)30251-8)
- Mariano, G., Farthing, R. J., Lale-Farjat, S. L. M., & Bergeron, J. R. C. (2020). Structural Characterization of SARS-CoV-2: Where We Are, and Where We Need to Be. In *Frontiers in Molecular Biosciences* (Vol. 7). Frontiers Media S.A. <https://doi.org/10.3389/fmolb.2020.605236>
- Medzhitov, R., & Janeway, C. A. (1997). Innate immunity: impact on the adaptive immune response. *Current Opinion in Immunology*, 9(1), 4–9. [https://doi.org/10.1016/S0952-7915\(97\)80152-5](https://doi.org/10.1016/S0952-7915(97)80152-5)
- Melo-González, F., Soto, J. A., González, L. A., Fernández, J., Duarte, L. F., Schultz, B. M., Gálvez, N. M. S., Pacheco, G. A., Ríos, M., Vázquez, Y., Rivera-Pérez, D., Moreno-Tapia, D., Iturriaga, C., Vallejos, O. P., Berríos-Rojas, R. v., Hoppe-Elsholz, G., Urzúa, M., Bruneau, N., Fasce, R. A., ... Bueno, S. M. (2021). Recognition of Variants of Concern by Antibodies and T Cells Induced by a SARS-

CoV-2 Inactivated Vaccine. *Frontiers in Immunology*, 12. <https://doi.org/10.3389/fimmu.2021.747830>

Mohammadi, M., Shayestehpour, M., & Mirzaei, H. (2021). The impact of spike mutated variants of SARS-CoV2 [Alpha, Beta, Gamma, Delta, and Lambda] on the efficacy of subunit recombinant vaccines. In *Brazilian Journal of Infectious Diseases* (Vol. 25, Issue 4). Elsevier Editora Ltda. <https://doi.org/10.1016/j.bjid.2021.101606>

Mullen, J. L., Tsueng, G., Latif, A. A., Alkuzweny, M., Cano, M., Haag, E., Zhou, J., Zeller, M., Hughes, L. D., & Center for Viral System Biology. (2022). *outbreak.info*. <https://doi.org/10.1016/j.outbreakinfo.2022.101606>

Murphy, K. (Kenneth M.), Weaver, C., & Janeway, C. (n.d.). *Janeway's immunobiology*.

Ni, L., Ye, F., Cheng, M. L., Feng, Y., Deng, Y. Q., Zhao, H., Wei, P., Ge, J., Gou, M., Li, X., Sun, L., Cao, T., Wang, P., Zhou, C., Zhang, R., Liang, P., Guo, H., Wang, X., Qin, C. F., ... Dong, C. (2020a). Detection of SARS-CoV-2-Specific Humoral and Cellular Immunity in COVID-19 Convalescent Individuals. *Immunity*, 52(6), 971-977.e3. <https://doi.org/10.1016/j.immuni.2020.04.023>

Ni, L., Ye, F., Cheng, M. L., Feng, Y., Deng, Y. Q., Zhao, H., Wei, P., Ge, J., Gou, M., Li, X., Sun, L., Cao, T., Wang, P., Zhou, C., Zhang, R., Liang, P., Guo, H., Wang, X., Qin, C. F., ... Dong, C. (2020b). Detection of SARS-CoV-2-Specific Humoral and Cellular Immunity in COVID-19 Convalescent Individuals. *Immunity*, 52(6), 971-977.e3. <https://doi.org/10.1016/j.immuni.2020.04.023>

Nooraei, S., Bahrulolum, H., Hoseini, Z. S., Katalani, C., Hajizade, A., Easton, A. J., & Ahmadian, G. (2021). Virus-like particles: preparation, immunogenicity and their roles as nanovaccines and drug nanocarriers. In *Journal of Nanobiotechnology* (Vol. 19, Issue 1). BioMed Central Ltd. <https://doi.org/10.1186/s12951-021-00806-7>

Paludan, S. R., & Mogensen, T. H. (2022). Innate immunological pathways in COVID-19 pathogenesis. In *Sci. Immunol* (Vol. 7). <https://www.science.org>

- Pamukcu, C., Celik, E., Zeynep Ergun, E., Karahan, Z. S., Turkoz, G., Aras, M., Eren, C., Sili, U., Bilgin, H., Suder, I., Can Mandaci, B., Dingiloglu, B., Tatli, O., Doganay, G. D., Baris, S., Ozoren, N., & Sutlu, T. (2020). Lentiviral vector-based SARS-CoV-2 pseudovirus enables analysis of neutralizing activity in COVID-19 convalescent plasma. *BioRxiv*. <https://doi.org/10.1101/2020.12.28.424590>
- Pereson, M. J., Mojsiejczuk, L., Martínez, A. P., Flichman, D. M., Garcia, G. H., & di Lello, F. A. (2021). Phylogenetic analysis of SARS-CoV-2 in the first few months since its emergence. *Journal of Medical Virology*, *93*(3), 1722–1731. <https://doi.org/10.1002/jmv.26545>
- Petersen, E., Ntoumi, F., Hui, D. S., Abubakar, A., Kramer, L. D., Obiero, C., Tambyah, P. A., Blumberg, L., Yapi, R., Al-Abri, S., Pinto, T. de C. A., Yeboah-Manu, D., Haider, N., Asogun, D., Velavan, T. P., Kapata, N., Bates, M., Ansumana, R., Montaldo, C., ... Zumla, A. (2022). Emergence of new SARS-CoV-2 Variant of Concern Omicron (B.1.1.529) - highlights Africa's research capabilities, but exposes major knowledge gaps, inequities of vaccine distribution, inadequacies in global COVID-19 response and control efforts. *International Journal of Infectious Diseases*, *114*, 268–272. <https://doi.org/10.1016/j.ijid.2021.11.040>
- Planas, D., Veyer, D., Baidaliuk, A., Staropoli, I., Guivel-Benhassine, F., Rajah, M. M., Planchais, C., Porrot, F., Robillard, N., Puech, J., Prot, M., Gallais, F., Gantner, P., Velay, A., le Guen, J., Kassis-Chikhani, N., Edriss, D., Belec, L., Seve, A., ... Schwartz, O. (2021). Reduced sensitivity of SARS-CoV-2 variant Delta to antibody neutralization. *Nature*, *596*(7871), 276–280. <https://doi.org/10.1038/s41586-021-03777-9>
- Polack, F. P., Thomas, S. J., Kitchin, N., Absalon, J., Gurtman, A., Lockhart, S., Perez, J. L., Pérez Marc, G., Moreira, E. D., Zerbini, C., Bailey, R., Swanson, K. A., Roychoudhury, S., Koury, K., Li, P., Kalina, W. v., Cooper, D., Frenck, R. W., Hammitt, L. L., ... Gruber, W. C. (2020). Safety and Efficacy of the BNT162b2

mRNA Covid-19 Vaccine. *New England Journal of Medicine*, 383(27), 2603–2615.
<https://doi.org/10.1056/nejmoa2034577>

Pollard, A. J., & Bijker, E. M. (2021). A guide to vaccinology: from basic principles to new developments. In *Nature Reviews Immunology* (Vol. 21, Issue 2, pp. 83–100). Nature Research. <https://doi.org/10.1038/s41577-020-00479-7>

Promptchara, E., Ketloy, C., & Palaga, T. (2020). Allergy and Immunology Immune responses in COVID-19 and potential vaccines: Lessons learned from SARS and MERS epidemic. *Asian Pacific Journal of Allergy and Immunology*.
<https://doi.org/10.12932/AP-200220-0772>

Raghuvamsi, P. v., Tulsian, N. K., Samsudin, F., Qian, X., Purushotorman, K., Yue, G., Kozma, M. M., Hwa, W. Y., Lescar, J., Bond, P. J., Macary, P. A., & Anand, G. S. (2021). Sars-cov-2 s protein: Ace2 interaction reveals novel allosteric targets. *ELife*, 10, 1–47. <https://doi.org/10.7554/eLife.63646>

Rahimi, A., Mirzazadeh, A., & Tavakolpour, S. (2021). Genetics and genomics of SARS-CoV-2: A review of the literature with the special focus on genetic diversity and SARS-CoV-2 genome detection. In *Genomics* (Vol. 113, Issue 1P2, pp. 1221–1232). Academic Press Inc. <https://doi.org/10.1016/j.ygeno.2020.09.059>

Rastogi, M., Pandey, N., Shukla, A., & Singh, S. K. (2020). SARS coronavirus 2: from genome to infectome. In *Respiratory Research* (Vol. 21, Issue 1). BioMed Central Ltd. <https://doi.org/10.1186/s12931-020-01581-z>

Redondo, N., Zaldívar-López, S., Garrido, J. J., & Montoya, M. (2021). SARS-CoV-2 Accessory Proteins in Viral Pathogenesis: Knowns and Unknowns. In *Frontiers in Immunology* (Vol. 12). Frontiers Media S.A.
<https://doi.org/10.3389/fimmu.2021.708264>

Ren, Y., Shu, T., Wu, D., Mu, J., Wang, C., Huang, M., Han, Y., Zhang, X. Y., Zhou, W., Qiu, Y., & Zhou, X. (2020). The ORF3a protein of SARS-CoV-2 induces apoptosis

- in cells. In *Cellular and Molecular Immunology* (Vol. 17, Issue 8, pp. 881–883). Springer Nature. <https://doi.org/10.1038/s41423-020-0485-9>
- Rohaim, M. A., el Naggar, R. F., Clayton, E., & Munir, M. (2021). Structural and functional insights into non-structural proteins of coronaviruses. In *Microbial Pathogenesis* (Vol. 150). Academic Press. <https://doi.org/10.1016/j.micpath.2020.104641>
- Rydyznski Moderbacher, C., Ramirez, S. I., Dan, J. M., Grifoni, A., Hastie, K. M., Weiskopf, D., Belanger, S., Abbott, R. K., Kim, C., Choi, J., Kato, Y., Crotty, E. G., Kim, C., Rawlings, S. A., Mateus, J., Tse, L. P. V., Frazier, A., Baric, R., Peters, B., ... Crotty, S. (2020). Antigen-Specific Adaptive Immunity to SARS-CoV-2 in Acute COVID-19 and Associations with Age and Disease Severity. *Cell*, 183(4), 996-1012.e19. <https://doi.org/10.1016/j.cell.2020.09.038>
- Sah, P., Fitzpatrick, M. C., Zimmer, C. F., Abdollahi, E., Juden-Kelly, L., Moghadas, S. M., Singer, B. H., & Galvani, A. P. (n.d.). *Asymptomatic SARS-CoV-2 infection: A systematic review and meta-analysis*. <https://doi.org/10.1073/pnas.2109229118/-/DCSupplemental>
- Saito, A., Irie, T., Suzuki, R., Maemura, T., Uriu, K., Kosugi, Y., Shirakawa, K., Kimura, I., Ito, J., Wu, J., Iwatsuki-Horimoto, K., Ito, M., Yamayoshi, S., Ozono, S., Butlertanaka, E. P., Shimizu, R., Shimizu, K., Yoshimatsu, K., Kawabata, R., ... Sato, K. (n.d.). *SARS-CoV-2 spike P681R mutation, a hallmark of the Delta variant, enhances viral fusogenicity and pathogenicity*. <https://doi.org/10.1101/2021.06.17.448820>
- Santos, J. C., & Passos, G. A. (n.d.). *The high infectivity of SARS-CoV-2 B.1.1.7 is associated with increased interaction force between Spike-ACE2 caused by the viral N501Y mutation*. <https://doi.org/10.1101/2020.12.29.424708>

- Satarker, S., & Nampoothiri, M. (2020). Structural Proteins in Severe Acute Respiratory Syndrome Coronavirus-2. In *Archives of Medical Research* (Vol. 51, Issue 6, pp. 482–491). Elsevier Inc. <https://doi.org/10.1016/j.arcmed.2020.05.012>
- Schoeman, D., & Fielding, B. C. (2019). Coronavirus envelope protein: Current knowledge. In *Virology Journal* (Vol. 16, Issue 1). BioMed Central Ltd. <https://doi.org/10.1186/s12985-019-1182-0>
- Sette, A., & Crotty, S. (2021). Adaptive immunity to SARS-CoV-2 and COVID-19. In *Cell* (Vol. 184, Issue 4, pp. 861–880). Elsevier B.V. <https://doi.org/10.1016/j.cell.2021.01.007>
- Sette, A., Moutaftsi, M., Moyron-Quiroz, J., McCausland, M. M., Davies, D. H., Johnston, R. J., Peters, B., Rafii-El-Idrissi Benhnia, M., Hoffmann, J., Su, H. P., Singh, K., Garboczi, D. N., Head, S., Grey, H., Felgner, P. L., & Crotty, S. (2008). Selective CD4+ T Cell Help for Antibody Responses to a Large Viral Pathogen: Deterministic Linkage of Specificities. *Immunity*, 28(6), 847–858. <https://doi.org/10.1016/j.immuni.2008.04.018>
- Shang, J., Wan, Y., Luo, C., Ye, G., Geng, Q., Auerbach, A., & Li, F. (2020). Cell entry mechanisms of SARS-CoV-2. *Proceedings of the National Academy of Sciences*, 117(21), 11727–11734. <https://doi.org/10.1073/PNAS.2003138117>
- Shereen, M. A., Khan, S., Kazmi, A., Bashir, N., & Siddique, R. (2020). COVID-19 infection: Emergence, transmission, and characteristics of human coronaviruses. *Journal of Advanced Research*, 24, 91–98. <https://doi.org/10.1016/J.JARE.2020.03.005>
- Shi, R., Shan, C., Duan, X., Chen, Z., Liu, P., Song, J., Song, T., Bi, X., Han, C., Wu, L., Gao, G., Hu, X., Zhang, Y., Tong, Z., Huang, W., Jun Liu, W., Wu, G., Zhang, B., Wang, L., ... Yan, J. (2020). A human neutralizing antibody targets the receptor-binding site of SARS-CoV-2. | *Nature* |, 584. <https://doi.org/10.1038/s41586-020-2381-y>

- Siu, K. L., Yuen, K. S., Castano-Rodriguez, C., Ye, Z. W., Yeung, M. L., Fung, S. Y., Yuan, S., Chan, C. P., Yuen, K. Y., Enjuanes, L., & Jin, D. Y. (2019). Severe acute respiratory syndrome Coronavirus ORF3a protein activates the NLRP3 inflammasome by promoting TRAF3-dependent ubiquitination of ASC. *FASEB Journal*, 33(8), 8865–8877. <https://doi.org/10.1096/fj.201802418R>
- Siu, Y. L., Teoh, K. T., Lo, J., Chan, C. M., Kien, F., Escriou, N., Tsao, S. W., Nicholls, J. M., Altmeyer, R., Peiris, J. S. M., Bruzzone, R., & Nal, B. (2008). The M, E, and N Structural Proteins of the Severe Acute Respiratory Syndrome Coronavirus Are Required for Efficient Assembly, Trafficking, and Release of Virus-Like Particles. *Journal of Virology*, 82(22), 11318–11330. <https://doi.org/10.1128/jvi.01052-08>
- Snijder, E. J., Decroly, E., & Ziebuhr, J. (2016). The Nonstructural Proteins Directing Coronavirus RNA Synthesis and Processing. In *Advances in Virus Research* (Vol. 96, pp. 59–126). Academic Press Inc. <https://doi.org/10.1016/bs.aivir.2016.08.008>
- Suthar, M. S., Zimmerman, M. G., Kauffman, R. C., Mantus, G., Linderman, S. L., Hudson, W. H., Vanderheiden, A., Nyhoff, L., Davis, C. W., Adekunle, O., Affer, M., Sherman, M., Reynolds, S., Verkerke, H. P., Alter, D. N., Guarner, J., Bryksin, J., Horwath, M. C., Arthur, C. M., ... Wrammert, J. (2020). Rapid Generation of Neutralizing Antibody Responses in COVID-19 Patients. *Cell Reports Medicine*, 1(3). <https://doi.org/10.1016/j.xcrm.2020.100040>
- Takeda, M. (2021). Proteolytic activation of SARS-CoV-2 spike protein. In *Microbiology and Immunology*. John Wiley and Sons Inc. <https://doi.org/10.1111/1348-0421.12945>
- Tangid, D., Comishid, P., & Kang, R. (2020). The hallmarks of COVID-19 disease. *PLOS Pathogens*. <https://doi.org/10.1371/journal.ppat.1008536>
- Tao, K., Tzou, P. L., Nouhin, J., Gupta, R. K., de Oliveira, T., Kosakovsky Pond, S. L., Fera, D., & Shafer, R. W. (2021). The biological and clinical significance of

emerging SARS-CoV-2 variants. In *Nature Reviews Genetics* (Vol. 22, Issue 12, pp. 757–773). Nature Research. <https://doi.org/10.1038/s41576-021-00408-x>

Troyano-Hernández, P., Reinoso, R., & Holguín, Á. (2021). Evolution of sars-cov-2 envelope, membrane, nucleocapsid, and spike structural proteins from the beginning of the pandemic to september 2020: A global and regional approach by epidemiological week. *Viruses*, *13*(2). <https://doi.org/10.3390/v13020243>

V'kovski, P., Kratzel, A., Steiner, S., Stalder, H., & Thiel, V. (2021). Coronavirus biology and replication: implications for SARS-CoV-2. In *Nature Reviews Microbiology* (Vol. 19, Issue 3, pp. 155–170). Nature Research. <https://doi.org/10.1038/s41579-020-00468-6>

Volz, E., Hill, V., McCrone, J. T., Price, A., Jorgensen, D., O'Toole, Á., Southgate, J., Johnson, R., Jackson, B., Nascimento, F. F., Rey, S. M., Nicholls, S. M., Colquhoun, R. M., da Silva Filipe, A., Shepherd, J., Pascall, D. J., Shah, R., Jesudason, N., Li, K., ... Pybus, O. G. (2021). Evaluating the Effects of SARS-CoV-2 Spike Mutation D614G on Transmissibility and Pathogenicity. *Cell*, *184*(1), 64-75.e11. <https://doi.org/10.1016/j.cell.2020.11.020>

Volz, E., Mishra, S., Chand, M., Barrett, J. C., Johnson, R., Geidelberg, L., Hinsley, W. R., Laydon, D. J., Dabrera, G., Amato, R., Ragonnet-Cronin, M., Harrison, I., Jackson, B., Ariani, C. v, Boyd, O., Loman, N. J., McCrone, J. T., Gonçalves, S., Jorgensen, D., ... Ferguson, N. M. (2021). Assessing transmissibility of SARS-CoV-2 lineage B.1.1.7 in England The COVID-19 Genomics UK (COG-UK) consortium. *Nature*, *593*. <https://doi.org/10.1038/s41586-021-03470-x>

Voysey, M., Clemens, S. A. C., Madhi, S. A., Weckx, L. Y., Folegatti, P. M., Aley, P. K., Angus, B., Baillie, V. L., Barnabas, S. L., Bhorat, Q. E., Bibi, S., Briner, C., Cicconi, P., Collins, A. M., Colin-Jones, R., Cutland, C. L., Darton, T. C., Dheda, K., Duncan, C. J. A., ... Zuidewind, P. (2021). Safety and efficacy of the ChAdOx1 nCoV-19 vaccine (AZD1222) against SARS-CoV-2: an interim analysis of four randomised

- controlled trials in Brazil, South Africa, and the UK. *The Lancet*, 397(10269), 99–111. [https://doi.org/10.1016/S0140-6736\(20\)32661-1](https://doi.org/10.1016/S0140-6736(20)32661-1)
- Walsh, E. E., Frenck, R. W., Falsey, A. R., Kitchin, N., Absalon, J., Gurtman, A., Lockhart, S., Neuzil, K., Mulligan, M. J., Bailey, R., Swanson, K. A., Li, P., Koury, K., Kalina, W., Cooper, D., Fontes-Garfias, C., Shi, P.-Y., Türeci, Ö., Tompkins, K. R., ... Gruber, W. C. (2020). Safety and Immunogenicity of Two RNA-Based Covid-19 Vaccine Candidates. *New England Journal of Medicine*, 383(25), 2439–2450. <https://doi.org/10.1056/nejmoa2027906>
- Wang, K., Long, Q.-X., Deng, H.-J., Hu, J., Gao, Q.-Z., Zhang, G.-J., He, C.-L., Huang, L.-Y., Hu, J.-L., Chen, J., Tang, N., & Huang, A.-L. (2021). Longitudinal Dynamics of the Neutralizing Antibody Response to Severe Acute Respiratory Syndrome Coronavirus 2 (SARS-CoV-2) Infection. *Clinical Infectious Disease*. <https://doi.org/10.1093/cid/ciaa1143>
- Wang, M. Y., Zhao, R., Gao, L. J., Gao, X. F., Wang, D. P., & Cao, J. M. (2020). SARS-CoV-2: Structure, Biology, and Structure-Based Therapeutics Development. In *Frontiers in Cellular and Infection Microbiology* (Vol. 10). Frontiers Media S.A. <https://doi.org/10.3389/fcimb.2020.587269>
- Ward, B. J., Gobeil, P., Séguin, A., Atkins, J., Boulay, I., Charbonneau, P.-Y., Couture, M., Finkle, C., Hager, K., Mahmood, A., Makarkov, A., Cheng, M., Pillet, S., Schimke, P., St-Martin, S., & Landry, N. (2020). Phase 1 trial of a Candidate Recombinant Virus-Like Particle Vaccine for Covid-19 1 Disease Produced in Plants 2 3. *MedRxiv*. <https://doi.org/10.1101/2020.11.04.20226282>
- Weiskopf, D., Schmitz, K. S., Raadsen, M. P., Grifoni, A., Okba, N. M. A., Endeman, H., van den Akker, J. P. C., Molenkamp, R., Koopmans, M. P. G., van Gorp, E. C. M., Haagmans, B. L., de Swart, R. L., Sette, A., & de Vries, R. D. (2020). Phenotype and kinetics of SARS-CoV-2-specific T cells in COVID-19 patients with acute respiratory distress syndrome. *Science Immunology*, 5(48). <https://doi.org/10.1126/SCIIMMUNOL.ABD2071>

- WHO. (2022, January). *Draft landscape of COVID-19 candidate vaccines*. <https://www.who.int/publications/m/item/draft-landscape-of-covid-19-candidate-vaccines>
- Wilhelm, A., Widera, M., Grikscheit, K., Toptan, T., Schenk, B., Pallas, C., Metzler, M., Kohmer, N., Hoehl, S., Helfritz, F. A., Wolf, T., Goetsch, U., & Ciesek, S. (n.d.). *Reduced Neutralization of SARS-CoV-2 Omicron Variant by Vaccine Sera and monoclonal antibodies*. <https://doi.org/10.1101/2021.12.07.21267432>
- World Health Organization. (2020). *Naming the coronavirus disease (COVID-19) and the virus that causes it*. [https://www.who.int/emergencies/diseases/novel-coronavirus-2019/technical-guidance/naming-the-coronavirus-disease-\(covid-2019\)-and-the-virus-that-causes-it](https://www.who.int/emergencies/diseases/novel-coronavirus-2019/technical-guidance/naming-the-coronavirus-disease-(covid-2019)-and-the-virus-that-causes-it)
- Wu, A., Peng, Y., Huang, B., Ding, X., Wang, X., Niu, P., Meng, J., Zhu, Z., Zhang, Z., Wang, J., Sheng, J., Quan, L., Xia, Z., Tan, W., Cheng, G., & Jiang, T. (2020). Genome Composition and Divergence of the Novel Coronavirus (2019-nCoV) Originating in China. *Cell Host and Microbe*, 27(3), 325–328. <https://doi.org/10.1016/j.chom.2020.02.001>
- Wu, F., Wang, A., Liu, M., Wang, Q., Chen, J., Xia, S., Ling, Y., Zhang, Y., Xun, J., Lu, L., Jiang, S., Lu, H., Wen, Y., & Huang, J. (2020). Neutralizing antibody responses to SARS-CoV-2 in a COVID-19 recovered patient cohort and their implications. *MedRxiv*. <https://doi.org/10.1101/2020.03.30.20047365>
- Wu, F., Zhao, S., Yu, B., Chen, Y. M., Wang, W., Song, Z. G., Hu, Y., Tao, Z. W., Tian, J. H., Pei, Y. Y., Yuan, M. L., Zhang, Y. L., Dai, F. H., Liu, Y., Wang, Q. M., Zheng, J. J., Xu, L., Holmes, E. C., & Zhang, Y. Z. (2020). A new coronavirus associated with human respiratory disease in China. *Nature*, 579(7798), 265–269. <https://doi.org/10.1038/s41586-020-2008-3>
- Yadav, R., Chaudhary, J. K., Jain, N., Chaudhary, P. K., Khanra, S., Dhamija, P., Sharma, A., Kumar, A., & Handu, S. (2021). *cells Role of Structural and Non-Structural*

Proteins and Therapeutic Targets of SARS-CoV-2 for COVID-19. 10, 821.
<https://doi.org/10.3390/cells>

Yang, C., Pan, X., Huang, Y., Cheng, C., Xu, X., Wu, Y., Xu, Y., Shang, W., Niu, X., Wan, Y., Li, Z., Zhang, R., Liu, S., Xiao, G., & Xu, W. (2021). Drug Repurposing of Itraconazole and Estradiol Benzoate against COVID-19 by Blocking SARS-CoV-2 Spike Protein-Mediated Membrane Fusion. *Advanced Therapeutics*, 4(5).
<https://doi.org/10.1002/adtp.202000224>

Yang, H., & Rao, Z. (2021). Structural biology of SARS-CoV-2 and implications for therapeutic development. In *Nature Reviews Microbiology* (Vol. 19, Issue 11, pp. 685–700). Nature Research. <https://doi.org/10.1038/s41579-021-00630-8>

Yang, J., Wang, W., Chen, Z., Lu, S., Yang, F., Bi, Z., Bao, L., Mo, F., Li, X., Huang, Y., Hong, W., Yang, Y., Zhao, Y., Ye, F., Lin, S., Deng, W., Chen, H., Lei, H., Zhang, Z., ... Wei, X. (2020). A vaccine targeting the RBD of the S protein of SARS-CoV-2 induces protective immunity. *Nature*, 586(7830), 572–577.
<https://doi.org/10.1038/s41586-020-2599-8>

Yilmaz, I. C., Ipekoglu, E. M., Bulbul, A., Turay, N., Yildirim, M., Evcili, I., Yilmaz, N. S., Guvencli, N., Aydin, Y., Gungor, B., Saraydar, B., Bartan, A. G., Ibibik, B., Bildik, T., Baydemir, İ., Sanli, H. A., Kayaoglu, B., Ceylan, Y., Yildirim, T., ... Gursel, M. (2021). Development and preclinical evaluation of virus-like particle vaccine against COVID-19 infection. *Allergy: European Journal of Allergy and Clinical Immunology*. <https://doi.org/10.1111/all.15091>

Zhang, Y., Chen, Y., Li, Y., Huang, F., Luo, B., Yuan, Y., Xia, B., Ma, X., Yang, T., Yu, F., Liu, J., Liu, B., Song, Z., Chen, J., Yan, S., Wu, L., Pan, T., Zhang, X., Li, R., ... Zhang, H. (n.d.). *The ORF8 protein of SARS-CoV-2 mediates immune evasion through down-regulating MHC-I.* <https://doi.org/10.1073/pnas.2024202118/-/DCSupplemental>

- Zhang, Y., & Zeng, G. (2020). Phase 2 Clinical Trial of SARS-CoV-2 Inactivated Vaccine. *MedRxiv*. <https://doi.org/10.1101/2020.07.31.20161216>
- Zhu, F. C., Guan, X. H., Li, Y. H., Huang, J. Y., Jiang, T., Hou, L. H., Li, J. X., Yang, B. F., Wang, L., Wang, W. J., Wu, S. P., Wang, Z., Wu, X. H., Xu, J. J., Zhang, Z., Jia, S. Y., Wang, B. sen, Hu, Y., Liu, J. J., ... Chen, W. (2020). Immunogenicity and safety of a recombinant adenovirus type-5-vectored COVID-19 vaccine in healthy adults aged 18 years or older: a randomised, double-blind, placebo-controlled, phase 2 trial. *The Lancet*, 396(10249), 479–488. [https://doi.org/10.1016/S0140-6736\(20\)31605-6](https://doi.org/10.1016/S0140-6736(20)31605-6)
- Zhu, J. (2012). Mammalian cell protein expression for biopharmaceutical production. *Biotechnology Advances*, 30(5), 1158–1170. <https://doi.org/10.1016/j.biotechadv.2011.08.022>
- Zhu, N., Zhang, D., Wang, W., Li, X., Yang, B., Song, J., Zhao, X., Huang, B., Shi, W., Lu, R., Niu, P., Zhan, F., Ma, X., Wang, D., Xu, W., Wu, G., Gao, G. F., & Tan, W. (2020). A Novel Coronavirus from Patients with Pneumonia in China, 2019. *New England Journal of Medicine*, 382(8), 727–733. <https://doi.org/10.1056/nejmoa2001017>

APPENDICES

A. Vector Maps and Sequences

Sequence of Envelope protein gene of SARS-CoV-2:

AAAATGCCTTTGCTTTTGTGCTTCCTCTTCTCTGGGCTGGGGCTTTGGC
CAAGCTTATGTATAGCTTTGTGTCAGAGGAGACTGGCACACTTATAGTT
AATAGCGTCCTCCTGTTCCCTCGCATTCTAGTCTTTTTGCTCGTCACTCT
CGCGATCTTGACGGCTTTGAGGTTGTGCGCTTACTGCTGCAACATTGTG
AATGTCAGTCTCGTAAACCTTCTTTCTACGTCTACTCCAGAGTAAAAA
ATCTTAATAGTTCCCGCGTGCCAGACTTGCTGGTAGGAAGCCTGGTACC
CAGAGGCTCTCCACACCATCATCACCACCACTAA

Sequence of Membrane glycoprotein gene of SARS-CoV-2:

GGATCCAAAATGCCTTTGCTTTTGTGCTTCCTCTTCTCTGGGCTGGGGC
TTTGGCCAAGCTTATGGCGGACAGTAATGGAACCTATTACGGTGGAGGA
ACTTAAGAACTGCTGGAACAATGGAACCTGGTAATAGGTTTCCTGTTT
CTCACATGGATCTGCCTCTTGCAATTCGCGTACGCGAACCGGAATAGAT
TTCTCTACATAATAAAGCTGATTTTCCTCTGGCTCCTGTGGCCCGTCACA
CTCGCCTGTTTCGTACTCGCAGCAGTGTACAGGATTAAGTGGATTACCG
GGGAATTGCGATTGCAATGGCTTGTCTGGTGGGACTGATGTGGCTTAG
CTATTTTATTGCTAGTTTTTCGACTTTTCGCAAGAACTCGAAGCATGTGGT
CCTTCAATCCTGAGACGAATATACTGTTGAATGTGCCTTTGCATGGAAC
AATTTTGACCCGACCGCTTCTTGAAAGCGAGCTTGTAATTGGGGCCGTG
ATACTTAGAGGTCCTTGCAGGATCGCAGGCCACCACCTTGGGCGGTGTG
ATATCAAGGATCTTCCTAAGGAAATCACGGTCGCAACGAGCCGCACGT

TGAGCTACTATAAACTCGGCGCGAGCCAGCGGGTTGCTGGTGATTTCAG
GTTTCGCCGCTTACTCTAGATACAGGATTGGTAATTACAACTCAATAC
AGACCACAGTTCCTCTTCCGATAACATTGCTCTTCTGGTACAGGGAAGC
CTGGTACCCAGAGGCTCTCCACACCATCATCACCACCACTAA

Sequence of Nucleocapsid gene of SARS-CoV-2:

AAAATGAGCGACAACGGCCACAAAATCAACGGAACGCCCCCGGATA
ACCTTCGGTGGGCCATCTGACAGTACTGGCTCTAATCAGAACGGAGAG
CGCTCCGGAGCAAGAAGCAAGCAACGACGGCCGCAAGGACTGCCAAT
AATACTGCCAGTTGGTTCACAGCACTGACCCAGCACGGGAAAGAGGAT
CTCAAATTTCCGCGCGGTCAAGGTGTCCCCATTAACACTAATTCATCTC
CCGATGATCAAATCGGGTACTATCGACGAGCAACGCGCCGAATAAGGG
GCGGCGACGGAAAAATGAAGGACCTGTCCCCAAGGTGGTACTTTTACT
ATCTTGGCACCGGGCCGGAAGCGGGTCTTCCGTATGGAGCAAACAAGG
ACGGAATAATTTGGGTTCGCGACCGAGGGTGCTCTTAATACTCCCAAAG
ATCACATTGGTACTCGCAATCCTGCTAACAACGCAGCCATCGTTCTCCA
GCTGCCGCAGGGAACAACGCTGCCCAAGGGTTTTTACGCGGAAGGCTC
AAGGGGTGGAAGCCAGGCGTCAAGTCGCAGCTCCAGCAGAAGTAGAA
ACAGTTCACGAAATAGCACCCCAGGCTCCTCACGCGGTACGAGTCCAG
CTAGAATGGCAGGAAACGGAGGGGACGCTGCTCTTGCCTTGCTGCTTCT
GGATCGGCTCAACCAGCTCGAAAGCAAGATGAGTGGTAAGGGGCAGCA
ACAACAGGGTCAGACCGTAACGAAAAAGTCTGCTGCAGAGGCTTCAA
GAAACCTAGGCAGAAGCGGACCGCAACCAAAGCCTACAATGTTACCCA
AGCCTTCGGGCGGAGAGGTCCGGAACAAACGCAAGGGAATTCGGTGA
TCAGGAACTGATTTCGGCAAGGAACCGATTACAAGCATTGGCCACAGAT
TGCTCAATTCGCCCAAGCGCGAGTGCTTTCTTTGGGATGTCACGCATC
GGGATGGAAGTAACTCCATCCGGAACGTGGTTGACGTATACAGGCGCG
ATAAAGCTGGACGATAAAGACCCTAATTTCAAGGATCAGGTTATTCTGT
TGAATAAACATATAGACGCGTATAAAACCTTCCCGCCTACCGAGCCCA

AGAAAGATAAGAAGAAAAAGCCGACGAAACCCAGGCTCTCCCTCAG
AGGCAAAAGAAACAGCAAACGGTTACTCTCCTCCCTGCCGCCGATTTG
GACGACTTTAGCAAACAGTTGCAGCAGAGTATGTCCAGTGCAGACTCC
ACTCAGGCATAA

Sequence of 6p-Spike gene of SARS-CoV-2:

GGATCCAAAATGCCTTTGCTTTTGTGCTTCCTCTTCTCTGGGCTGGGGC
TTTGGCCAAGCTTGTGAACCTTACCACACGCACCCAATTGCCCCAGCT
TACACAAACAGCTTTACTAGGGGCGTCTACTATCCCGACAAGGTGTTTC
GGAGTAGCGTGCTGCACTCTACTCAAGACCTCTTCCTGCCCTTCTTTTCC
AATGTCACTTGGTTCCACGCCATCCATGTCAGCGGTACCAATGGGACCA
AAAGGTTTGACAACCCAGTGTTGCCATTTAACGATGGCGTGTATTTTCGC
CAGTACTGAAAAGAGCAATATCATCAGGGGCTGGATCTTCGGTACTAC
CCTGGATAGCAAGACCCAGTCTTTGCTGATTGTGAACAATGCTACAAAT
GTGGTAATCAAAGTTTGTGAGTTTCAATTCTGCAATGACCCATTCTGG
GCGTCTATTACCACAAGAATAACAAAAGTTGGATGGAATCCGAGTTTC
GGGTGTACAGCTCCGCTAACAACTGCACATTCGAATATGTGTCCCAGCC
GTTCTGATGGACCTTGAGGGGAAGCAGGGAAATTTCAAGAACCTGCG
GGAGTTCGTATTTAAAAATATCGACGGCTACTTTAAAATCTATAGTAAG
CACACCCCATTAACCTGGTCCGAGACCTTCCGCAGGGATTTTCCGCTC
TGGAGCCTCTGGTTGACCTCCCTATAGGCATTAACATCACCAGATTCCA
GACCCTCCTGGCCCTGCACCGCTCATATTTGACCCCGGGGACTCAAGT
AGTGGATGGACAGCCGGGGCTGCTGCTTATTATGTAGGCTATCTGCAGC
CTCGGACATTCCTGCTGAAGTACAACGAAAACGGGACTATCACTGATG
CCGTCGACTGCGCCCTTGACCCTCTTTCTGAGACCAAGTGTACACTTAA
ATCATTACCGTGGAGAAAGGTATCTACCAGACCTCTAATTTCCGAGTC
CAGCCTACAGAGTCCATCGTGAGGTTTCCGAACATTACAAATCTTTGTC
CCTTTGGCGAAGTGTTTAATGCCACTAGATTTGCAAGTGTGTACGCTTG
GAACCGAAAGAGAATCTCCAACCTGTGTCGCTGACTATTCTGTGCTCTAC

AACAGCGCTAGCTTTAGCACATTTAAGTGTTACGGAGTTTCCCCACCA
AGCTGAATGACCTGTGCTTTACCAACGTCTATGCAGACTCCTTTGTGAT
TAGAGGCGATGAAGTGCGACAAATTGCACCTGGCCAAACGGGCAAAT
TGCTGATTATAACTACAAGCTGCCCGACGATTTACAGGCTGCGTTATC
GCCTGGAACAGCAACAACCTGGACAGTAAGGTTGGCGGAAATTATAAC
TACCTGTATCGGCTGTTCAGGAAGAGCAATCTTAAGCCCTTTGAAAGAG
ACATTAGTACCGAAATATAACCAGGCCGGCTCTACCCCATGCAATGGCGT
TGAGGGCTTCAATTGCTATTTTCCCCTTCAGTCATATGGGTTTCAGCCAA
CCAATGGGGTGGGGTACCAGCCTTATCGCGTAGTGGTACTGAGCTTTGA
GCTGTTGCACGCACCAGCAACAGTGTGCGGGCCGAAGAAATCTACAAA
TCTCGTGAAGAACAATGTGTCAATTTAACTTTAACGGTCTGACCGGC
ACGGGGGTCTGACAGAATCTAACAAGAAATTTCTCCCCTTTCAGCAGT
TCGGAAGAGATATCGCAGATACAACTGATGCTGTGCGCGATCCTCAGA
CGCTTGAGATTTTGGATATTACACCTTGCTCTTTCGGGGGGGTCAGCGT
CATCACTCCCGGAACAAATACAAGCAACCAGGTGGCAGTCCTGTACCA
GGACGTAAACTGCACCGAAGTGCCCGTTGCAATTCATGCTGACCAGCTT
ACTCCACATGGAGGGTGTACTCCACCGGATCTAATGTCTTTCAGACAA
GAGCTGGCTGCCTGATCGGTGCCGAACATGTGAATAATAGCTACGAGT
GTGACATTCCCATCGGAGCCGGCATTGTGCATCCTACCAAACCTCAGAC
GAACAGCCCCGGCAGCGCCAGCAGTGTGGCCTCCAGAGCATTATCGC
ATACACTATGTCTCTGGGTGCTGAAAACCTCCGTGGCATATTCAAACAAC
TCAATCGCCATTCCAACCTTTACCATTTTCAGTCACAACCGAAATCC
TGCCAGTGTCTATGACCAAGACAAGCGTGGATTGCACTATGTATATTTG
CGGCGACTCCACAGAATGCTCTAATTTGCTTCTGCAGTACGGCTCCTTTT
GCACTCAATTGAATAGGGCATTGACTGGCATTGCTGTGGAGCAAGATA
AAAATACTCAGGAGGTATTTGCTCAGGTGAAACAAATCTACAAAACCTC
CACCAATTAAGACTTCGGAGGTTTTAATTTCTCACAGATTCTGCCTGA
TCCATCAAAGCCTTCTAAGCGGAGTCCCATCGAAGACTTGCTCTTTAAC
AAAGTCACTCTGGCTGACGCCGGCTTTATCAAGCAGTACGGTGACTGCT
TGGGCGACATCGCTGCTCGCGACCTGATCTGCGCTCAGAAGTTCAATGG

CCTGACCGTCCTGCCACCACTGCTGACAGACGAAATGATTGCCCAGTAC
ACCTCTGCATTGCTTGCCGGGACCATCACATCTGGGTGGACCTTCGGAG
CTGGACCCGCTCTCCAGATCCCCTTCCCCATGCAAATGGCCTATCGCTT
CAATGGCATCGGGGTCACCCAGAATGTGCTGTACGAAAACCAGAACT
TATTGCCAATCAGTTTAATAGCGCGATCGGCAAGATTCAGGACAGTCTG
TCTTCTACTCCCTCTGCCCTGGGAAAGTTGCAGGATGTGGTGAATCAGA
ATGCCCAGGCTCTGAATACACTGGTCAAGCAACTCAGCAGCAACTTCG
GCGCAATTTCTTCCGTTCTGAACGATATCCTGTCTAGACTCGACCCACC
AGAAGCTGAGGTACAGATTGATAGGCTTATCACAGGCCGGCTCCAATC
ACTGCAAACATACGTGACTCAGCAGCTGATCCGGGCTGCCGAAATTAG
GGCCAGTGCAAACCTGGCTGCGACTAAGATGTCTGAGTGCGTTCTGGGT
CAGTCCAAGAGGGTAGATTTTTGTGGCAAGGGGTACCATCTCATGTCTT
TTCCTCAGAGTGCACCACATGGAGTGGTCTTCCTCCACGTGACCTACGT
GCCCCGCCAAGAGAAAAATTTACAACCGCTCCAGCTATCTGCCACGAT
GGAAAAGCTCATTTCGCGGGAGGGCGTGTTTCGTCAGTAATGGAACG
CACTGGTTCGTGACCCAGAGAACTTTTACGAGCCCCAGATAATTACCA
CCGATAATACATTTGTTAGCGGCAACTGCGATGTCGTGATCGGGATAGT
GAATAACACAGTGTACGACCCACTCCAGCCCGAACTCGACTCATTAAAG
GAAGAGCTTGACAAGTACTTTAAGAATCACACCAGCCCAGATGTGGAC
CTGGGAGATATCAGCGGCATTAATGCCTCAGTGGTGAATATTCAGAAG
GAAATAGATAGACTGAATGAAGTGGCAAAGAATCTGAACGAGTCCCTC
ATTGATCTGCAGGAGCTCGGCAAGTACGAGCAATATATTAATGGCCG
TGGTACATTTGGCTGGGATTTATCGCAGGACTCATTGCCATCGTGATGG
TGAATATCATGCTGTGTTGTATGACCAGCTGCTGCAGCTGTTTGAAAGG
TTGTTGCAGCTGTGGTTCCTGTTGCAAGTTCGATGAAGATGATAGCGAG
CCAGTTCTGAAGGGCGTTAAGCTGCACTATACTGAAAACCTGTATTTTC
AGAGCGGATCTGGGTACATCCCCGAGGCACCAAGAGATGGTCAGGCAT
ATGTTAGGAAGGATGGGGAATGGGTCCCTCCTGAGCACATTTTTGGGAG
GAAGCCTGGTACCCAGAGGCTCTCCACACCATCATCACCACCACTAAG
GATCC

Sequence of Spike gene of Alpha variant:

GGATCCGCCGCCACCATGCCTTTGCTTTTGTTGCTTCCTCTTCTCTGGGC
TGGGGCTTTGGCCAAGCTTGTGAACCTTACCACACGCACCCAATTGCC
CCAGCTTACACAAACAGCTTTACTAGGGGCGTCTACTATCCCGACAAGG
TGTTTCGGAGTAGCGTGCTGCACTCTACTCAAGACCTCTTCCTGCCCTT
TTTTCCAATGTCACCTTGGTTCCACGCCATCAGCGGTACCAATGGGACCA
AAAGGTTTGACAACCCAGTGTTGCCATTTAACGATGGCGTGTATTTGCG
CAGTACTGAAAAGAGCAATATCATCAGGGGCTGGATCTTCGGTACTAC
CCTGGATAGCAAGACCCAGTCTTTGCTGATTGTGAACAATGCTACAAAT
GTGGTAATCAAAGTTTGTGAGTTTCAATTCTGCAATGACCCATTCTGG
GCGTCTATTACCACAAGAATAACAAAAGTTGGATGGAATCCGAGTTTC
GGGTGTACAGCTCCGCTAACAACTGCACATTCGAATATGTGTCCCAGCC
GTTCTGATGGACCTTGAGGGGAAGCAGGGAAATTTCAAGAACCTGCG
GGAGTTCGTATTTAAAAATATCGACGGCTACTTTAAAATCTATAGTAAG
CACACCCCATTAACCTGGTCCGAGACCTTCCGCAGGGATTTTCCGCTC
TGGAGCCTCTGGTTGACCTCCCTATAGGCATTAACATCACCAGATTCCA
GACCCTCCTGGCCCTGCACCGCTCATATTTGACCCCGGGGACTCAAGT
AGTGGATGGACAGCCGGGGCTGCTGCTTATTATGTAGGCTATCTGCAGC
CTCGGACATTCTGCTGAAGTACAACGAAAACGGGACTATCACTGATG
CCGTCGACTGCGCCCTTGACCCTCTTTCTGAGACCAAGTGTACTTAA
ATCATTACCCGTGGAGAAAGGTATCTACCAGACCTCTAATTTCCGAGTC
CAGCCTACAGAGTCCATCGTGAGGTTTCCGAACATTACAAATCTTTGTC
CCTTTGGCGAAGTGTTTAATGCCACTAGATTTGCAAGTGTGTACGCTTG
GAACCGAAAGAGAATCTCCAACCTGTGTGCTGACTATTCTGTGCTCTAC
AACAGC

GCTAGCTTTAGCACATTTAAGTGTTACGGAGTTTCCCCACCAAGCTGA
ATGACCTGTGCTTTACCAACGTCTATGCAGACTCCTTTGTGATTAGAGG
CGATGAAGTGCGACAAATTGCACCTGGCCAAACGGGCAAATTTGCTGA
TTATAACTACAAGCTGCCCGACGATTTACAGGCTGCGTTATCGCCTGG
AACAGCAACAACCTGGACAGTAAGGTTGGCGGAAATTATAACTACCTG
TATCGGCTGTTTACAGGAAGAGCAATCTTAAGCCCTTTGAAAGAGACATTA
GTACCGAAATATACCAGGCCGGCTCTACCCCATGCAATGGCGTTGAGG
GCTTCAATTGCTATTTTCCCCTTCAGTCATATGGGTTTCAGCCAACCTAC

GGGGTGGGGTACCAGCCTTATCGCGTAGTGGTACTGAGCTTTGAGCTGT
TGCACGCACCAGCAACAGTGTGCGGGCCGAAGAAATCTACAAATCTCG
TGAAGAACAATGTGTCAATTTTAACTTTAACGGTCTGACCGGCACGGG
GGTCTGACAGAATCTAACAAGAAATTTCTCCCCTTTCAGCAGTTCGGA
AGAGATATCGCAGATACAACCTGATGCTGTGCGGATCCTCAGACGCTTG

AGATTTTGGATATTACACCTTGCTCTTTCGGGGGGGTCAGCGTCATCAC
TCCCGGAACAAATACAAGCAACCAGGTGGCAGTCCTGTACCAG GGC
GTAAACTGCACCGAAGTGCCCGTTGCAATTCATGCTGACCAGCTTACTC
CCACATGGAGGGTGTACTCCACCGGATCTAATGTCTTTCAGACAAGAGC
TGGCTGCCTGATCGGTGCCGAACATGTGAATAATAGCTACGAGTGTGAC
ATTCCCATCGGAGCCGGCATTGTGCATCCTACCAAACCTCAGACGAACA
GCCCCGGCAGCGCCAGCAGTGTGGCCTCCAGAGCATTATCGCATAACA
CTATGTCTCTGGGTGCTGAAAACCTCCGTGGCATATTCAAACAACCTCAAT
CGCCATTCCAACCTAACTTTACCATTTCAGTCACAACCGAAATCCTGCCA
GTGTCTATGACCAAGACAAGCGTGGATTGCACTATGTATATTTGCGGCG
ACTCCACAGAATGCTCTAATTTGCTTCTGCAGTACGGCTCCTTTTGCCT
CAATTGAATAGGGCATTGACTGGCATTGCTGTGGAGCAAGATAAAAAT
ACTCAGGAGGTATTTGCTCAGGTGAAACAAATCTACAAAACCTCCACCA
ATTAAAGACTTCGGAGGTTTTAATTTCTCACAGATTCTGCCTGATCCATC
AAAGCCTTCTAAGCGGAGTCCCATCGAAGACTTGCTCTTTAACAAAGTC
ACTCTGGCTGACGCCGGCTTTATCAAGCAGTACGGTGACTGCTTGGGCG
ACATCGCTGCTCGCGACCTGATCTGCGCTCAGAAGTTCAATGGCCTGAC
CGTCTGCCACCACTGCTGACAGACGAAATGATTGCCAGTACACCTCT
GCATTGCTTGCCGGGACCATCACATCTGGGTGGACCTTCGGAGCTGGAC
CCGCTCTCCAGATCCCCTTCCCCATGCAAATGGCCTATCGCTTCAATGG
CATCGGGGTCACCCAGAATGTGCTGTACGAAAACCAGAACTTATTGC
CAATCAGTTTAATAGCGCGATCGGCAAGATTCAGGACAGTCTGTCTTCT
ACTCCCTCTGCCCTGGGAAAGTTGCAGGATGTGGTGAATCAGAATGCC
AGGCTCTGAATACACTGGTCAAGCAACTCAGCAGCAACTTCGGCGCAA
TTTCTTCCGTTCTGAACGATATCCTGTCTAGACTCGACCCACCAGAAGC
TGAGGTACAGATTGATAGGCTTATCACAGGCCGGCTCCAATCACTGCAA
ACATACGTGACTCAGCAGCTGATCCGGGCTGCCGAAATTAGGGCCAGT
GCAAACCTGGCTGCGACTAAGATGTCTGAGTGCCTTCTGGGTGAGTCCA
AGAGGGTAGATTTTTGTGGCAAGGGGTACCATCTCATGTCTTTTCCTCA
GAGTGCACCACATGGAGTGGTCTTCCTCCACGTGACCTACGTGCCCGCC

CAAGAGAAAAATTTTACAACCGCTCCAGCTATCTGCCACGATGGAAAA
GCTCATTTCCCGCGGGAGGGCGTGTTCGTTCAGTAATGGAACGCACTGGT
TCGTGACCCAGAGAACTTTTACGAGCCCCAGATAATTACCACCGATAA
TACATTTGTTAGCGGCAACTGCGATGTCGTGATCGGGATAGTGAATAAC
ACAGTGTACGACCCACTCCAGCCCGAACTCGACTCATTTAAGGAAGAG
CTTGACAAGTACTTTAAGAATCACACCAGCCCAGATGTGGACCTGGGA
GATATCAGCGGCATTAATGCCTCAGTGGTGAATATTCAGAAGGAAATA
GATAGACTGAATGAAGTGGCAAAGAATCTGAACGAGTCCCTCATTGAT
CTGCAGGAGCTCGGCAAGTACGAGCAATATATTAATGGCCGTGGTAC
ATTTGGCTGGGATTTATCGCAGGACTCATTGCCATCGTGATGGTGACTA
TCATGCTGTGTTGTATGACCAGCTGCTGCAGCTGTTTGAAAGGTTGTTG
CAGCTGTGGTTCCTGTTGCAAGTTCGATGAAGATGATAGCGAGCCAGTT
CTGAAGGGCGTTAAGCTGCACTATACTGAAAACCTGTATTTTCAGAGCG
GATCTGGGTACATCCCCGAGGCACCAAGAGATGGTCAGGCATATGTTA
GGAAGGATGGGGAATGGGTCCTCCTGAGCACATTTTGGGAGGAAGCC
TGGTACCCAGAGGCTCTCCACACCATCATCACCACCACTAAGGATCC

Sequence of Spike gene of Delta variant:

GGATCCCCCGCCACCATGCCTTTGCTTTTGTGGCTTCCTCTTCTCTGGGC
TGGGGCTTTGGCCGTGAACCTGAGAACCAGAACACAGCTGCCTCCAGC
CTACACCAACAGCTTTACCAGAGGCGTGTACTACCCCGACAAGGTGTTT
AGATCCAGCGTGCTGCACTCTACCCAGGACCTGTTCCCTGCCTTTCTTCA
GCAACGTGACCTGGTTCCACGCCATCCACGTGTCCGGCACCAATGGCAC
CAAGAGATTCGACAACCCCGTGCTGCCCTTCAACGACGGGGTGTACTTT
GCCAGCACCGAGAAGTCCAACATCATCAGAGGCTGGATCTTCGGCACC
ACACTGGACAGCAAGACCCAGAGCCTGCTGATCGTGAACAACGCCACC
AACGTGGTCATCAAAGTGTGCGAGTTCCAGTTCTGCAACGACCCCTTCC
TGGACGTCTACTACCACAAGAACAACAAGAGCTGGATGGAAAGCGGCG
TGTACAGCAGCGCCAACAACACTGCACCTTCGAGTACGTGTCCCAGCCTTT

CCTGATGGACCTGGAAGGCAAGCAGGGCAACTTCAAGAACCTGCGCGA
GTTTCGTGTTTAAGAACATCGACGGCTACTTCAAGATCTACAGCAAGCAC
ACCCCTATCAACCTCGTGCGGGATCTGCCTCAGGGCTTCTCTGCTCTGG
AACCCCTGGTGGATCTGCCATCGGCATCAACATCACCCGGTTTCAGAC
ACTGCTGGCCCTGCACAGAAGCTACCTGACACCTGGCGATAGCAGCAG
CGGATGGACAGCTGGTGCCGCCGCTTACTATGTGGGCTACCTGCAGCCT
AGAACCTTCCTGCTGAAGTACAACGAGAACGGCACCATCACCGACGCC
GTGGATTGTGCTCTGGACCCT

CTGAGCGAGACAAAGTGCACCCTGAAGTCCTTCACCGTGGAAGGGC
ATCTACCAGACCAGCAACTTCCGGGTGCAGCCCACCGAATCCATCGTGC
GGTTCCCAATATCACCAATCTGTGCCCTTCGGCGAGGTGTTCAATGC
CACCAGATTCGCCTCTGTGTACGCCTGGAACCGGAAGCGGATCAGCAA
TTGCGTGGCCGACTACTCCGTGCTGTACAACCTCC

GCTAGCTTCAGCACCTTCAAGTGCTACGGCGTGTCCCCTACCAAGCTGA
ACGACCTGTGCTTCACAAACGTGTACGCCGACAGCTTCGTGATCCGGGG
AGATGAAGTGCGGCAGATTGCCCTGGACAGACAGGCAATATCGCCGA
CTACAACCTACAAGCTGCCCCGACGACTTCACCGGCTGTGTGATTGCCTGG
AACAGCAACAACCTGGACTCCAAAGTCGGCGGCAACTACAATTACAGA
TACCGGCTGTTCCGGAAGTCCAATCTGAAGCCCTTCGAGCGGGACATCT
CCACCGAGATCTATCAGGCCGGCAGCAAGCCTTGTAACGGCGTGGAAG
GCTTCAACTGCTACTTCCCCTGCAGTCCTACGGCTTTCAGCCCACAAA
TGGCGTGGGCTATCAGCCCTACAGAGTGGTGGTGCTGAGCTTCGAACTG
CTGCATGCCCCTGCCACAGTGTGCGGCCCTAAGAAAAGCACCAATCTCG
TGAAGAACAATGCGTGAACCTCAACTTCAACGGCCTGACCGGCACCG
GCGTGCTGACAGAGAGCAACAAGAAGTTCCTGCCATTCCAGCAGTTTG
GCCGGGATATCGCCGATACCACAGACGCCGTTAGAGATCCCCAGACAC
TGGAATCCTGGACATCACCCCTTGCAGCTTCGGCGGAGTGTCTGTGAT
CACCCCTGGCACCAACACCAGCAATCAGGTGGCAGTGCTGTACCAGGG
CGTGAACCTGTACCGAAGTGCCCGTGGCCATTCACGCCGATCAGCTGACA

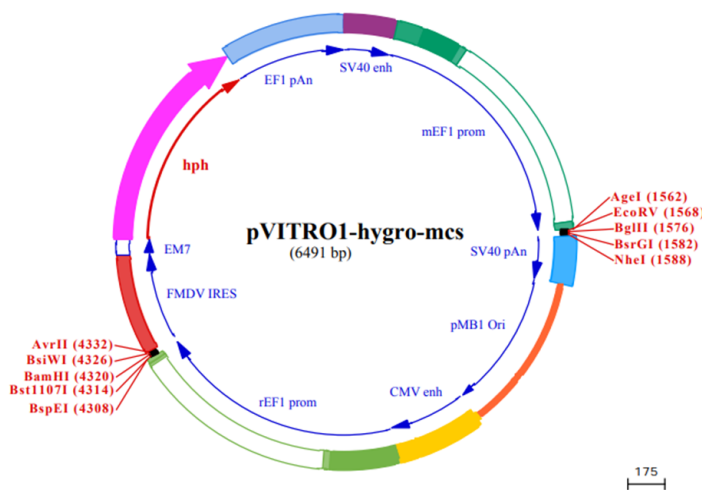
CCTACATGGCGGGTGTACTCCACCGGCAGCAATGTGTTTCAGACCAGAG
CCGGCTGTCTGATCGGAGCCGAGCACGTGAACAATAGCTACGAGTGCG
ACATCCCCATCGGCGCTGGAATCTGCGCCAGCTACCAGACACAGACAA
ACAGCAGAGGCAGCGCCTCC

AGCGTGGCCAGCCAGAGCATCATTGCCTACACAATGTCTCTGGGCGCCG
AGAACAGCGTGGCCTACTCCAACAACCTCTATCGCTATCCCCACCAACTT
CACCATCAGCGTGACCACAGAGATCCTGCCTGTGTCCATGACCAAGACC
AGCGTGGACTGCACCATGTACATCTGCGGCGATTCCACCGAGTGCTCCA
ACCTGCTGCTGCAGTACGGCAGCTTCTGCACCCAGCTGAATAGAGCCCT
GACAGGGATCGCCGTGGAACAGGACAAGAACACCCAAGAGGTGTTTCGC
CCAAGTGAAGCAGATCTACAAGACCCCTCCTATCAAGGACTTCGGCGG
CTTCAATTCAGCCAGATTCTGCCCCGATCCTAGCAAGCCCAGCAAGCGG
AGC

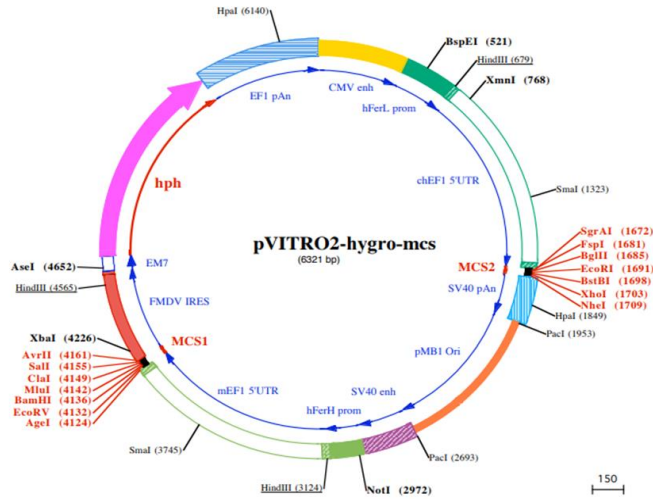
CCCATCGAGGACCTGCTGTTCAACAAAGTGACACTGGCCGACGCCGGC
TTCATCAAGCAGTATGGCGATTGTCTGGGCGACATTGCCGCCAGGGATC
TGATTTGCGCCCAGAAGTTTAAACGGACTGACAGTGCTGCCTCCTCTGCT
GACCGATGAGATGATCGCCCAGTACACATCTGCCCTGCTGGCCGGCAC
AATCACAAGCGGCTGGACATTTGGAGCAGGCCCCCGCTCTGCAGATCCC
CTTTCCTATGCAGATGGCCTACCGGTTCAACGGCATCGGAGTGACCCAG
AATGTGCTGTACGAGAACCAGAAGCTGATCGCCAACCAGTTCAACAGC
GCCATCGGCAAGATCCAGGACAGCCTGAGCAGCACACCCAGCGCCCTG
GGAAAGCTGCAGAACGTGGTCAACCAGAATGCCCAGGCACTGAACACC
CTGGTCAAGCAGCTGTCCTCCAACCTTCGGCGCCATCAGCTCTGTGCTGA
ACGATATCCTGAGCAGACTGGACCCTCCTGAGGCCGAGGTGCAGATCG
ACAGACTGATCACAGGCAGACTGCAGAGCCTCCAGACATACGTGACCC
AGCAGCTGATCAGAGCCGCCGAGATTAGAGCCTCTGCCAATCTGGCCG
CCACCAAGATGTCTGAGTGTGTGCTGGGCCAGAGCAAGAGAGTGGACT
TTTGC GGCAAGGGCTACCACCTGATGAGCTTCCCTCAGTCTGCCCTCA
CGGCGTGGTGTCTTCTGCACGTGACATATGTGCCCGCTCAAGAGAAGAAT
TTCACCACCGCTCCAGCCATCTGCCACGACGGCAAAGCCCACCTTTCCTA

GAGAAGGCGTGTTTCGTGTCCAACGGCACCCATTGGTTCGTGACACAGC
 GGAACTTCTACGAGCCCCAGATCATCACCACCGACAACACCTTCGTGTC
 TGGCAACTGCGACGTCGTGATCGGCATTGTGAACAATACCGTGTACGAC
 CCTCTGCAGCCCGAGCTGGACAGCTTCAAAGAGGAACTGGACAAGTAC
 TTTAAGAACCACACAAGCCCCGACGTGGACCTGGGCGATATCAGCGGA
 ATCAATGCCAGCGTCGTGAACATCCAGAAAGAGATCGACCGGCTGAAC
 GAGGTGGCCAAGAATCTGAACGAGAGCCTGATCGACCTGCAAGAAGTGG
 GGAAGTACGAGCAGTACATCAAGTGGCCCTGGTACATCTGGCTGGGC
 TTTATCGCCGGACTGATTGCCATCGTGATGGTCAATCATGCTGTGTT
 GCATGACCAGCTGCTGTAGCTGCCTGAAGGGCTGTTGTAGCTGTGGCAG
 CTGCTGCAAGTTCGACGAGGACGATTCTGAGCCCGTGCTGAAGGGCGT
 GAAACTGCACTACACAGAAAACCTGTATTTTCAGAGCGGATCTGGGTA
 CATCCCCGAGGCACCAAGAGATGGTCAGGCATATGTTAGGAAGGATGG
 GGAATGGGTCCCTCCTGAGCACATTTTTGGGAGGAAGCCTGGTACCCAG
 AGGCTCTCCACACCATCATCACCACCACTGATGAGGATCC

pVITro1-hygro-mcs Vector map:



pVITRO2-hygro-mcs vector map:



Next Generation Sequencing result of pVITRO2 hexapS-E for Alpha variant:

CCCGCGGGCCTGGCCTCTTTACGGGTTATGGCCCTTGCGTGCCTTGAAT
 TACTTCCATGCCCTGGCTGCAGTACGTGATTCTTGATCCCGAGCTTCG
 GGTTGGAAGTGGGTGGGAGAGTTCGAGGCCTTGCGCTTAAGGAGCCCC
 TTCGCCTCGTGCTTGAGTTGAGGCCTGGCTTGGGCGCTGGGGCCGCCGC
 GTGCTAATCTGGTGGCACCTTCGCGCCTGTCTCGCTGCTTTCGCTAAGTC
 TCTAGCCATTTAAAATTTTGTAAACCAGCTGCGACGCTTTTTTCTGGC
 GAGATAGTCTTGTAATGCGGGCCAGGATCTGCACACTGGTATTTCCGGT
 TTTTGGGGCCCGGGCGGGCGACGGGGCCCGTGCCTCCAGCGCACATG
 TTCGGCGAGGCGGGGCCTGCGAGCGCGGCCACCGAGAATCGGACGGGG
 GTAGTCTCAAACCTGGCCGGCCTGCTCTGGTGCCTGGCCTCGCGCCGCCG
 TGTATCGCCCCGCCCTGGGCGGCAAGGCTGGCCCGGTCGGCACCAGTTG
 CGTGAGCGGAAAGATGGCCGCTTCCCGGCCCTGCTGCAGGGAGCTCAA
 AATGGAGGACGCGGGCGCCCGGGAGAGCGGGCGGGTGAGTCACCCACA

CAAAGGAAAAGGGCCTTTCCTTCCTCATCCGTCGCTTCATGTGACTCCA
CGGAGTACCGGGCGCCGTCCAGGCACCTCGATTAGTTGTCGAGCTTTTG
GAGTACGTCGTCTTTAGGTTGGGGGGAGGGGTTTTATGCGATGGAGTTT
CCCCACACTGAGTGGGTGGAGACTGAAGAGTTAGGCCAGCTTGGCACT
TGATGTAATTCTCCTTGGAATTTGCCCTTTTTGAGTTT

GGATCTTGCCTCATTCTCAAGCCTCAGACAGTGGTTCAAAGTTTTTTTCT
TCCATTTAGGTGTCGTGAAAACCTACCCTAAAAGCCACCGGCGTGCGC
AAGATCC

AAAATGCCTTTGCTTTTGTTGCTTCCTCTTCTCTGGGCTGGGGCTTTGGC
CAAGCTTATGTATAGCTTTGTGTCAGAGGAGACTGGCACACTTATAGTT
AATAGCGTCCTCCTGTTCCCTCGCATTCTAGTCTTTTTGCTCGTCACTCT
CGCGATCTTGACGGCTTTGAGGTTGTGCGCTTACTGCTGCAACATTGTG
AATGTCAGTCTCGTAAACCTTCTTTCTACGTCTACTCCAGAGTAAAAA
ATCTTAATAGTTCCCGCGTGCCAGACTTGCTGGTAGGAAGCCTGGTACC
CAGAGGCTCTCCACACCATCATCACCACCACTAA

GGATCT

GAATTCTTCGAACTCGAGGCTAGCTGGCCAGACATGATAAGATAACATTG
ATGAGTTTGGACAAACCACAACCTAGAATGCAGTGAAAAAATGCTTTA
TTTGTGAAATTTGTGATGCTATTGCTTTATTTGTAACCATTATAAGCTGC
AATAAACAAGTTAACAACAACAATTGCATTCATTTTATGTTTCAGGTTC
AGGGGGAGGTGTGGGAGGTTTTTTAAAGCAAGTAAAACCTCTACAAAT
GTGGTATGGAAATGTTAATTAACCTAGCCATGACCAAAAATCCCTTAACGT
GAGTTTTTCGTTCCACTGAGCGTCAGACCCCGTAGAAAAGATCAAAGGA
TCTTCTTGAGATCCTTTTTTTCTGCGCGTAATCTGCTGCTTGCAAACAAA
AAAACCACCGCTACCAGCGGTGGTTTGTGGCCGGATCAAGAGCTACCA
ACTTTTTTCCGAAGGTAACCTGGCTTCAGCAGAGCGCAGATACCAAATA
CTGTTCTTCTAGTGTAGCCGTAGTTAGGCCACCACTTCAAGAACTCTGT
AGCACCGCCTACATACCTCGCTCTGCTAATCCTGTTACCAGTGGCTGCT

GCCAGTGGCGATAAGTCGTGTCTTACCGGGTTGGACTCAAGACGATAGT
TACCGGATAAGGCGCAGCGGTTCGGGCTGAACGGGGGTTTCGTGCACACA
GCCCAGCTTGGAGCGAACGACCTACACCGAACTGAGATACCTACAGCG
TGAGCTATGAGAAAGCGCCACGCTTCCCGAAGGGAGAAAGGCGGACAG
GTATCCGGTAAGCGGCAGGGTTCGGAACAGGAGAGCGCACGAGGGAGC
TTCCAGGGGGAAACGCCTGGTATCTTTATAGTCCTGTCGGGTTTCGCCA
CCTCTGACTTGAGCGTCGATTTTTGTGATGCTCGTCAGGGGGGCGGAGC
CTATGGAAAACGCCAGCAACGCGGCCTTTTTACGGTTCCTGGCCTTTT
GCTGGCCTTTTGCTCACATGTTCTTAATTAACCTGCAGGGCCTGAAATA
ACCTCTGAAAGAGGAACTTGGTTAGGTACCTTCTGAGGCTGAAAGAAC
CAGCTGTGGAATGTGTGTCAGTTAGGGTGTGGAAAGTCCCCAGGCTCCC
CAGCAGGCAGAAGTATGCAAAGCATGCATCTCAATTAGTCAGCAACCA
GGTGTGGAAAGTCCCCAGGCTCCCCAGCAGGCAGAAGTATGCAAAGCA
TGCATCTCAATTAGTCAGCAACCATAGTCCCCTAGTTCCGCCAGAGCG
CGCGAGGGCCTCCAGCGGCCGCCCTCCCCACAGCAGGGGCGGGGTC
CCGCGCCCACCGGAAGGAGCGGGCTCGGGGCGGGCGGCGCTGATTGGC
CGGGGCGGGCCTGACGCCGACGCGGCTATAAGAGACCACAAGCGACCC
GCAGGGCCAGACGTTCTTCGCCGAAGCTTGCCGTCAGAACGCAGGTGA
GGGGCGGGTGTGGCTTCCGCGGGCCGCCGAGCTGGAGGTCCTGCTCCG
AGCGGGCCGGGCCCGCTGTCGTCGGCGGGGATTAGCTGCGAGCATTC
CCGCTTCGAGTTGCGGGCGGCGCGGGAGGCAGAGTGCGAGGCCTAGCG
GCAACCCCGTAGCCTCGCCTCGTGTCCGGCTTGAGGCCTAGCGTGGTGT
CCGCGCCGCCCGCCGCGTGCTACTCCGGCCGCACTCTGGTCTTTTTTTTTT
TTGTTGTTGTTGCCCTGCTGCCTTCGATTGCCGTTTCAGCAATAGGGGCTA
ACAAAGGGAGGGTGCGGGGCTTGCTCGCCCGGAGCCCGGAGAGGTCAT
GGTTGGGGAGGAATGGAGGGACAGGAGTGGCGGCTGGGGCCCCGCCCG
CCTTCGGAGCACATGTCCGACGCCACCTGGATGGGGCGAGGCCTGGGG
TTTTTCCCGAAGCAACCAGGCTGGGGTTAGCGTGCCGAGGCCATGTGGC
CCCAGCACCCGGCACGATCTGGCTTGGCGGCGCCGCGTTGCCCTGCCTC
CCTAACTAGGGTGAGGCCATCCCGTCCGGCACCAAGTTGCGTGCGTGGA

AAGATGGCCGCTCCCGGGCCCTGTTGCAAGGAGCTCAAATGGAGGAC
GCGGCAGCCCGGTGGAGCGGGCGGGTGAGTACCCACACAAAGGAAG
AGGGCCTGGTCCCTCACCGGCTGCTGCTTCCTGTGACCCCGTGGTCCTA
TCGGCCGCAATAGTCACCTCGGGCTTTTGAGCACGGCTAGTCGCGGCGG
GGGGAGGGGATGTAATGGCGTTGGAGTTTGTTACATTTGGTGGGTGG
AGACTAGTCAGGCCAGCCTGGCGCTGGAAGTCATTTTTGGAATTTGTCC
CCTTGAGTTTTGAGCGGAGCTAATTCTCGGGCTTCTTAGCGGTTCAAAG
GTATCTTTTAAACCCTTTTTTAGGTGTTGTGAAAACCACCGCTAATTCAA
AGCAACCGGTGATATC

GGATCCGCCGCCACCATGCCTTTGCTTTTGTTGCTTCCTCTTCTGCGG
TGGGGCTTTGGCCAAGCTTGTGAACCTTACCACACGCACCCAATTGCCC
CCAGCTTACACAAACAGCTTTACTAGGGGCGTCTACTATCCCGACAAGG
TGTTTCGGAGTAGCGTGCTGCACTCTACTCAAGACCTTTCCTGCCCTTC
TTTTCCAATGTCACTTGGTTCCACGCCATC

AGCGGTACCAATGGGACCAAAGGTTTGACAACCCAGTGTTGCCATTT
AACGATGGCGTGTATTTCCGCCAGTACTGAAAAGAGCAATATCATCAGG
GGCTGGATCTTCGGTACTACCCTGGATAGCAAGACCCAGTCTTTGCTGA
TTGTGAACAATGCTACAAATGTGGTAATCAAAGTTTGTGAGTTTCAATT
CTGCAATGACCCATTCCTGGGCGTCTATTACCACAAGAATAACAAAAGT
TGGATGGAATCCGAGTTTCGGGTGTACAGCTCCGCTAACAACTGCACAT
TCGAATATGTGTCCCAGCCGTTCTGATGGACCTTGAGGGGAAGCAGG
GAAATTTCAAGAACCTGCGGGAGTTCGTATTTAAAATATCGACGGCTA
CTTTAAAATCTATAGTAAGCACACCCCCATTAACCTGGTCCGAGACCTT
CCGCAGGGATTTTCCGCTCTGGAGCCTCTGGTTGACCTCCCTATAGGCA
TTAACATCACCAGATTCCAGACCCTCCTGGCCCTGCACCGCTCATATTT
GACCCCGGGGACTCAAGTAGTGGATGGACAGCCGGGGCTGCTGCTTA
TTATGTAGGCTATCTGCAGCCTCGGACATTCCTGCTGAAGTACAACGAA
AACGGGACTATCACTGATGCCGTGACTGCGCCCTTGACCCTCTTTCTG
AGACCAAGTGTACACTTAAATCATTACCGTGGAGAAAGGTATCTACC

AGACCTCTAATTTCCGAGTCCAGCCTACAGAGTCCATCGTGAGGTTTCC
GAACATTACAAATCTTTGTCCCTTTGGCGAAGTGTTAATGCCACTAGA
TTTGCAAGTGTGTACGCTTGGAAACCGAAAGAGAATCTCCAACCTGTGTGCG
CTGACTATTCTGTGCTCTACAACAGC

GCTAGCTTTAGCACATTTAAGTGTTACGGAGTTTCCCCACCAAGCTGA
ATGACCTGTGCTTTACCAACGTCTATGCAGACTCCTTTGTGATTAGAGG
CGATGAAGTGCGACAAATTGCACCTGGCCAAACGGGCAAATTGCTGA
TTATAACTACAAGCTGCCCCGACGATTTACAGGCTGCGTTATCGCCTGG
AACAGCAACAACCTGGACAGTAAGGTTGGCGGAAATTATAACTACCTG
TATCGGCTGTTTACAGGAAGAGCAATCTTAAGCCCTTTGAAAGAGACATTA
GTACCGAAATATACCAGGCCGGCTCTACCCCATGCAATGGCGTTGAGG
GCTTCAATTGCTATTTTCCCCTTCAGTCATATGGGTTTCAGCCAACCTAC
GGGGTGGGGTACCAGCCTTATCGCGTAGTGGTACTGAGCTTTGAGCTGT
TGCACGCACCAGCAACAGTGTGCGGGCCGAAGAAATCTACAAATCTCG
TGAAGAACAAATGTGTCAATTTTAACTTTAACGGTCTGACCGGCACGGG
GGTCCTGACAGAATCTAACAAGAAATTTCTCCCCTTTCAGCAGTTCGGA
AGAGATATCGCAGATACAACTGATGCTGTGCGCGATCCTCAGACGCTTG
AGATTTTGGATATTACACCTTGCTCTTTCGGGGGGGTCAGCGTCATCAC
TCCCGGAACAAATACAAGCAACCAGGTGGCAGTCCTGTACCAG GGC

GTAAACTGCACCGAAGTGCCCGTTGCAATTCATGCTGACCAGCTTACTC
CCACATGGAGGGTGTACTCCACCGGATCTAATGTCTTTCAGACAAGAGC
TGGCTGCCTGATCGGTGCCGAACATGTGAATAATAGCTACGAGTGTGAC
ATTCCCATCGGAGCCGGCATTGTGTCATCCTACCAAACCTCAGACGAACA
GCCCCGGCAGCGCCAGCAGTGTGGCCTCCCAGAGCATTATCGCATACA
CTATGTCTCTGGGTGCTGAAAACCTCCGTGGCATATTCAAACAACCTCAAT
CGCCATTCCAACCTAACTTTACCATTTCAGTCACAACCGAAATCCTGCCA
GTGTCTATGACCAAGACAAGCGTGGATTGCACTATGTATATTTGCGGCG
ACTCCACAGAATGCTCTAATTTGCTTCTGCAGTACGGCTCCTTTTGCCT
CAATTGAATAGGGCATTGACTGGCATTGCTGTGGAGCAAGATAAAAAT

ACTCAGGAGGTATTTGCTCAGGTGAAACAAATCTACAAAACCTCCACCA
ATTAAAGACTTCGGAGGTTTTAATTTCTCACAGATTCTGCCTGATCCATC
AAAGCCTTCTAAGCGGAGTCCCATCGAAGACTTGCTCTTTAACAAAGTC
ACTCTGGCTGACGCCGGCTTTATCAAGCAGTACGGTGACTGCTTGGGCG
ACATCGCTGCTCGCGACCTGATCTGCGCTCAGAAGTTCAATGGCCTGAC
CGTCCTGCCACCACTGCTGACAGACGAAATGATTGCCCAGTACACCTCT
GCATTGCTTGCCGGGACCATCACATCTGGGTGGACCTTCGGAGCTGGAC
CCGCTCTCCAGATCCCCTTCCCCATGCAAATGGCCTATCGCTTCAATGG
CATCGGGGTCACCCAGAATGTGCTGTACGAAAACCAGAACTTATTGC
CAATCAGTTTAATAGCGCGATCGGCAAGATTCAGGACAGTCTGTCTTCT
ACTCCCTCTGCCCTGGGAAAGTTGCAGGATGTGGTGAATCAGAATGCC
AGGCTCTGAATACACTGGTCAAGCAACTCAGCAGCAACTTCGGCGCAA
TTTCTTCCGTTCTGAACGATATCCTGTCTAGACTCGACCCACCAGAAGC
TGAGGTACAGATTGATAGGCTTATCACAGGCCGGCTCCAATCACTGCAA
ACATACGTGACTCAGCAGCTGATCCGGGCTGCCGAAATTAGGGCCAGT
GCAAACCTGGCTGCGACTAAGATGTCTGAGTGCCTTCTGGGTGAGTCCA
AGAGGGTAGATTTTTGTGGCAAGGGGTACCATCTCATGTCTTTTCCTCA
GAGTGCACCACATGGAGTGGTCTTCCCTCCACGTGACCTACGTGCCCGCC
CAAGAGAAAAATTTTACAACCGCTCCAGCTATCTGCCACGATGGAAAA
GCTCATTTCCCGCGGGAGGGCGTGTTTCGTCAGTAATGGAACGCACTGGT
TCGTGACCCAGAGAACTTTTACGAGCCCCAGATAATTACCACCGATAA
TACATTTGTTAGCGGCAACTGCGATGTCGTGATCGGGATAGTGAATAAC
ACAGTGTACGACCCACTCCAGCCCGAACTCGACTCATTTAAGGAAGAG
CTTGACAAGTACTTTAAGAATCACACCAGCCCAGATGTGGACCTGGGA
GATATCAGCGGCATTAATGCCTCAGTGGTGAATATTCAGAAGGAAATA
GATAGACTGAATGAAGTGGCAAAGAATCTGAACGAGTCCCTCATTGAT
CTGCAGGAGCTCGGCAAGTACGAGCAATATATTAATGGCCGTGGTAC
ATTTGGCTGGGATTTATCGCAGGACTCATTGCCATCGTGATGGTACTA
TCATGCTGTGTTGTATGACCAGCTGCTGCAGCTGTTTGAAAGGTTGTTG
CAGCTGTGGTTCCTGTTGCAAGTTCGATGAAGATGATAGCGAGCCAGTT

CTGAAGGGCGTTAAGCTGCACTATACTGAAAACCTGTATTTTCAGAGCG
GATCTGGGTACATCCCCGAGGCACCAAGAGATGGTCAGGCATATGTTA
GGAAGGATGGGGAATGGGTCCTCCTGAGCACATTTTTGGGAGGAAGCC
TGGTACCCAGAGGCTCTCCACACCATCATCACCACCACTAAGGATCC

ACGCGTATCGATTGTCGACCCTAGGAGCAGGTTTCCCCAATGACACAAA
ACGTGCAACTTGAAACTCCGCCTGGTCTTTCCAGGTCTAGAGGGGTAAC
ACTTTGTA CTGCGTTTGGCTCCACGCTCGATCCACTGGCGAGTGTTAGT
AACAGCACTGTTGCTTCGTAGCGGAGCATGACGGCCGTGGGAACTCCTC
CTTGGTAACAAGGACCCACGGGGCCAAAAGCCACGCCACACGGGGCC
GTCATGTGTGCAACCCAGCACGGCGACTTTACTGCGAAACCCACTTTA
AAGTGACATTGAAACTGGTACCCACACACTGGTGACAGGCTAAGGATG
CCCTTCAGGTACCCCGAGGTAACACGCGACACTCGGGATCTGAGAAGG
GGACTGGGGCTTCTATAAAAGCGCTCGGTTTAAAAAGCTTCTATGCCTG
AATAGGTGACCGGAGGTCCGGCACCTTTCCTTTGCAATTA CTGACCCTAT
GAATACA ACTGACTGTTTGACAATTAATCATCGGCATAGTATATCGGCA
TAGTATAATACGACTCACTATAGGAGGGCCACCATGAAGAAACCTGAA
CTGACAGCAACTTCTGTTGAGAAGTTTCTCATTGAAAAATTTGATTCTG
TTTCTGATCTCATGCAGCTGTCTGAAGGTGAAGAAAGCAGAGCCTTTTC
TTTTGATGTTGGAGGAAGAGGTTATGTTCTGAGGGTCAATTCTTGCTGCT
GATGGTTTTTACAAAGACAGATATGTTTACAGACACTTTGCCTCTGCTG
CTCTGCCAATTCCAGAAGTTCTGGACATTGGAGAATTTTCTGAATCTCT
CACCTACTGCATCAGCAGAAGAGCACAAGGAGTCACTCTCCAGGATCT
CCCTGAAACTGAGCTGCCAGCTGTTCTGCAACCTGTTGCTGAAGCAATG
GATGCCATTGCAGCAGCTGATCTGAGCCAAACCTCTGGATTTGGTCCTT
TTGGTCCCCAAGGCATTGGTCAGTACACCACTTGGAGGGATTTCAATTG
TGCCATTGCTGATCCTCATGTCTATCACTGGCAGACTGTGATGGATGAC
ACAGTTTCTGCTTCTGTTGCTCAGGCACTGGATGAACTCATGCTGTGGG
CAGAAGATTGTCCTGAAGTCAGACACCTGGTCCATGCTGATTTTGGAAG
CAACAATGTTCTGACAGACAATGGCAGAATCACTGCAGTCATTGACTG

GTCTGAAGCCATGTTTGGAGATTCTCAATATGAGGTTGCCAACATTTTT
TTTTGGAGACCTTGGCTGGCTTGCATGGAACAACAACAAGATATTTTG
AAAGAAGACACCCAGAACTGGCTGGTTCACCCAGACTGAGAGCCTACA
TGCTCAGAATTGGCCTGGACCAACTGTATCAATCTCTGGTTGATGGAAA
CTTTGATGATGCTGCTTGGGCACAAGGAAGATGTGATGCCATTGTGAGG
TCTGGTGCTGGAAGTGTGGAAGAACTCAAATTGCAAGAAGGTCTGCTG
CTGTTTGGACTGATGGATGTGTTGAAGTTCTGGCTGACTCTGGAAACAG
GAGACCCTCCACAAGACCCAGAGCCAAGGAATGAATATTAGCTAGATT
ATCCCTAATACCTGCCACCCCACTCTTAATCAGTGGTGGGAAGAACGGTC
TCAGAACTGTTTGTTCATTGGCCATTTAAGTTTAGTAGTAAAAGACT
GGTTAATGATAACAATGCATCGTAAAACCTTCAGAAGGAAAGGAGAAT
GTTTTGTGGACCACTTTGGTTTTCTTTTTTGCCTGTGGCAGTTTTAAGTT
ATTAGTTTTTAAAATCAGTACTTTTTAATGGAAACAACCTTGACCAAAAA
TTTGTCACAGAATTTTGAGACCCATTAAAAAAGTTAAATGAGAAACCTG
TGTGTTCCTTTGGTCAACACCGAGACATTTAGGTGAAAGACATCTAATT
CTGGTTTTACGAATCTGGAAACTTCTTGAAAATGTAATTCTTGAGTTAA
CACTTCTGGGTGGAGAATAGGGTTGTTTTCCCCCACATAATTGGAAGG
GGAAGGAATATCATTAAAGCTATGGGAGGGTTGCTTTGATTACAACAC
TGGAGAGAAATGCAGCATGTTGCTGATTGCCTGTCACTAAAACAGGCC
AAAAACTGAGTCCTTGGGTTCATAGAAAGCTGCCTGCAGGCGTTACAT
AACTTACGGTAAATGGCCCGCCTGGCTGACCGCCCAACGACCCCCGCC
ATTGACGTCAAT

Next Generation Sequencing result of pViro2 hexapS-E for Delta variant:

CCTGCAGGCGTTACATAACTTACGGTAAATGGCCCGCCTGGCTGACCGC
CCAACGACCCCGCCATTGACGTCAATAATGACGTATGTTCCCATAGT
AACGCCAATAGGGACTTTCATTGACGTCAATGGGTGGAGTATTTACGG
TAAACTGCCCACTTGGCAGTACATCAAGTGTATCATATGCCAAGTACGC
CCCCTATTGACGTCAATGACGGTAAATGGCCCGCCTGGCATTATGCCCA
GTACATGACCTTATGGGACTTTCCTACTTGGCAGTACATCTACGTATTA
GTCATCGCTATTACCATGATGATGCGGTTTTGGCAGTACATCAATGGGC
GTGGATAGCGGTTTGACTCACGGGGATTTCCAAGTCTCCACCCCATTGA
CGTCAATGGGAGTTTGTTTTACTAGTCAGGGCCCCAACCCCCCAAGC
CCCCATTCACAACACGCTGGCGCTACAGGCGCGTGACTTCCCCTTGCT
TTGGGGCGGGGGGCTGAGACTCCTATGTGCTCCGGATTGGTCAGGCAC
GGCCTTCGGCCCCGCCTCCTGCCACCGCAGATTGGCCGCTAGGCCTCCC
CGAGCGCCCTGCCTCCGAGGGGCCGGCGCACCATAAAAGAAGCCGCCCT
AGCCACGTCCCCTCGCAGTTCGGCGGTCCCGCGGGTCTGTCTCAAGCTT
GCCGCCAGAACACAGGTAAGTGCCGTGTGTGGTTCCCGCGGGCCTGGC
CTCTTTACGGGTTATGGCCCTTGCGTGCCTTGAATTAATTCCATGCCCT
GGCTGCAGTACGTGATTCTTGATCCCGAGCTTCGGGTTGGAAGTGGGTG
GGAGAGTTCGAGGCCTTGCGCTTAAGGAGCCCCTTCGCCTCGTGCTTGA
GTTGAGGCCTGGCTTGGGCGCTGGGGCCGCCGCGTGCTAATCTGGTGGC
ACCTTCGCGCCTGTCTCGCTGCTTTCGCTAAGTCTCTAGCCATTTAAAAT
TTTTGATAACCAGCTGCGACGCTTTTTTTCTGGCGAGATAGTCTTGTA
TGCGGGCCAGGATCTGCACACTGGTATTTTCGGTTTTTTGGGGCCGCGGGC
GGCGACGGGGCCCGTGCGTCCCAGCGCACATGTTTCGGCGAGGCGGGGC
CTGCGAGCGCGGCCACCGAGAATCGGACGGGGGTAGTCTCAAACCTGGC
CGGCCTGCTCTGGTGCCTGGCCTCGCGCCGCCGTGTATCGCCCCGCCCT
GGGCGGCAAGGCTGGCCCGGTCCGGCACCAAGTTGCGTGAGCGGAAAGAT
GGCCGCTTCCCGGCCCTGCTGCAGGGAGCTCAAAATGGAGGACGCGGC
GCCCCGGAGAGCGGGCGGGTGAGTCACCCACACAAAGGAAAAGGGCC
TTTCCTTCCTCATCCGTCGCTTCATGTGACTCCACGGAGTACCGGGCGCC
GTCCAGGCACCTCGATTAGTTGTTCGAGCTTTTGGAGTACGTGCTTTTA

GGTTGGGGGGAGGGGTTTTATGCGATGGAGTTTCCCCACACTGAGTGG
GTGGAGACTGAAGAGTTAGGCCAGCTTGGCACTTGATGTAATTCTCCTT
GGAATTTGCCCTTTTTGAGTTTGGATCTTGCCTCATTCTCAAGCCTCAGA
CAGTGGTTCAAAGTTTTTTTCTTCCATTTTCAGGTGTCGTGAAAACCTACCC
CTAAAAGCCACCGGCGTGCGCAA

AAAATGCCTTTGCTTTTGTGCTTCTCTTCTCTGGGCTGGGGCTTTGGC
CAAGCTTATGTATAGCTTTGTGTCAGAGGAGACTGGCACACTTATAGTT
AATAGCGTCCTCCTGTTCCCTCGCATTCGTAGTCTTTTTGCTCGTCACTCT
CGCGATCTTGACGGCTTTGAGGTTGTGCGCTTACTGCTGCAACATTGTG
AATGTCAGTCTCGTAAAACCTTCTTTCTACGTCTACTCCAGAGTAAAAA
ATCTTAATAGTTCCCGCGTGCCAGACTTGCTGGTAGGAAGCCTGGTACC
CAGAGGCTCTCCACACCATCATCACCACCACTAA

GATCCGAATTCTTCGAACTCGAGGCTAGCTGGCCAGACATGATAAGAT
ACATTGATGAGTTTGGACAAACCACAACCTAGAATGCAGTGAAAAAAT
GCTTTATTTGTGAAATTTGTGATGCTATTGCTTTATTTGTAACCATTATA
AGCTGCAATAAACAAGTTAACAACAACAATTGCATTCATTTTATGTTTC
AGGTTCAAGGGGGAGGTGTGGGAGGTTTTTTAAAGCAAGTAAAACCTCT
ACAAATGTGGTATGGAAATGTTAATTAAGTCCATGACCAAATCCCT
TAACGTGAGTTTTTCGTTCCACTGAGCGTCAGACCCCGTAGAAAAGATCA
AAGGATCTTCTTGAGATCCTTTTTTTCTGCGCGTAATCTGCTGCTTGCAA
ACAAAAAAACCACCGCTACCAGCGGTGGTTTGTGGCCGGATCAAGAG
CTACCAACTCTTTTTCCGAAGGTAAGTGGCTTCAGCAGAGCGCAGATAC
CAAATACTGTTCTTCTAGTGTAGCCGTAGTTAGGCCACCACTTCAAGAA
CTCTGTAGCACCGCCTACATACCTCGCTCTGCTAATCCTGTTACCAGTG
GCTGCTGCCAGTGGCGATAAGTCGTGTCTTACCGGGTTGGACTCAAGAC
GATAGTTACCGGATAAGGCGCAGCGGTTCGGGCTGAACGGGGGGTTCGT
GCACACAGCCCAGCTTGGAGCGAACGACCTACACCGAACTGAGATACC
TACAGCGTGAGCTATGAGAAAGCGCCACGCTTCCCGAAGGGAGAAAGG
CGGACAGGTATCCGGTAAGCGGCAGGGTCGGAACAGGAGAGCGCACG

AGGGAGCTTCCAGGGGGAAACGCCTGGTATCTTTATAGTCCTGTCGGGT
TTCGCCACCTCTGACTTGAGCGTCGATTTTTGTGATGCTCGTCAGGGGG
GCGGAGCCTATGGAAAAACGCCAGCAACGCGGCCTTTTTACGGTTCCTG
GCCTTTTGCTGGCCTTTTGCTCACATGTTCTTAATTAACCTGCAGGGCCT
GAAATAACCTCTGAAAGAGGAACTTGGTTAGGTACCTTCTGAGGCTGA
AAGAACCAGCTGTGGAATGTGTGTCAGTTAGGGTGTGGAAAGTCCCCA
GGCTCCCCAGCAGGCAGAAGTATGCAAAGCATGCATCTCAATTAGTCA
GCAACCAGGTGTGGAAAGTCCCCAGGCTCCCCAGCAGGCAGAAGTATG
CAAAGCATGCATCTCAATTAGTCAGCAACCATAGTCCCAGTACTAGTTCGC
CAGAGCGCGCGAGGGCCTCCAGCGGCCGCCCCCTCCCCACAGCAGGGG
CGGGGTCCCGCGCCACCGGAAGGAGCGGGCTCGGGGCGGGCGGGCGCT
GATTGGCCGGGGCGGGCCTGACGCCGACGCGGCTATAAGAGACCACAA
GCGACCCGCAGGGCCAGACGTTCTTCGCCGAAGCTTGCCGTCAGAACG
CAGGTGAGGGGCGGGTGTGGCTTCCGCGGGCCGCCGAGCTGGAGGTCC
TGCTCCGAGCGGGCCGGGCCCGCTGTCGTCGGCGGGGATTAGCTGCG
AGCATTCCCGCTTCGAGTTGCGGGCGGGCGGGGAGGCAGAGTGCGAGG
CCTAGCGGCAACCCCGTAGCCTCGCCTCGTGTCCGGCTTGAGGCCTAGC
GTGGTGTCCGCGCCGCCGCGGTGCTACTCCGGCCGCACTCTGGTCTT
TTTTTTTTTTGTTGTTGTTGCCCTGCTGCCTTCGATTGCCGTTTCAGCAATA
GGGGCTAACAAAGGGAGGGTGCGGGGCTTGCTCGCCCGGAGCCCGGAG
AGGTCATGGTTGGGGAGGAATGGAGGGACAGGAGTGGCGGCTGGGGC
CCGCCCCGCTTCGGAGCACATGTCCGACGCCACCTGGATGGGGCGAGG
CCTGGGGTTTTTTCCCGAAGCAACCAGGCTGGGGTTAGCGTGCCGAGGCC
ATGTGGCCCCAGCACCCGGCACGATCTGGCTTGCGGGCGCCGCGTTGCC
CTGCCTCCCTAACTAGGGTGAGGCCATCCCGTCCGGCACCAAGTTGCGTG
CGTGGAAGATGGCCGCTCCCGGGCCCTGTTGCAAGGAGCTCAAAATG
GAGGACGCGGCAGCCCGGTGGAGCGGGCGGGTGAGTCACCCACACAA
AGGAAGAGGGCCTGGTCCCTCACCGGCTGCTGCTTCCTGTGACCCCGTG
GTCCTATCGGCCGCAATAGTCACCTCGGGCTTTTGAGCACGGCTAGTCG
CGGCGGGGGGAGGGGATGTAATGGCGTTGGAGTTTGTTCACATTTGGT

GGGTGGAGACTAGTCAGGCCAGCCTGGCGCTGGAAGTCATTTTTGGAA
TTTGTCCCCTTGAGTTTTGAGCGGATCCCCGCCACCATGCCTTTGCTTT
TGTTGCTTCTCTTCTCTGGGCTGGGGCTTTGGCCGGTGAACCTGAGAA
CCAGAACACAGCTGCCTCCAGCCTACACCAACAGCTTTACCAGAGGCG
TGTA TACTACCCCGACAAGGTGTT CAGATCCAGCGTGCTGCACTCTACCCA
GGACCTGTTCTGCCTTTCTTCAGCAACGTGACCTGGTTCCACGCCATCC
ACGTGTCCGGCACCAATGGCACCAAGAGATTCGACAACCCCGTGCTGC
CCTTCAACGACGGGGTGTACTTTGCCAGCACCGAGAAGTCCAACATCAT
CAGAGGCTGGATCTTCGGCACCACTGGACAGCAAGACCCAGAGCCT
GCTGATCGTGAACAACGCCACCAACGTGGTCATCAAAGTGTGCGAGTT
CCAGTTCTGCAACGACCCCTTCTGGACGTCTACTACCACAAGAACAAC
AAGAGCTGGATGGAAAGCGGCGTGTACAGCAGCGCCAACA ACTGCACC
TTCGAGTACGTGTCCAGCCTTTCCTGATGGACCTGGAAGGCAAGCAGG
GCAACTTCAAGAACCTGCGCGAGTTCGTGTTTAAGAACATCGACGGCTA
CTTCAAGATCTACAGCAAGCACACCCTATCAACCTCGTGCGGGATCTG
CCTCAGGGCTTCTCTGCTCTGGAACCCCTGGTGGATCTGCCCATCGGCA
TCAACATCACCCGGTTTCAGACACTGCTGGCCCTGCACAGAAGCTACCT
GACACCTGGCGATAGCAGCAGCGGATGGACAGCTGGTGCCGCCGCTTA
CTATGTGGGCTACCTGCAGCCTAGAACCTTCTGCTGAAGTACAACGAG
AACGGCACCATCACCGACGCCGTGGATTGTGCTCTGGACCCT
CTGAGCGAGACAAAGTGCACCCTGAAGTCCTTACCCTGGAAAAGGGC
ATCTACCAGACCAGCAACTTCCGGGTGCAGCCCACCGAATCCATCGTGC
GGTTCCCAATATCACCAATCTGTGCCCTTCGGCGAGGTGTTCAATGC
CACCAGATTCGCCTCTGTGTACGCCTGGAACCGGAAGCGGATCAGCAA
TTGCGTGGCCGACTACTCCGTGCTGTACA ACTCC

GCTAGCTTCAGCACCTTCAAGTGCTACGGCGTGTCCCCTACCAAGCTGA
ACGACCTGTGCTTCAAAACGTGTACGCCGACAGCTTCGTGATCCGGGG
AGATGAAGTGCGGCAGATTGCCCTGGACAGACAGGCAATATCGCCGA
CTACA ACTACAAGCTGCCCGACGACTTACC GGCTGTGTGATTGCCTGG

AACAGCAACAACCTGGACTCCAAAGTCGGCGGCAACTACAATTACAGA
TACCGGCTGTTCCGGAAGTCCAATCTGAAGCCCTTCGAGCGGGACATCT
CCACCGAGATCTATCAGGCCGGCAGCAAGCCTTGTAACGGCGTGGAAG
GCTTCAACTGCTACTTCCCCTGCAGTCCTACGGCTTTCAGCCCACAAA
TGGCGTGGGCTATCAGCCCTACAGAGTGGTGGTGCTGAGCTTCGAACTG
CTGCATGCCCCTGCCACAGTGTGCGGCCCTAAGAAAAGCACCAATCTCG
TGAAGAACAAATGCGTGAACCTTCAACTTCAACGGCCTGACCGGCACCG
GCGTGCTGACAGAGAGCAACAAGAAGTTCCTGCCATTCCAGCAGTTTG
GCCGGGATATCGCCGATACCACAGACGCCGTTAGAGATCCCCAGACAC
TGAAATCCTGGACATCACCCCTTGCGAGCTTCGGCGGAGTGTCTGTGAT
CACCCCTGGCACCAACACCAGCAATCAGGTGGCAGTGCTGTACCAGGG
CGTGAACGTGACCGAAGTGCCCGTGGCCATTCACGCCGATCAGCTGACA
CCTACATGGCGGGTGTACTCCACCGGCAGCAATGTGTTTCAGACCAGAG
CCGGCTGTCTGATCGGAGCCGAGCACGTGAACAATAGCTACGAGTGCG
ACATCCCCATCGGCGCTGGAATCTGCGCCAGCTACCAGACACAGACAA
ACAGCAGAGGCAGCGCCTCC
AGCGTGGCCAGCCAGAGCATCATTGCCTACACAATGTCTCTGGGCGCCG
AGAACAGCGTGGCCTACTCCAACAACCTCTATCGCTATCCCCACCAACTT
CACCATCAGCGTGACCACAGAGATCCTGCCTGTGTCCATGACCAAGACC
AGCGTGGACTGCACCATGTACATCTGCGGCGATTCCACCGAGTGCTCCA
ACCTGCTGCTGCAGTACGGCAGCTTCTGCACCCAGCTGAATAGAGCCCT
GACAGGGATCGCCGTGGAACAGGACAAGAACACCCAAGAGGTGTTTCGC
CCAAGTGAAGCAGATCTACAAGACCCCTCCTATCAAGGACTTCGGCGG
CTTCAATTTTCAGCCAGATTCTGCCCCGATCCTAGCAAGCCCAGCAAGCGG
AGC
CCCATCGAGGACCTGCTGTTCAACAAAGTGACACTGGCCGACGCCGGC
TTCATCAAGCAGTATGGCGATTGTCTGGGCGACATTGCCGCCAGGGATC
TGATTTGCGCCCAGAAGTTTAACGGACTGACAGTGCTGCCTCCTCTGCT
GACCGATGAGATGATCGCCCAGTACACATCTGCCCTGCTGGCCGGCAC
AATACAAGCGGCTGGACATTTGGAGCAGGCCCCCGCTCTGCAGATCCC

CTTTCCTATGCAGATGGCCTACCGGTTCAACGGCATCGGAGTGACCCAG
AATGTGCTGTACGAGAACCAGAAGCTGATCGCCAACCAGTTCAACAGC
GCCATCGGCAAGATCCAGGACAGCCTGAGCAGCACACCCAGCGCCCTG
GGAAAGCTGCAGAACGTGGTCAACCAGAATGCCCAGGCACTGAACACC
CTGGTCAAGCAGCTGTCCTCCAACCTTCGGCGCCATCAGCTCTGTGCTGA
ACGATATCCTGAGCAGACTGGACCCTCCTGAGGCCGAGGTGCAGATCG
ACAGACTGATCACAGGCAGACTGCAGAGCCTCCAGACATACTGACCC
AGCAGCTGATCAGAGCCGCCGAGATTAGAGCCTCTGCCAATCTGGCCG
CCACCAAGATGTCTGAGTGTGTGCTGGGCCAGAGCAAGAGAGTGGACT
TTTGCGGCAAGGGCTACCACCTGATGAGCTTCCCTCAGTCTGCCCTCA
CGGCGTGGTGTCTCTGCACGTGACATATGTGCCCGCTCAAGAGAAGAAT
TTCACCACCGCTCCAGCCATCTGCCACGACGGCAAAGCCCACCTTCCTA
GAGAAGGCGTGTTCGTGTCCAACGGCACCCATTGGTTCGTGACACAGC
GGAACCTTCTACGAGCCCCAGATCATCACCACCGACAACACCTTCGTGTC
TGCCAACCTGCGACGTCGTGATCGGCATTGTGAACAATACCGTGTACGAC
CCTCTGCAGCCCGAGCTGGACAGCTTCAAAGAGGAACTGGACAAGTAC
TTAAGAACCACACAAGCCCCGACGTGGACCTGGGCGATATCAGCGGA
ATCAATGCCAGCGTCGTGAACATCCAGAAAGAGATCGACCGGCTGAAC
GAGGTGGCCAAGAATCTGAACGAGAGCCTGATCGACCTGCAAGAAGTGG
GGGAAGTACGAGCAGTACATCAAGTGGCCCTGGTACATCTGGCTGGGC
TTTATCGCCGGACTGATTGCCATCGTGATGGTCACAATCATGCTGTGTT
GCATGACCAGCTGCTGTAGCTGCCTGAAGGGCTGTTGTAGCTGTGGCAG
CTGCTGCAAGTTCGACGAGGACGATTCTGAGCCCGTGCTGAAGGGCGT
GAAACTGCACTACACAGAAAACCTGTATTTTCAGAGCGGATCTGGGTA
CATCCCCGAGGCACCAAGAGATGGTCAGGCATATGTTAGGAAGGATGG
GGAATGGGTCCTCCTGAGCACATTTTTGGGAGGAAGCCTGGTACCCAG
AGGCTCTCCACACCATCATCACCACCACTGATGAGAGCTAATTCTCGGG
CTTCTTAGCGGTTCAAAGGTATCTTTTAAACCCTTTTTTAGGTGTTGTGA
AAACCACCGCTAATTCAAAGCAACCGGTGATATCGGATCCACGCGTAT
CGATTGTCGACCCTAGGAGCAGGTTTCCCCAATGACACAAAACGTGCA

ACTTGAAACTCCGCCTGGTCTTTCCAGGTCTAGAGGGGTAACACTTTGT
ACTGCGTTTTGGCTCCACGCTCGATCCACTGGCGAGTGTTAGTAACAGCA
CTGTTGCTTCGTAGCGGAGCATGACGGCCGTGGGAACTCCTCCTTGGTA
ACAAGGACCCACGGGGCCAAAAGCCACGCCCACACGGGCCCCGTCATGT
GTGCAACCCCAGCACGGCGACTTTACTGCGAAACCCACTTTAAAGTGAC
ATTGAAACTGGTACCCACACACTGGTGACAGGCTAAGGATGCCCTTCA
GGTACCCCGAGGTAACACGCGACACTCGGGATCTGAGAAGGGGACTGG
GGCTTCTATAAAAGCGCTCGGTTTAAAAAGCTTCTATGCCTGAATAGGT
GACCGGAGGTCGGCACCTTTCTTTGCAATTACTGACCCTATGAATACA
ACTGACTGTTTGACAATTAATCATCGGCATAGTATATCGGCATAGTATA
ATACGACTCACTATAGGAGGGCCACCATGAAGAAACCTGAACTGACAG
CAACTTCTGTTGAGAAGTTTCTCATTGAAAAATTTGATTCTGTTTCTGAT
CTCATGCAGCTGTCTGAAGGTGAAGAAAGCAGAGCCTTTTCTTTTGATG
TTGGAGGAAGAGGTTATGTTCTGAGGGTCAATTCTTGTGCTGATGGTTT
TTACAAAGACAGATATGTTTACAGACACTTTGCCTCTGCTGCTCTGCCA
ATTCCAGAAGTTCTGGACATTGGAGAATTTTCTGAATCTCTCACCTACT
GCATCAGCAGAAGAGCACAAGGAGTCACTCTCCAGGATCTCCCTGAAA
CTGAGCTGCCAGCTGTTCTGCAACCTGTTGCTGAAGCAATGGATGCCAT
TGCAGCAGCTGATCTGAGCCAAACCTCTGGATTTGGTCCTTTTGGTCCC
CAAGGCATTGGTCAGTACCACTTGGAGGGATTTCAATTTGTGCCATTG
CTGATCCTCATGTCTATCACTGGCAGACTGTGATGGATGACACAGTTTC
TGCTTCTGTTGCTCAGGCACTGGATGAACTCATGCTGTGGGCAGAAGAT
TGTCCTGAAGTCAGACACCTGGTCCATGCTGATTTTGGGAAGCAACAATG
TTCTGACAGACAATGGCAGAATCACTGCAGTCATTGACTGGTCTGAAGC
CATGTTTGGAGATTCTCAATATGAGGTTGCCAACATTTTTTTTTTGGAGAC
CTTGGCTGGCTTGCATGGAACAACAAACAAGATATTTTGAAGAAGAC
ACCCAGAACTGGCTGGTTCCCCCAGACTGAGAGCCTACATGCTCAGAAT
TGGCCTGGACCAACTGTATCAATCTCTGGTTGATGGAACTTTGATGAT
GCTGCTTGGGCACAAGGAAGATGTGATGCCATTGTGAGGTCTGGTGCTG
GAACTGTTGGAAGAACTCAAATTGCAAGAAGGTCTGCTGCTGTTTGGAC

TGATGGATGTGTTGAAGTTCTGGCTGACTCTGGAAACAGGAGACCCTCC
ACAAGACCCAGAGCCAAGGAATGAATATTAGCTAGATTATCCCTAATA
CCTGCCACCCCACTCTTAATCAGTGGTGGGAAGAACGGTCTCAGAACTGT
TTGTTTCAATTGGCCATTTAAGTTTAGTAGTAAAAGACTGGTTAATGAT
ACAATGCATCGTAAAACCTTCAGAAGGAAAGGAGAATGTTTTGTGGA
CCACTTTGGTTTTCTTTTTTGCGTGTGGCAGTTTTAAGTTATTAGTTTTTA
AAATCAGTACTTTTTAATGGAAACAACCTTGACCAAAAATTTGTCACAGA
ATTTTGAGACCCATTAAAAAAGTTAAATGAGAAACCTGTGTGTTTCCTTT
GGTCAACACCGAGACATTTAGGTGAAAGACATCTAATTCTGGTTTTACG
AATCTGGAAACTTCTTGAAAATGTAATTCTTGAGTTAACACTTCTGGGT
GGAGAATAGGGTTGTTTTCCCCCACATAATTGGAAGGGGAAGGAATA
TCATTTAAAGCTATGGGAGGGTTGCTTTGATTACAACACTGGAGAGAAA
TGCAGCATGTTGCTGATTGCCTGTCACTAAAACAGGCCAAAAACTGAGT
CCTTGGGTTGCATAGAAAGCTG

Next Generation Sequencing Result of pVitro1 M+N:

GCAAGGAGCTCAAAATGGAGGACGCGGCAGCCCGGTGGAGCGGGCGG
GTGAGTCACCCACACAAAGGAAGAGGGCCTTGCCCCTCGCCGGCCGCT
GCTTCCTGTGACCCCGTGGTCTATCGGCCGCATAGTCACCTCGGGCTTC
TCTTGAGCACCGCTCGTCGCGGGCGGGGGAGGGGATCTAATGGCGTTG
GAGTTTGTTCACATTTGGTGGGTGGAGACTAGTCAGGCCAGCCTGGCGC
TGGAAGTCATTCTTGGAATTTGCCCTTTGAGTTTGGAGCGAGGCTAAT
TCTCAAGCCTCTTAGCGGTTCAAAGGTATTTTCTAAACCCGTTTCCAGGT
GTTGTGAAAGCCACCGCTAATTCAAAGCAATCCGGAGTATAC

GGATCCAAAATGCCTTTGCTTTTGTGCTTCCTCTTCTCTGGGCTGGGGC
TTTGGCCAAGCTTATGGCGGACAGTAATGGAACCTATTACGGTGGAGGA
ACTTAAGAACTGCTGGAACAATGGAACCTGGTAATAGGTTTCCTGTTC
CTCACATGGATCTGCCTCTTGCAATTCGCGTACGCGAACCGGAATAGAT
TTCTCTACATAATAAAGCTGATTTTCCTCTGGCTCCTGTGGCCCGTCACA
CTCGCCTGTTTCGTACTCGCAGCAGTGTACAGGATTAACCTGGATTACCG
GGGGAATTGCGATTGCAATGGCTTGTCTGGTGGGACTGATGTGGCTTAG
CTATTTTATTGCTAGTTTTTCGACTTTTCGCAAGAACTCGAAGCATGTGGT
CCTTCAATCCTGAGACGAATATACTGTTGAATGTGCCTTTGCATGGAAC
AATTTTGACCCGACCGCTTCTTGAAAGCGAGCTTGTAATTGGGGCCGTG
ATACTTAGAGGTCACCTTGCGGATCGCAGGCCACCACCTTGGGCGGTGTG
ATATCAAGGATCTTCCTAAGGAAATCACGGTCGCAACGAGCCGCACGT
TGAGCTACTATAAACTCGGCGCGAGCCAGCGGGTTGCTGGTGATTCAG
GTTTCGCCGCTTACTCTAGATACAGGATTGGTAATTACAACTCAATAC
AGACCACAGTTCCTCTTCCGATAACATTGCTCTTCTGGTACAGGGAAGC
CTGGTACCCAGAGGCTCTCCACACCATCATCACCACCACTAA

GGATCC

CGTACGCCTAGGAGCAGGTTTCCCAATGACACAAAACGTGCAACTTG
AAACTCCGCCTGGTCTTTCAGGTCTAGAGGGGTAACACTTTGTACTGC

GTTTGGCTCCACGCTCGATCCACTGGCGAGTGTTAGTAACAGCACTGTT
GCTTCGTAGCGGAGCATGACGGCCGTGGGAACTCCTCCTTGGTAACAA
GGACCCACGGGGCCAAAAGCCACGCCACACGGGCCCCGTCATGTGTGC
AACCCAGCACGGCGACTTTACTGCGAAACCCACTTTAAAGTGACATTG
AAACTGGTACCCACACACTGGTGACAGGCTAAGGATGCCCTTCAGGTA
CCCCGAGGTAACACGCGACACTCGGGATCTGAGAAGGGGACTGGGGCT
TCTATAAAAGCGCTCGGTTTAAAAAGCTTCTATGCCTGAATAGGTGACC
GGAGGTCGGCACCTTTCCTTTGCAATTACTGACCCTATGAATACACTGA
CTGTTTGACAATTAATCATCGGCATAGTATATCGGCATAGTATAATACG
ACTCACTATAGGAGGGCCACCATGAAGAAACCTGAACTGACAGCAACT
TCTGTTGAGAAGTTTCTCATTGAAAAATTTGATTCTGTTTCTGATCTCAT
GCAGCTGTCTGAAGGTGAAGAAAGCAGAGCCTTTTCTTTTGATGTTGGA
GGAAGAGGTTATGTTCTGAGGGTCAATTCTTGTGCTGATGGTTTTTACA
AAGACAGATATGTTTACAGACACTTTGCCTCTGCTGCTCTGCCAATTCC
AGAAGTTCTGGACATTGGAGAATTTTCTGAATCTCTCACCTACTGCATC
AGCAGAAGAGCACAAGGAGTCACTCTCCAGGATCTCCCTGAAACTGAG
CTGCCAGCTGTTCTGCAACCTGTTGCTGAAGCAATGGATGCCATTGCAG
CAGCTGATCTGAGCCAAACCTCTGGATTTGGTCCTTTTGGTCCCCAAGG
CATTGGTCAGTACACCACTTGGAGGGATTTCAATTTGTGCCATTGCTGAT
CCTCATGTCTATCACTGGCAGACTGTGATGGATGACACAGTTTCTGCTT
CTGTTGCTCAGGCACTGGATGAACTCATGCTGTGGGCAGAAGATTGTCC
TGAAGTCAGACACCTGGTCCATGCTGATTTTGGAAAGCAACAATGTTCTG
ACAGACAATGGCAGAATCACTGCAGTCATTGACTGGTCTGAAGCCATG
TTTGGAGATTCTCAATATGAGGTTGCCAACATTTTTTTTTGGAGACCTTG
GCTGGCTTGCATGGAACAACAACAAGATATTTTGAAGAAGACACCC
AGAACTGGCTGGTTCCCCCAGACTGAGAGCCTACATGCTCAGAATTGGC
CTGGACCAACTGTATCAATCTCTGGTTGATGGAACTTTGATGATGCTG
CTTGGGCACAAGGAAGATGTGATGCCATTGTGAGGTCTGGTGCTGGAA
CTGTTGGAAGAACTCAAATTGCAAGAAGGTCTGCTGCTGTTTGGACTGA
TGGATGTGTTGAAGTTCTGGCTGACTCTGGAAACAGGAGACCCTCCACA

AGACCCAGAGCCAAGGAATGAATATTAGCTAGATTATCCCTAATACCT
GCCACCCCACTCTTAATCAGTGGTGAAGAACGGTCTCAGAACTGTTTG
TTCAATTGGCCATTTAAGTTTAGTAGTAAAAGACTGGTTAATGATAAC
AATGCATCGTAAAACCTTCAGAAGGAAAGGAGAATGTTTTGTGGACCA
CTTTGGTTTTCTTTTTTGCCTGTGGCAGTTTTAAGTTATTAGTTTTTAAAA
TCAGTACTTTTTAATGGAAACAACCTTGACCAAAAATTTGTCACAGAATT
TTGAGACCCATTAAAAAAGTTAAATGAGAAACCTGTGTGTTCCTTTGGT
CAACACCGAGACATTTAGGTGAAAGACATCTAATTCTGGTTTTACGAAT
CTGGAAACTTCTTGAAAATGTAATTCCTGAGTTAACACTTCTGGGTGGA
GAATAGGGTTGTTTTCCCCCACATAATTGGAAGGGGAAGGAATATCAT
TTAAAGCTATGGGAGGGTTGCTTTGATTACAACACTGGAGAGAAATGC
AGCATGTTGCTGATTGCCTGTCACTAAAACAGGCCAAAACCTGAGTCCT
TGGGTTGCATAGAAAGCTGCCTGCAGGGCCTGAAATAACCTCTGAAAG
AGGAACTTGGTTAGGTACCTTCTGAGGCGGAAAGAACCAGCTGTGGAA
TGTGTGTCAGTTAGGGTGTGGAAAGTCCCCAGGCTCCCCAGCAGGCAG
AAGTATGCAAAGCATGCATCTCAATTAGTCAGCAACCAGGTGTGGAAA
GTCCCCAGGCTCCCCAGCAGGCAGAAAGTATGCAAAGCATGCATCTCAA
TTAGTCAGCAACCATAGTCCCCTAGTGGAGCCGAGAGTAATTCATACA
AAAGGAGGGATCGCCTTCGCAAGGGGAGAGCCCAGGGACCGTCCCTAA
ATTCTCACAGACCCAAATCCCTGTAGCCGCCCCACGACAGCGCGAGGA
GCATGCGCTCAGGGCTGAGCGCGGGGAGAGCAGAGCACACAAGCTCAT
AGACCCTGGTCGTGGGGGGGAGGACCGGGGAGCTGGCGCGGGGCAAA
CTGGGAAAGCGGTGTCGTGTGCTGGCTCCGCCCTCTTCCCGAGGGTGGG
GGAGAACGGTATATAAGTGCGGCAGTCGCCTTGGACGTTCTTTTTCGCA
ACGGGTTTGCCGTCAGAACGCAGGTGAGGGGCGGGTGTGGCTTCCGCG
GGCCGCCGAGCTGGAGGTCCTGCTCCGAGCGGGCCGGGCCCCGCTGTC
GTCGGCGGGGATTAGCTGCGAGCATTCCCGCTTCGAGTTGCGGGCGGC
GCGGGAGGCAGAGTGCGAGGCCTAGCGGCAACCCCGTAGCCTCGCCTC
GTGTCCGGCTTGAGGCCTAGCGTGGTGTCCGCGCCGCCGCGCGTGCTA
CTCCGGCCGCACTCTGGTCTTTTTTTTTTTTTTGTGTTGTTGCCCTGCTGCC

TTCGATTGCCGTTTCAGCAATAGGGGCTAACAAAGGGAGGGTGCGGGGC
TTGCTCGCCCCGGAGCCCCGGAGAGGTCATGGTTGGGGAGGAATGGAGGG
ACAGGAGTGGCGGCTGGGGCCCCGCCCTTCGGAGCACATGTCCGAC
GCCACCTGGATGGGGCGAGGCCTGGGGTTTTTCCCGAAGCAACCAGGC
TGGGGTTAGCGTGCCGAGGCCATGTGGCCCCAGCACCCGGCACGATCT
GGCTTGGCGGCGCCGCGTTGCCCTGCCTCCCTAACTAGGGTGAGGCCAT
CCCGTCCGGCACCAAGTTGCGTGCGTGGAAGATGGCCGCTCCCGGGCC
CTGTTGCAAGGAGCTCAAAATGGAGGACGCGGCAGCCCCGGTGGAGCGG
GCGGGTGAGTCACCCACACAAAGGAAGAGGGCCTGGTCCCTCACCGGC
TGCTGCTTCCCTGTGACCCCGTGGTCCTATCGGCCGCAATAGTCACCTCG
GGCTTTTGAGCACGGCTAGTCGCGGCGGGGGGAGGGGATGTAATGGCG
TTGGAGTTTGTTCACATTTGGTGGGTGGAGACTAGTCAGGCCAGCCTGG
CGCTGGAAGTCATTTTTGGAATTTGTCCCCTTGAGTTTTGAGCGGAGCT
AATTCTCGGGCTTCTTAGCGGTTCAAAGGTATCTTTTAAACCCTTTTTTA
GGTGTGTGAAAACCACCGCTAATTCAAAGCAACCGGTGATATCAAAG
ATCC

AAAATGAGCGACAACGGCCACAAAATCAACGGAACGCCCCCGGATA
ACCTTCGGTGGGCCATCTGACAGTACTGGCTCTAATCAGAACGGAGAG
CGCTCCGGAGCAAGAAGCAAGCAACGACGGCCGCAAGGACTGCCCAAT
AATACTGCCAGTTGGTTCACAGCACTGACCCAGCACGGGAAAGAGGAT
CTCAAATTTCCGCGCGGTCAAGGTGTCCCATTAACTAATTCATCTC
CCGATGATCAAATCGGGTACTATCGACGAGCAACGCGCCGAATAAGGG
GCGGCGACGGAAAAATGAAGGACCTGTCCCCAAGGTGGTACTTTTACT
ATCTTGGCACCGGGCCGGAAGCGGGTCTTCCGTATGGAGCAAACAAGG
ACGGAATAATTTGGGTGCGGACCGAGGGTGCTCTTAATACTCCCAAAG
ATCACATTGGTACTCGCAATCCTGCTAACAACGCAGCCATCGTTCTCCA
GCTGCCGCAGGGAACAACGCTGCCCAAGGGTTTTTACGCGGAAGGCTC
AAGGGGTGGAAGCCAGGCGTCAAGTCGCAGCTCCAGCAGAAGTAGAA
ACAGTTCACGAAATAGCACCCCAGGCTCCTCACGCGGTACGAGTCCAG

CTAGAATGGCAGGAAACGGAGGGGACGCTGCTCTTGCCTTGCTGCTTCT
GGATCGGCTCAACCAGCTCGAAAGCAAGATGAGTGGTAAGGGGCAGCA
ACAACAGGGTCAGACCGTAACGAAAAAGTCTGCTGCAGAGGCTTCAA
GAAACCTAGGCAGAAGCGGACCGCAACCAAAGCCTACAATGTTACCA
AGCCTTCGGGCGGAGAGGTCCGGAACAAACGCAAGGGAATTTGGTGA
TCAGGAAGTATTGCGCAAGGAACCGATTACAAGCATTGGCCACAGAT
TGCTCAATTCGCCCCAAGCGCGAGTGCTTTCTTTGGGATGTCACGCATC
GGGATGGAAGTAACTCCATCCGGAACGTGGTTGACGTATACAGGCGCG
ATAAAGCTGGACGATAAAGACCCTAATTTCAAGGATCAGGTTATTCTGT
TGAATAAACATATAGACGCGTATAAAACCTTCCCGCCTACCGAGCCCA
AGAAAGATAAGAAGAAAAAAGCCGACGAAACCCAGGCTCTCCCTCAG
AGGCAAAGAAACAGCAAACGGTTACTCTCCTCCCTGCCGCCGATTTG
GACGACTTTAGCAAACAGTTGCAGCAGAGTATGTCCAGTGCAGACTCC
ACTCAGGCATAA

GGATCTTGTACAGCTAGCTGGCCAGACATGATAAGATACATTGATGAGT
TTGGACAAACCACAACCTAGAATGCAGTGAAAAAATGCTTTATTTGTG
AAATTTGTGATGCTATTGCTTTATTTGT
AACCATTATAAGCTGCAATAAACAAGTTAACAACAACAATTGCATTCAT
TTTATGTTTTAGGTTTCAGGGGGAGGTGTGGGAGGTTTTTTAAAGCAAGT
AA
AACCTCTACAAATGTGGTATGGAAATGTTAATTAAGTACCATGACCAA
AATCCCTTAACGTGAGTTTTTCGTTCCACTGAGCGTCAGACCCCGTAGAA
AA
GATCAAAGGATCTTCTTGAGATCCTTTTTTTCTGCGCGTAATCTGCTGCT
TGCAAACAAAAAACCACCGCTACCAGCGGTGGTTTGTTTGCCGGATC
AA
GAGCTACCAACTCTTTTTCCGAAGGTAAGTGGCTTCAGCAGAGCGCAGA
TACCAAATACTGTTCTTCTAGTGTAGCCGTAGTTAGGCCACCACTTCAA
GA

ACTCTGTAGCACCGCCTACATACCTCGCTCTGCTAATCCTGTTACCAGT
GGCTGCTGCCAGTGGCGATAAGTCGTGTCTTACCGGGTTGGACTCAAGA
CG
ATAGTTACCGGATAAGGCGCAGCGGTTCGGGCTGAACGGGGGGTTCGTG
CACACAGCCCAGCTTGGAGCGAACGACCTACACCGAACTGAGATACCT
ACAG
CGTGAGCTATGAGAAAGCGCCACGCTTCCCGAAGGGAGAAAGGCGGAC
AGGTATCCGGTAAGCGGCAGGGTTCGGAACAGGAGAGCGCACGAGGGA
GCTTC
CAGGGGGAAACGCCTGGTATCTTTATAGTCCTGTCGGGTTTTCGCCACCT
CTGACTTGAGCGTCGATTTTTGTGATGCTCGTCAGGGGGGCGGAGCCTA
TG
GAAAAACGCCAGCAACCGCGCCTTTTTACGGTTCCTGGCCTTTTGCTGG
CCTTTTGCTCACATGTTCTTAATTAACCTGCAGGCGTTACATAACTTACG
G
TAAATGGCCCGCCTGGCTGACCGCCCAACGACCCCCGCCCATTTGACGTC
AATAATGACGTATGTTCCCATAGTAACGCCAATAGGGACTTTCCATTGA
CG
TCAATGGGTGGAGTATTTACGGTAAACTGCCCACTTGGCAGTACATCAA
GTGTATCATATGCCAAGTACGCCCCCTATTGACGTCAATGACGGTAAAT
GG
CCCGCCTGGCATTATGCCAGTACATGACCTTATGGGACTTTCCTACTT
GGCAGTACATCTACGTATTAGTCATCGCTATTACCATGATGATGCGGTT
TT
GGCAGTACATCAATGGGCGTGGATAGCGGTTTGACTCACGGGGATTTCC
AAGTCTCCACCCATTGACGTCAATGGGAGTTTGTTTTGACTAGTGGAG
CC
GAGAGTAATTCATACAAAAGGAGGGATCGCCTTCGCAAGGGGAGAGCC
CAGGGACCGTCCCTAAATTCTCACAGACCCAAATCCCTGTAGCCGCCCC
ACG

ACAGCGCGAGGAGCATGCGCCCAGGGCTGAGCGCGGGTAGATCAGAGC
ACACAAGCTCACAGTCCCCGGCGGTGGGGGGAGGGGCGCGCTGAGCGG
GGGC
CAGGGAGCTGGCGCGGGGCAAACCTGGGAAAGTGGTGTTCGTGTGCTGGC
TCCGCCCTCTTCCCGAGGGTGGGGGAGAACGGTATATAAGTGCGGTAG
TCGC
CTTGGACGTTCTTTTTTCGCAACGGGTTTGCCGTCAGAACGCAGGTGAGT
GGCGGGTGTGGCTTCCGCGGGCCCCGGAGCTGGAGCCCTGCTCTGAGC
GGG
CCGGGCTGATATGCGAGTGTTCGTCCGCAGGGTTTAGCTGTGAGCATTCC
CACTTCGAGTGGCGGGCGGTGCGGGGGTGAGAGTGCGAGGCCTAGCGG
CAA
CCCCGTAGCCTCGCCTCGTGTCCGGCTTGAGGCCTAGCGTGGTGTCCGC
CGCCGCGTGCCTACTCCGGCCGCACTATGCGTTTTTTTGTCTTGCTGCCCT
C
GATTGCCTTCCAGCAGCATGGGCTAACAAAGGGAGGGTGTGGGGCTCA
CTCTTAAGGAGCCCATGAAGCTTACGTTGGATAGGAATGGAAGGGCAG
GAGG
GGCGACTGGGGCCCCGCCCGCCTTCGGAGCACATGTCCGACGCCACCTG
GATGGGGCGAGGCCTGTGGCTTTCCGAAGCAATCGGGCGTGAGTTTAG
CCTA
CCTGGGCCATGTGGCCCTAGCACTGGGCACGGTCTGGCCTGGCGGTGCC
GCGTTCCCTTGCCCTCCAACAAGGGTGAGGCCGTCCCGCCCGGCACCAG
TT GCTTGCGCGGAAAGATGGCCGCTCCCGGGGCCCTGTT

B. Media and Buffer Recipes

Low Salt LB Media

- 10 g Tryptone
- 5 g NaCl
- 5 g Yeast Extract
- 10 g Agar (For Solid Media)

Finalize to 1L with distilled water and autoclave. Add Hygromycin B gold at 100 µg/mL final concentration for antibiotic selection.

10 % Regular DMEM Medium (500 mL)

- 375.5 mL high glucose DMEM (Biological Industries, USA, cat. #01-052-1A)
- 10 mL heat inactivated Fetal bovine serum (Biological Industries, USA, cat. #04-127-1A)
- 5 mL Penicillin/Streptomycin Solution (Biological Industries, USA, cat. #03-031-1B)
- 5 mL MEM Non-Essential Amino Acids Solution 100X (Biological Industries, USA, cat. #03-340-1B)
- 5 mL Sodium Pyruvate Solution (Biological Industries, USA, cat. #03-042-1B)

Multimodal Chromatography Equilibration Buffer (1X DPBS)

- 0.2 g Potassium Chloride (KCl)
- 0.2 g Potassium Phosphate Monobasic (KH₂PO₄)
- 8 g Sodium Chloride (NaCl)
- 1.15 Sodium Phosphate Dibasic (Na₂HPO₄)

Adjust pH to 7.2 and finalize to 1 L with distilled water. 0.22 µm filter sterilize and store at room temperature.

Multimodal Chromatography Elution Buffer

- 11.9 g HEPES (50 mM)
- 116.9 g NaCl (2M)

Adjust pH to 7.2, finalize to 1L with distilled water and 0.22 µm filter sterilize.

Multimodal Chromatography Cleaning-In-Place (CIP) Solution

- 40 g NaOH (1M)
- 300 mL isopropanol
- 700 mL distilled water

0.22 µm filter sterilize and store at room temperature.

4X Laemmli Buffer

- 62.5 mM Tris-HCl, pH 6.8
- 10% glycerol
- 1% SDS
- 0.005% Bromophenol Blue

For reducing conditions add 100 µl of 2-mercaptoethanol per 900 µl (final concentration of 355 mM).

Phosphate buffered saline- Tween Solution (1X PBS-T)

- 0.2 g Potassium Chloride (KCl)
- 0.2 g Potassium Phosphate Monobasic (KH₂PO₄)
- 8 g Sodium Chloride (NaCl)
- 1.15 Sodium Phosphate Dibasic (Na₂HPO₄)
- 1 mL Tween 20

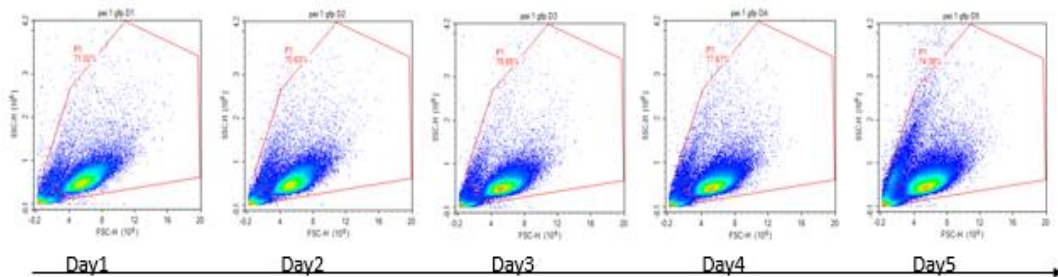
Adjust pH to 7.4 and finalize to 1 L with distilled water.

Immunoblotting Blocking Solution

- 5 g Non-Fat dry milk (5%)

Dissolve in 100 mL 1X PBS-T solution, store at 4 °C.

C. Gating Strategy for tracking pcDNA 3.1 (+) eGFP transfected HEK293 Suspension Cells



C.1. pcDNA 3.1 (+) eGFP transfected HEK293 Suspension Cells were tracked for 5 days after transfection. Viability of the cells were determined according to this gating strategy.

D. Viability Tracking of pViro2 6p-Delta-Variant-S+E and pViro1 M+N transfected HEK293 Suspension Cells (Representative for Both Variants)

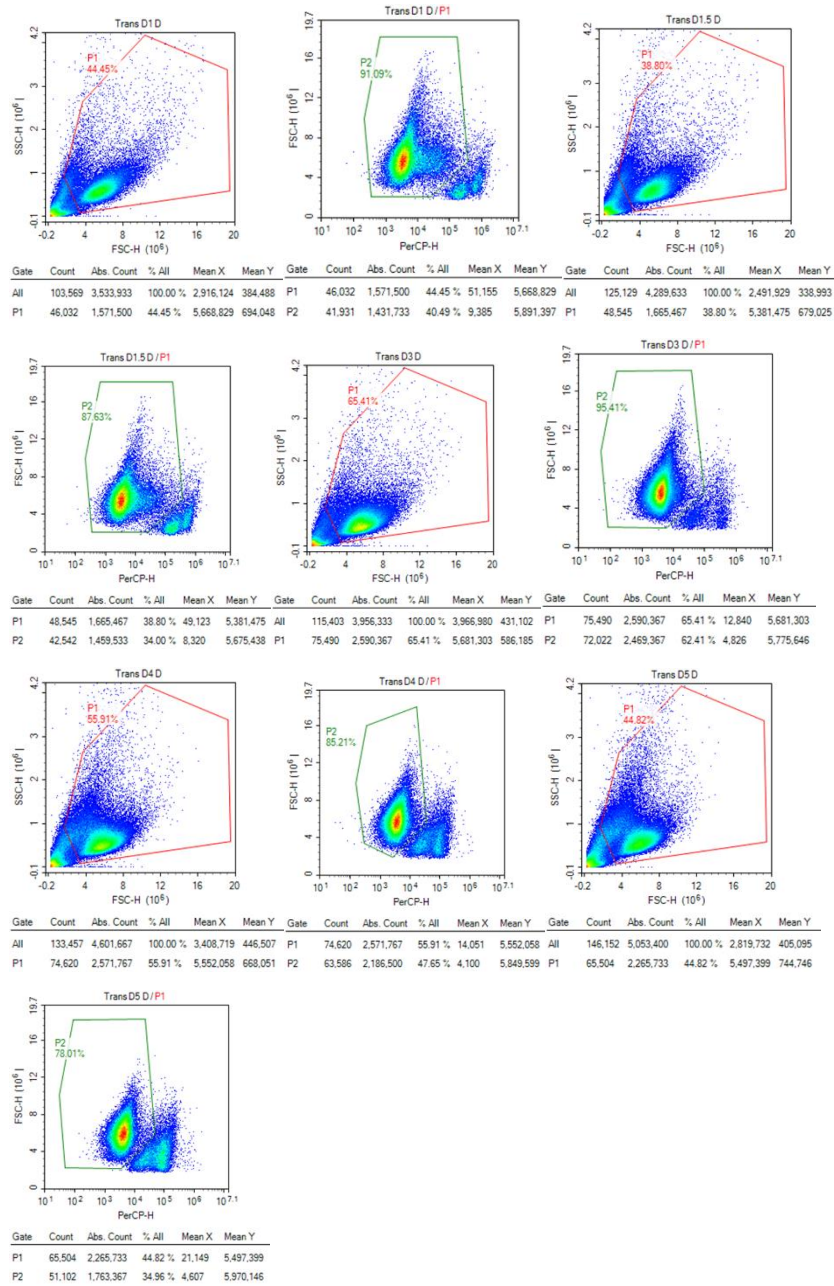
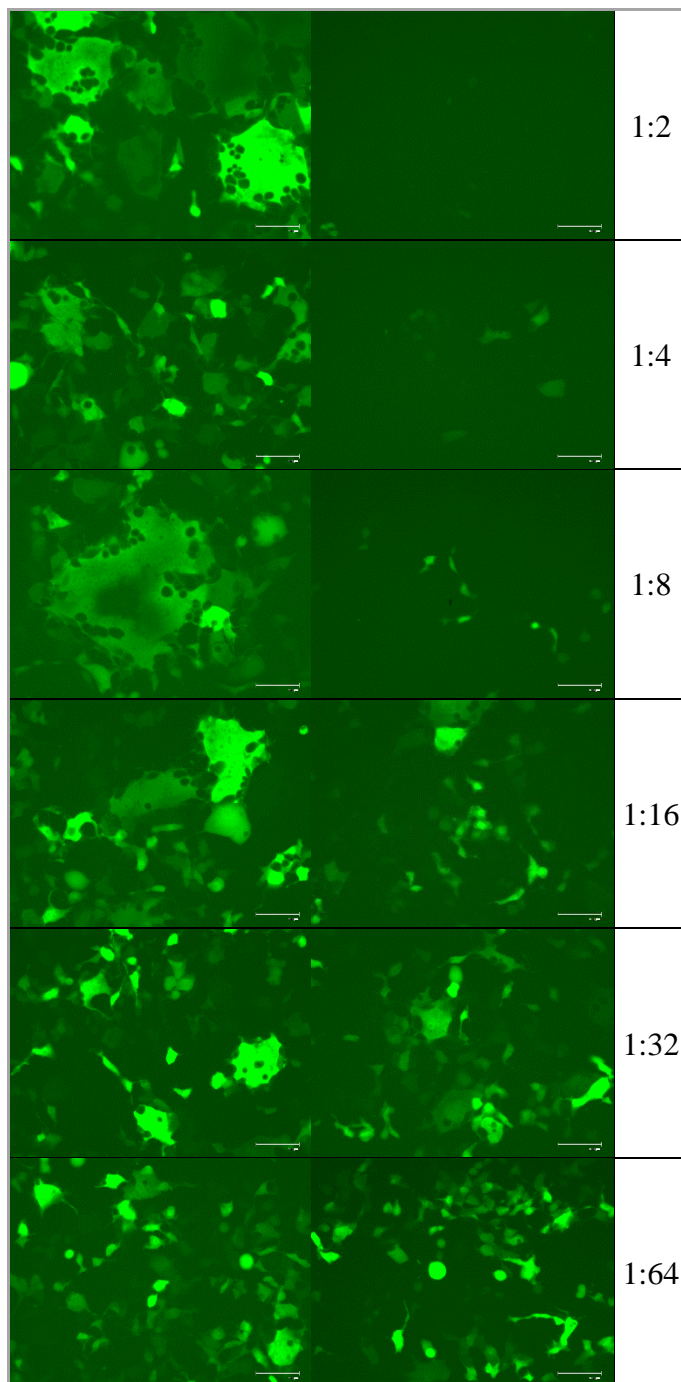


Figure D.1. Viability Tracking of the Transfected Cells with Variant Specific Constructs.

E. Negative and Positive Controls of Pseudotyped Virus Neutralization Assay



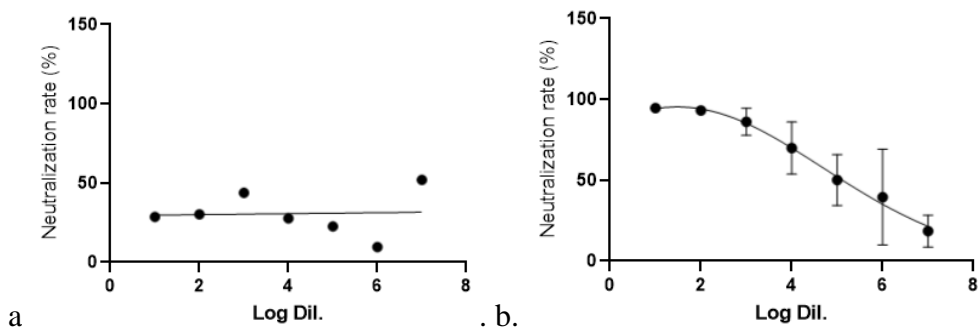
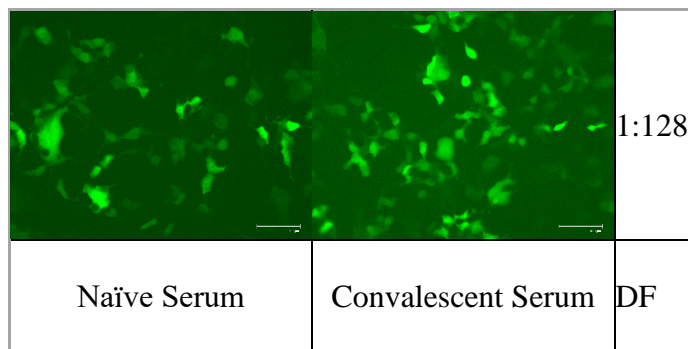


Figure E.1. Fluorescent Microscopy Images and Neutralization Activity Analysis from the Sera of Naïve (Negative control) and Convalescent (Positive control) (DF: dilution factor).

In the upper panel, each column represents FLoid™ images of an individual according to dilutions of the sera indicated at right marginst.

Graphs in the lower panel depict the changes in neutralization rate according to log dilutions of the sera from Naïve (a) and (b) Convalescent.

F. Flow Cytometric Analysis of Mean Fluorescent Intensity Levels

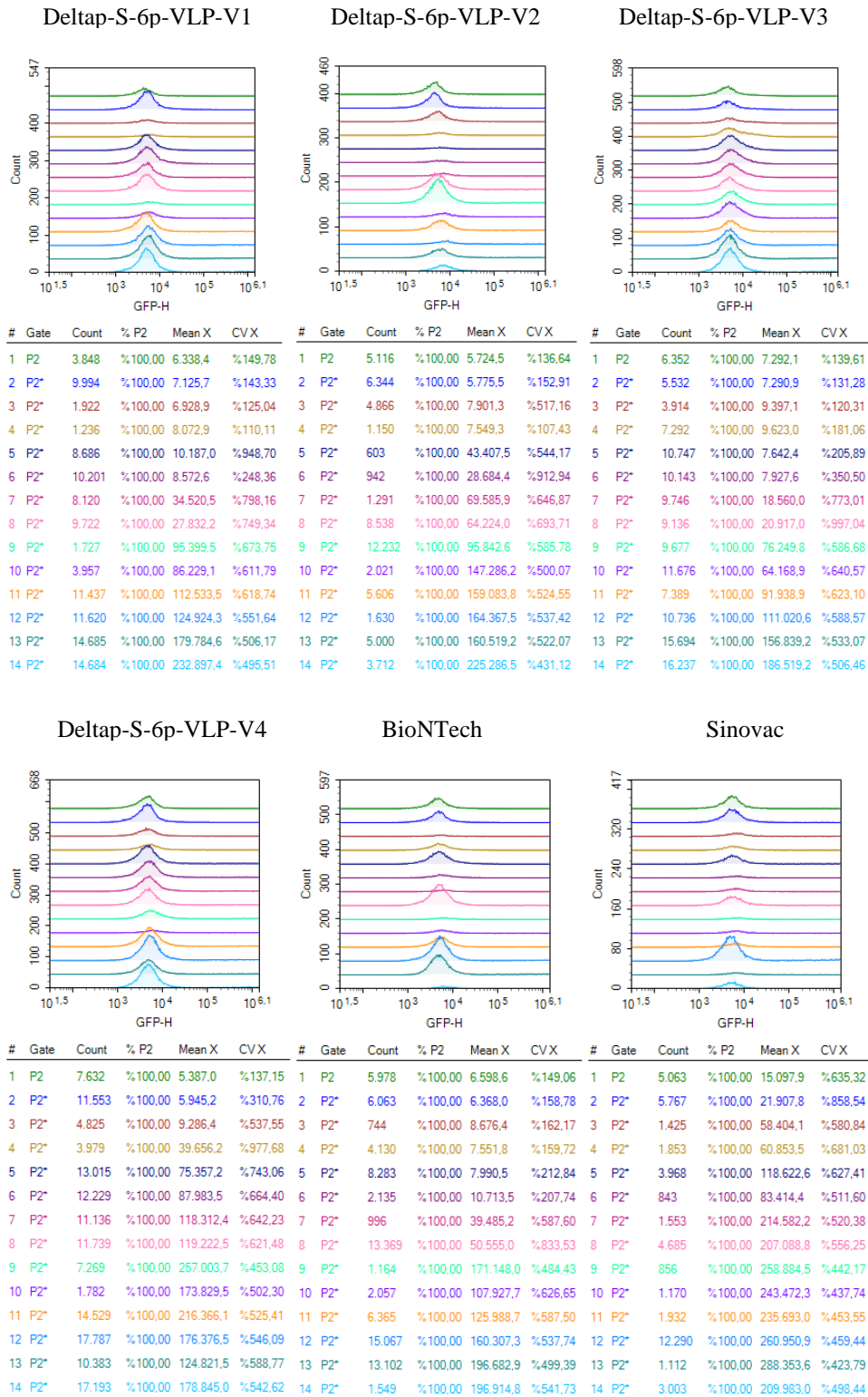
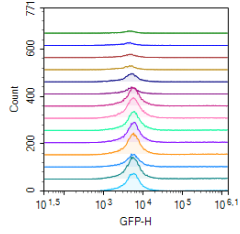
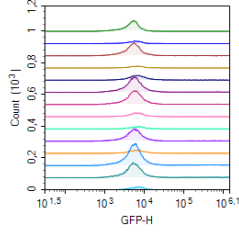


Figure F.1. Mean Fluorescent Intensity Levels of Neutralization Samples conducted with DeltaplusS-6p-VLP Vaccinated Mice and BioNTech & Sinovac Vaccinated Sera. Changes in mean fluorescence intensity according to dilutions were quantified in Flow Cytometry. MFI values were depicted as half-offset histograms. Sera dilutions were performed in duplicates starting from the top (1:2) to the bottom (1:128).

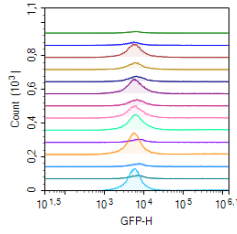
Alpha-S-6p-VLP-V1



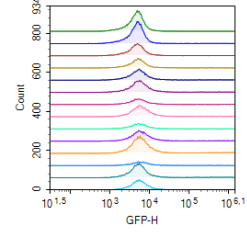
Alpha-S-6p-VLP-V2



Alpha-S-6p-VLP-V3

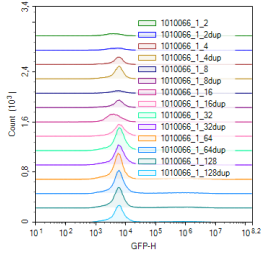


Alpha-S-6p-VLP-V4

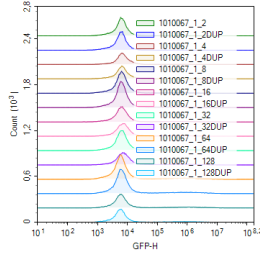


#	Gate	Count	% P2	Mean X	CV X	#	Gate	Count	% P2	Mean X	CV X	#	Gate	Count	% P2	Mean X	CV X	#	Gate	Count	% P2	Mean X	CV X
1	P2	1.577	%100.00	4.917.2	%80.56	1	P2	11.262	%100.00	7.667.1	%1.221.54	1	P2	1.841	%100.00	8.278.1	%117.57	1	P2	18.008	%100.00	9.336.4	%1.128.27
2	P2*	1.972	%100.00	4.923.8	%216.77	2	P2*	2.650	%100.00	6.984.4	%234.17	2	P2*	3.565	%100.00	8.060.3	%154.42	2	P2*	18.931	%100.00	11.986.2	%969.76
3	P2*	2.581	%100.00	5.663.9	%221.80	3	P2*	15.307	%100.00	29.420.6	%871.54	3	P2*	16.671	%100.00	9.149.1	%415.84	3	P2*	12.029	%100.00	45.386.2	%799.82
4	P2*	3.003	%100.00	5.452.4	%151.86	4	P2*	2.204	%100.00	26.716.0	%717.59	4	P2*	8.701	%100.00	10.003.9	%414.84	4	P2*	9.047	%100.00	29.964.4	%836.01
5	P2*	6.571	%100.00	22.342.4	%868.12	5	P2*	7.290	%100.00	82.282.8	%599.44	5	P2*	7.446	%100.00	36.109.0	%672.47	5	P2*	12.080	%100.00	96.008.9	%573.52
6	P2*	5.302	%100.00	20.420.3	%837.40	6	P2*	20.640	%100.00	73.212.6	%615.98	6	P2*	19.227	%100.00	33.103.6	%735.07	6	P2*	13.737	%100.00	83.703.7	%568.36
7	P2*	15.983	%100.00	64.747.9	%657.88	7	P2*	19.143	%100.00	82.187.4	%570.13	7	P2*	8.568	%100.00	46.121.0	%572.95	7	P2*	6.786	%100.00	134.430.0	%545.25
8	P2*	18.714	%100.00	56.000.1	%668.77	8	P2*	5.161	%100.00	67.766.2	%711.37	8	P2*	17.121	%100.00	64.731.1	%574.35	8	P2*	13.514	%100.00	135.127.7	%531.78
9	P2*	16.186	%100.00	64.028.2	%581.39	9	P2*	3.099	%100.00	69.644.2	%643.58	9	P2*	22.383	%100.00	128.860.2	%512.28	9	P2*	6.577	%100.00	188.310.8	%532.41
10	P2*	17.272	%100.00	79.764.8	%582.37	10	P2*	16.363	%100.00	99.156.7	%552.65	10	P2*	3.811	%100.00	49.357.4	%595.54	10	P2*	12.864	%100.00	195.813.0	%494.68
11	P2*	19.061	%100.00	108.653.3	%525.93	11	P2*	4.624	%100.00	80.428.3	%583.45	11	P2*	27.387	%100.00	89.957.6	%578.22	11	P2*	20.852	%100.00	222.287.8	%467.07
12	P2*	10.959	%100.00	78.216.2	%603.06	12	P2*	28.878	%100.00	104.874.1	%571.32	12	P2*	3.523	%100.00	56.142.5	%555.10	12	P2*	4.435	%100.00	86.940.3	%619.78
13	P2*	19.808	%100.00	160.580.8	%514.93	13	P2*	20.399	%100.00	132.111.8	%552.48	13	P2*	4.366	%100.00	85.972.2	%573.05	13	P2*	15.801	%100.00	164.210.9	%519.10
14	P2*	16.844	%100.00	136.697.4	%507.43	14	P2*	4.153	%100.00	102.255.5	%505.73	14	P2*	28.326	%100.00	139.133.9	%509.63	14	P2*	11.244	%100.00	103.259.8	%610.77

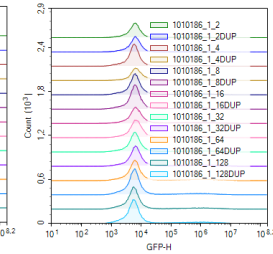
Alpha-S-6p-VLP-V5



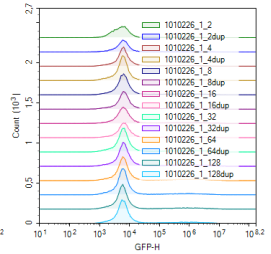
Alpha-S-6p-VLP-V6



Alpha-S-6p-VLP-V7



Alpha-S-6p-VLP-V8



#	Gate	Count	% P4	Mean X	CV X	#	Gate	Count	% P4	Mean X	CV X	#	Gate	Count	% P4	Mean X	CV X	#	Gate	Count	% P4	Mean X	CV X
1	P4	5.736	%100.00	4.881.9	%205.58	1	P4	27.040	%100.00	7.721.7	%295.86	1	P4	25.271	%100.00	48.888.8	%735.95	1	P4	24.674	%100.00	33.657.5	%800.22
2	P4*	5.692	%100.00	6.421.5	%249.38	2	P4*	28.308	%100.00	9.078.6	%536.76	2	P4*	25.914	%100.00	38.880.7	%822.32	2	P4*	19.664	%100.00	58.259.1	%687.38
3	P4*	13.450	%100.00	18.020.3	%11026.06	3	P4*	18.079	%100.00	14.246.6	%610.25	3	P4*	39.457	%100.00	88.680.7	%556.16	3	P4*	31.272	%100.00	124.042.1	%497.41
4	P4*	22.354	%100.00	16.054.9	%803.08	4	P4*	20.864	%100.00	24.732.5	%763.67	4	P4*	24.293	%100.00	92.426.0	%597.40	4	P4*	40.921	%100.00	100.000.0	%483.06
5	P4*	6.030	%100.00	44.751.3	%887.67	5	P4*	36.465	%100.00	41.020.8	%714.96	5	P4*	41.043	%100.00	170.194.9	%461.53	5	P4*	31.470	%100.00	198.456.0	%449.42
6	P4*	14.278	%100.00	33.265.4	%771.35	6	P4*	43.635	%100.00	56.847.3	%642.41	6	P4*	45.330	%100.00	117.210.1	%508.66	6	P4*	31.378	%100.00	194.572.1	%457.84
7	P4*	20.311	%100.00	16.573.6	%1193.39	7	P4*	27.428	%100.00	75.280.9	%614.68	7	P4*	34.317	%100.00	210.592.9	%452.36	7	P4*	31.909	%100.00	250.727.8	%435.36
8	P4*	26.840	%100.00	80.282.0	%608.48	8	P4*	25.830	%100.00	94.823.8	%529.68	8	P4*	38.922	%100.00	179.475.2	%459.77	8	P4*	28.488	%100.00	228.464.4	%449.07
9	P4*	52.540	%100.00	191.593.8	%452.87	9	P4*	38.957	%100.00	167.538.6	%485.54	9	P4*	40.178	%100.00	237.591.1	%435.45	9	P4*	45.514	%100.00	314.779.6	%404.15
10	P4*	45.944	%100.00	176.398.8	%477.10	10	P4*	26.541	%100.00	176.638.8	%473.61	10	P4*	42.696	%100.00	290.347.8	%417.46	10	P4*	43.477	%100.00	297.481.2	%427.24
11	P4*	54.761	%100.00	192.268.4	%451.80	11	P4*	45.979	%100.00	196.008.9	%458.89	11	P4*	43.096	%100.00	355.029.7	%400.83	11	P4*	42.352	%100.00	299.263.7	%402.06
12	P4*	51.487	%100.00	196.516.9	%469.97	12	P4*	49.945	%100.00	257.757.6	%432.62	12	P4*	52.907	%100.00	215.800.8	%447.41	12	P4*	46.906	%100.00	236.900.0	%440.32
13	P4*	45.531	%100.00	192.791.7	%456.73	13	P4*	27.977	%100.00	320.322.0	%407.15	13	P4*	45.576	%100.00	278.443.2	%419.40	13	P4*	42.579	%100.00	264.848.6	%419.53
14	P4*	39.180	%100.00	235.578.0	%444.42	14	P4*	24.677	%100.00	200.378.1	%452.96	14	P4*	48.932	%100.00	248.579.0	%433.49	14	P4*	42.935	%100.00	263.292.2	%424.15

Alpha-S-6p-VLP-V9

Alpha-S-6p-VLP-V10

Alpha-S-6p-VLP-V11

Alpha-S-6p-VLP-V12

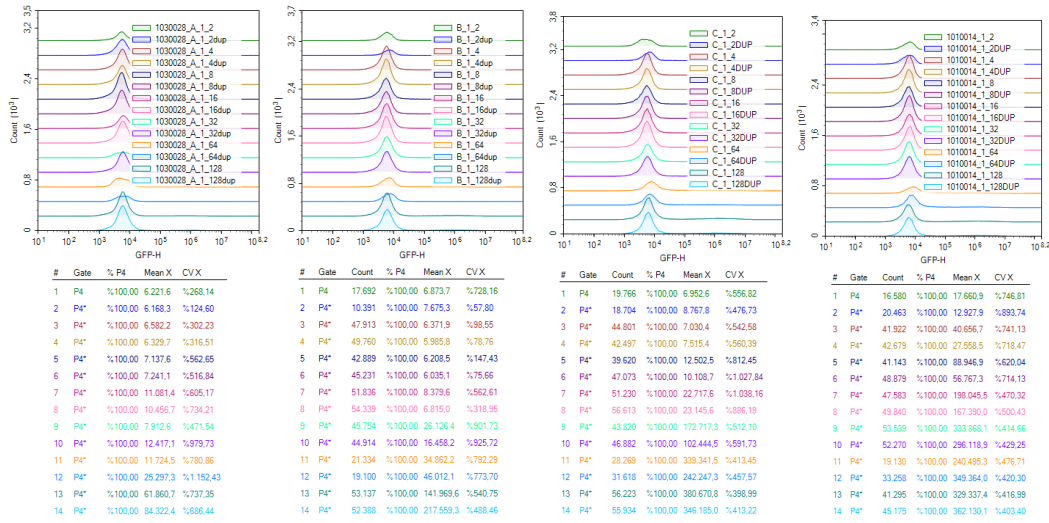


Figure F.2. Mean Fluorescent Intensity Levels of Neutralization Samples conducted with the sera of AlphaS-6p-VLP Vaccinated Volunteers. Changes in mean fluorescence intensity according to dilutions were quantified in Flow Cytometry. MFI values were depicted as half-offset histograms. Sera dilutions were performed in duplicates starting from the top (1:2) to the bottom (1:128).

